Australian Government
Geoscience Australia

Investigating Earthquake Risk Models and Uncertainty in Probabilistic Seismic Risk Analyses

Patchett A, Robinson D, Dhu T, Sanabria A.

Record
2005/02

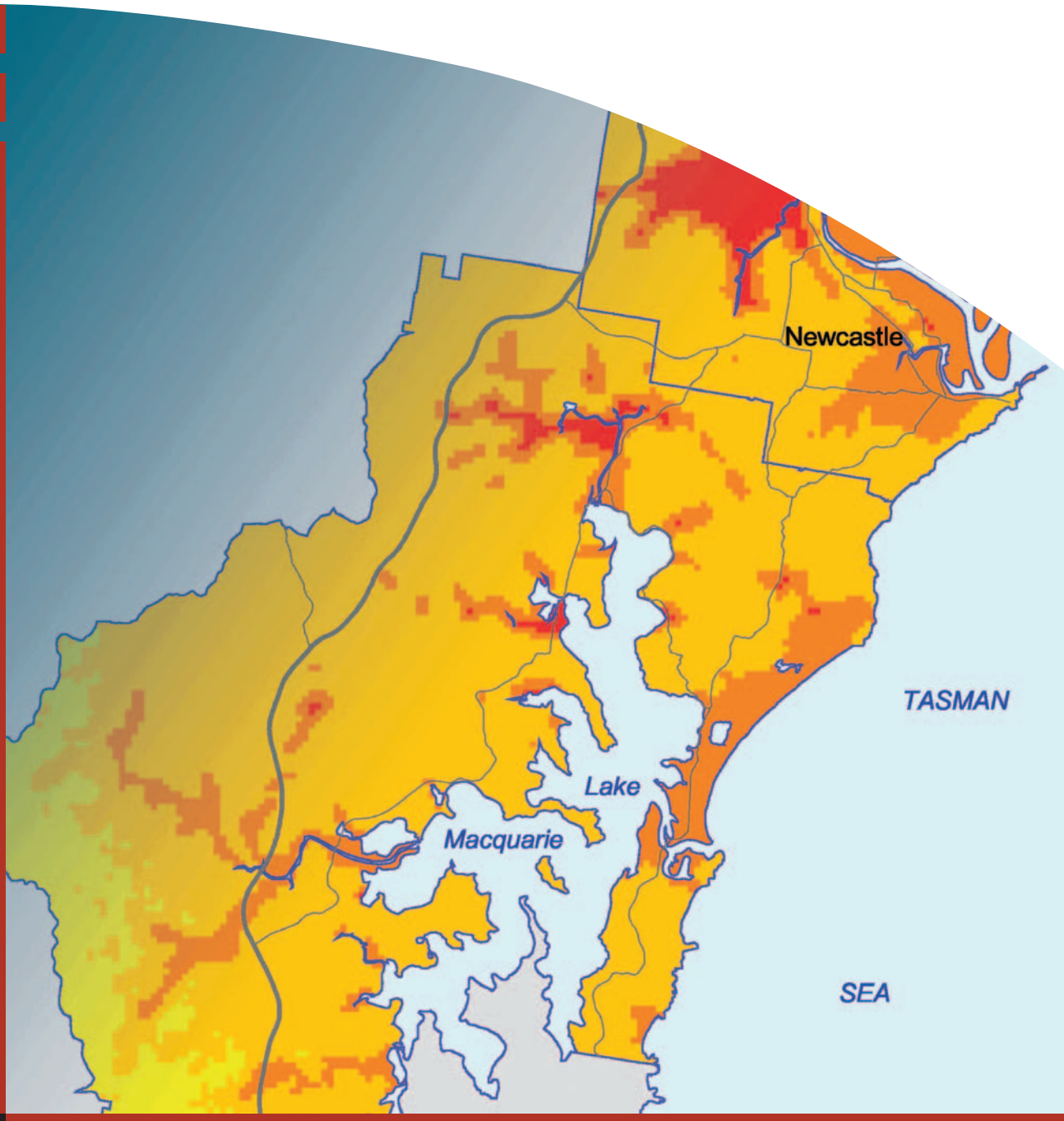

Investigating Earthquake Risk Models and Uncertainty in Probabilistic Seismic Risk Analyses

GEOSCIENCE AUSTRALIA
RECORD 2005/02

by

A.M. Patchett, D. Robinson, T. Dhu, A. Sanabria

Australian Government
Geoscience Australia

Geoscience Australia
Chief Executive Officer: Dr Neil Williams

Department of Industry, Tourism and Resources
Minister for Industry, Tourism and Resources: Senator The Hon. Ian Macfarlane MP
Parliamentary Secretary: The Hon. Warren Entsch, MP

ISSN 1448-2177
ISBN 1 920871 25 x (Hardcopy and CD-ROM)
ISBN 1 920871 61 6 (Web)

GeoCat No. 61752

Bibliographic reference: Patchett, A.M., Robinson, D., Dhu, T., Sanabria, A., 2005. *Investigating Earthquake Risk Models and Uncertainty in Probabilistic Seismic Risk Analyses.* Geoscience Australia, Record 2005/02

TABLE OF CONTENTS

1 Introduction

Natural disasters are common in Australia, causing over $1.14 billion damage annually to homes, businesses and infrastructure, and resulting in widespread disruption to communities (COAG, 2004). Although natural hazards cannot be prevented, their effects can be reduced by understanding the potential risk, identifying areas that are vulnerable and recommending and implementing mitigation strategies.

In December 2003, the Council of Australian Governments (COAG) endorsed a review of Australia's approach in dealing with a range of natural disasters (COAG, 2004). The review proposed 12 Reform Commitments (incorporating 66 recommendations) and concluded that a new approach to natural disasters in Australia was needed to develop safer, more sustainable communities in addition to achieving a reduction in risk, damage and losses from natural disasters likely to occur in the future. The COAG review essentially reflects a fundamental shift in priority beyond disaster response and reaction towards cost-effective, evidence-based disaster mitigation.

Local, State and Federal governments consented in principle to the 12 Reform Commitments which encompass disaster risk assessments, nationally consistent data and research, disaster mitigation strategies, resilient infrastructure and community awareness and warnings. Geoscience Australia is involved in addressing Reform Commitments 1 and 2 which deal with the development and implementation of "a five-year national programme of systematic and rigorous disaster risk assessments" and establishing "a nationally consistent system of data collection, research and analysis to ensure a sound knowledge base on natural disasters and disaster mitigation" respectively.

In order to appropriately address Reform Commitments 1 and 2, the development of a computational framework for assessing the natural hazard risk faced by Australian cities is required. Geoscience Australia has developed an earthquake risk model (EQRM) which models the likely impacts of earthquakes using probabilistic seismic hazard analyses (PSHA) and probabilistic seismic risk analyses (PSRA). PSHAs and PSRAs are typically undertaken via an event-based approach whereby individual events that obey *a priori* statistical information are synthetically generated through Monte Carlo techniques. This *a priori* information consists of probability density functions (PDFs, typically log-normal) described by moment parameters such as mean and standard deviation. Levels of ground motion or loss are estimated for each synthetic event and then aggregated to form hazard and risk estimates.

Incorporating uncertainties in risk estimates is critical to capturing the natural variation likely to be encountered during a natural disaster and therefore accurately model the associated risk. Two broad categories of uncertainty are associated with PSHA and PSRA and have been investigated herein – aleatory uncertainty and epistemic uncertainty. Aleatory uncertainty refers to the randomness inherent in a natural event and is modelled by sampling a PDF associated with each stage in the PSRA. Random sampling and spawning are two different techniques used by the EQRM to sample the PDFs within a Monte-Carlo approach.

Epistemic uncertainty arrises from knowledge limitations regarding the PDFs incorporated into the PSHA and PSRA. For example, inaccuracies in the value of the mean or standard deviation, or inaccuracies associated with assumptions about the shape (e.g. log-normal) of the PDF are forms of epistemic uncertainty. In this report, epistemic uncertainty for attenuation is considered by incorporating a range of alternative PDFs describing the propagation of motion.

Currently the event-based approach is not available to other hazards being considered in response to the COAG review. For example, wind studies currently estimate risk directly from hazard information rather than synthetic scenarios. In such cases hazard information must be converted to evaluations of risk. The primary aim of this project is to evaluate whether earthquake risk assessments derived from event-based and hazard-based approaches lead to consistent results. Case studies in the Perth and Newcastle regions were developed to answer this question.

The Perth and Newcastle case studies demonstrate that the hazard-based approach leads to higher estimates of risk than the event-based approach when used with random sampling. When used with spawning however, the event- and hazard- based approaches lead to similar estimates of risk, both of which are comparable with the hazard-random sampling combination. The differences between the four

results can be explained by the introduction of an artificial spatial correlation that is introduced when either the spawning or hazard based approaches are used. This report therefore demonstrates that the application of spawning requires a re-formulation and that care must be taken when estimating risk from hazard-based approaches.

The choice of attenuation model was also demonstrated to have a direct influence on risk. Furthermore, the uncertainty (epistemic) associated with using different attenuation models appears to be significantly greater than the uncertainty (aleatory) observed by using different sampling techniques. Uncertainty associated with the synthetic earthquake catalogue also influences risk estimates.

2 Background

Modelling earthquake risk involves the integration of source, attenuation, site response, building damage and financial loss models. A complicated element of earthquake risk assessments lies in the modelling of uncertainties, which are associated with each model component. Given the enormous uncertainty surrounding the timing, location and magnitude of future earthquakes, it is necessary to employ a probabilistic approach to describe the range of ground motions that a building or site may experience in the future.

PSRA provide an effective and logical basis for quantifying uncertainty and require an understanding of the location, frequency of occurrence and severity of hazard (Somerville and Moriwaki, 2003). Both the hazard- and event-based methods use a probabilistic approach to compute the level of ground shaking that is expected to be exceeded in a probabilistic sense.

Once the intensity of the ground motion is determined the associated risk is assessed. The computational methods used in this study estimate risk in terms of direct financial loss associated with damage to residential buildings. Other types of risk including social risk, indirect economic loss, damage to infrastructure, commercial buildings and essential services are not considered in this analysis.

Geoscience Australia's earthquake risk model EQRM uses PSRA and PSHA to estimate earthquake risk for both the event- and hazard-based approaches (Robinson and Fulford, 2005). In summary, EQRM

1. generates a catalogue of synthetic earthquakes using an earthquake source model;
2. models the associated ground motion and probability of occurrence;
3. estimates how the level of ground shaking propagates in the bedrock by using an attenuation model;
4. accounts for the local regolith and its affect on ground shaking by incorporating a site response model; and
5. estimates the probability of different damage states using the capacity spectrum method and models the direct financial loss to a suite of buildings and the probability of occurrence.

Robinson and Fulford (2005) provide a detailed description of this methodology.

This section describes the types of uncertainty in PSRA and the ways in which uncertainty is incorporated. It outlines the key differences between the event- and hazard-based methods for modelling earthquake risk.

2.1 UNCERTAINTY IN PSRA

Toro *et al.* (1997) introduced two broad categories of uncertainty into risk assessments:

1. *Aleatory uncertainty:* refers to the natural randomness of future events. Significant parameters of the PSRA are treated as random variables. Each random variable is defined by a probability density function (PDF) which describes the probability density of a variable taking on a specific value. It has a mean (μ) and standard deviation (σ). In this paper, aleatory uncertainty is incorporated mathematically by sampling the PDF associated with each random variable to include variation from the mean. Different techniques for sampling the PDF are discussed in detail later in this section.
2. *Epistemic uncertainty:* relates to knowledge limitation and can be associated with uncertainty in a model's ability to adequately describe a process. Mathematically this can be handled by using a range of models with different PDFs. In such cases it is argued that analysing the collection of PDFs provides an improved understanding of the true process. For example, alternative attenuation models are often used in PSHA and PSRA (Frankel *et al*., 2000; Adams and Halchuk, 2003).

Uncertainties are associated with each stage in earthquake risk assessments (see below).

2.1.1 Synthetic Earthquake Generation – Source Zone Model

The generation of a synthetic earthquake catalogue using a source zone model is the first integral component of the PSRA. The source zone model describes the probability of an earthquake of particular moment magnitude occurring in 1 year within the zone.

Source zones are defined by historical seismicity and the interpretation of earthquake occurrence on local geological structures. They are typically considered to be regions of homogeneous seismicity i.e. regions within which earthquakes of a given magnitude are equally likely to be located anywhere (Dhu and Jones, 2002). The ranges of moment magnitudes generated for Perth and Newcastle are 3.3 to 6.5 and 3.3 to 7.5 respectively. The source zones for the two study areas are discussed in detail later in this chapter.

The recurrence of earthquakes in each source zone is described by the bounded cumulative Gutenberg Richter relationship (BCGR. The BCGR estimates the number of earthquakes of equal or higher magnitude that are expected in the source zone for any magnitude of interest (Kramer, 1996). The term *bounded* indicates that the earthquake magnitude is bounded by a lower magnitude m_{min} that often corresponds to a measurement threshold and an upper bound m_{max} associated with the maximum expected earthquake in the zone. There is a separate PDF of the BCGR for each source zone which describes the probability density of an event in that source zone having any magnitude between m_{min} and m_{max}.

The generation of a synthetic earthquake catalogue involves the sampling of several PDFs. Firstly the user specifies the desired number of samples (N_s). In this study N_s was typically 1200 with the synthetic earthquakes distributed across a number of source zones. A location for each of the samples was generated by the random sampling of two uniform PDFs, one describing the latitude range of the source zone in question and the other describing the longitude range. This location of the event corresponds to the start of the rupture trace. A rupture orientation for each event is then assigned by using random sampling to take N_s samples from a uniform PDF covering the range -180 to 180. Each event is assigned a magnitude by using Stratified Monte Carlo sampling with the PDF of the BCGR for each source zone. This process ensures that all magnitudes between m_{min} and m_{max} are equally represented. Empirical rules are then used to calculate the remaining dimensions of each rupture trace such as depth and surface area (see Robinson and Fulford, 2005). Note that the process undertaken involves the incorporation of aleatory uncertainty only. Epistemic uncertainty in synthetic earthquake generation is not considered in this study and hence all source zones and empirical rules are assumed correct.

2.1.2 Attenuation

The attenuation model describes how the intensity of shaking varies with increasing distance from the earthquake source, and defines both the mean and standard deviation of the response spectra (Robinson and Fulford, 2005). Sampling the PDF is, in effect, sampling the output of the attenuation model.

Epistemic uncertainty associated with attenuation has been investigated by considering three different attenuation models, specifically those of Atkinson and Boore (1997), Toro *et al.* (1997) and Somerville *et al.* (2001). Each model generates a different PDF with a unique mean and standard deviation. Aleatory uncertainty associated with attenuation has been considered by applying different sampling techniques to each attenuation model.

2.1.3 Regolith Amplification and Uncertainty

Regolith plays an important role in terms of ground shaking during an earthquake, the presence of which can act to intensify and prolong ground movement. The site response model accounts for differences in response to ground shaking between regolith and the underlying unweathered bedrock. The type of regolith present at a building site can therefore be correlated with the level of damage experienced. Regolith effectively decreases the seismic wave velocity thereby increasing the amplitude and wavelength, giving rise to a much larger, more destructive seismic wave (Robinson *et al.*, 2006.

In order to identify regional changes in earthquake hazard due to variation in regolith, the Newcastle study area has been divided into six distinct regolith profiles (or site classes), each of which is considered to be essentially homogeneous. Amplification factors are used to account for the presence of regolith by representing the transfer of earthquake motion from the unweathered bedrock through the regolith to the ground surface.

Amplification factors for each site class are represented by a PDF to reflect inhomogeniety within the site class. Amplification uncertainty, and therefore aleatory uncertainty, is considered only by random sampling of the PDF. When amplification uncertainty is excluded, mean amplification factors are assumed.

Epistemic uncertainty in amplification is not considered in this study and hence all regolith site classes and amplification factor PDFs are assumed correct. In addition, the effect of regolith

amplification and uncertainty has only been investigated for Newcastle, as this information was not available for Perth at the time this work was conducted.

2.1.4 Building Damage Model

EQRM models damage to buildings using the capacity spectrum method, which estimates the peak response spectral acceleration and displacement for each building corresponding to a synthetic event.

Response spectral acceleration describes the total *acceleration* (or shaking) experienced by a building, or a suite of buildings, during an event. Response spectral displacement (RSD), however, describes the maximum *displacement* of a building relative to the displacement of the ground (Chopra, 2001). When computing RSA the buildings are assumed to behave as single degree of freedom oscillators (Kramer, 1996) with a range of fundamental periods (T_0). Typically an increase in T_0 corresponds to a taller building. RSA also form the basis for design spectra which are used in building codes and design criteria for major structural developments.

The capacity spectrum method employs two types of curves – the demand curve (or demand spectra) and the capacity curve (Figure 1).

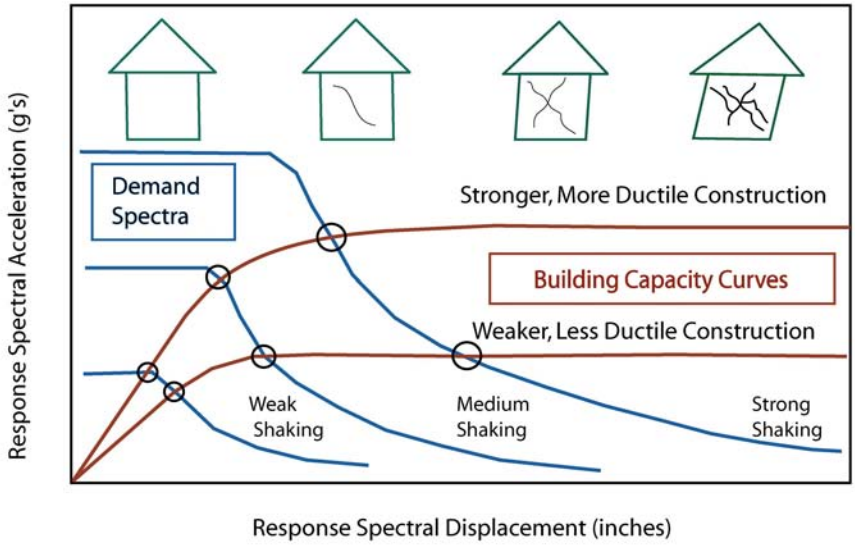

Figure 1 Intersection of demand spectra and building capacity curves. The intersection point indicates the peak displacement and acceleration which a single degree of freedom oscillator has undergone (after Kircher et al., 1997a).

The ***demand curve*** describes the load that is placed on a building during an earthquake (Kircher *et al.*, 1997a) and the way in which this curve is calculated forms the fundamental difference between the event- and hazard-based methods. As such, EQRM computes the demand curve in two different ways:

1. ***Event-based; response spectral acceleration -*** the demand curve is defined by the RSA for each individual earthquake at each individual building site, and is computed directly from the attenuation model. That is, it takes into account the event magnitude and distance to each individual building site.

2. ***Hazard-based; uniform hazard spectra (UHS) -*** the demand curve is defined by the UHS from the entire catalogue of earthquakes on the basis of maximum hazard at a particular level of return period. A range of return periods are used to produce a suite of UHS. Each individual UHS (i.e. for each different return period) is then used to describe the load on each building and hence 'mimic' an event.

The ***capacity curve*** is used to estimate the peak response of a building for a given level of spectral demand (Kircher *et al.*, 1997a). Capacity curves are plotted on the same axes as demand curves, the intersection of which indicates the peak acceleration and displacement (Figure 1). Figure 2 illustrates how the capacity curve is described by three segments separated by the yield and ultimate points.

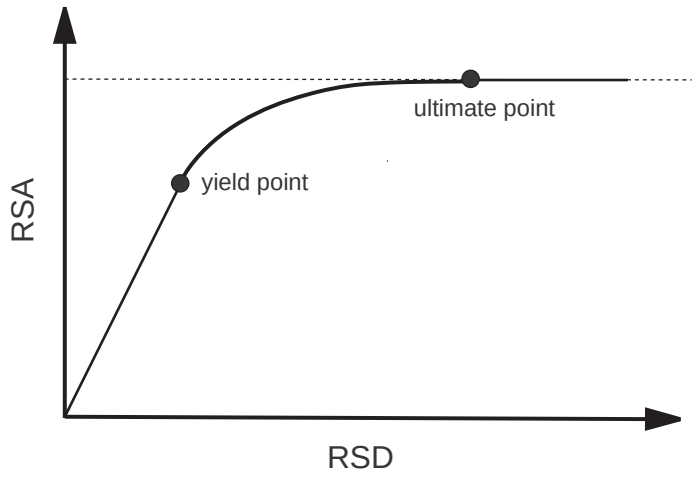

Figure 2 Capacity curve, defined by a straight line to the yield point, an exponential curve to the ultimate point and a horizontal line thereafter.

The vertical position of the capacity curve ultimate point is assumed to follow a log-normal probability density function with standard deviation of 0.3 (FEMA, 1999) as illustrated in Figure 3. Random sampling is used to pick a different ultimate point and hence capacity curve for each earthquake (return period in the case of the hazard method). Note that the PDF of the ultimate point is assumed to be correct for each building structural type. That is, there has been no attempt to consider any epistemic uncertainty in this study.

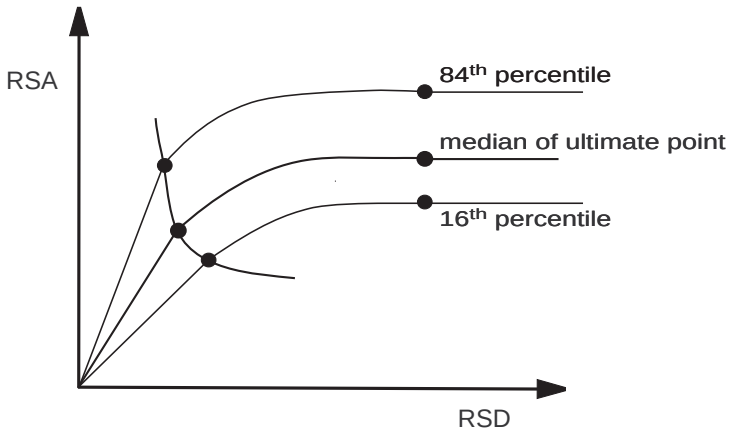

Figure 3 Log-normal distribution of the capacity curve illustrated by the median, 84th percentile and 16th percentile. In this study random sampling is used to incorporate aleatory uncertainty about the median capacity curve.

A third class of curve, ***building fragility curves***, describe the probability of reaching or exceeding a range of damage states. Fragility curves distribute damage among four key damage states - Slight, Moderate, Extensive and Complete damage (Kircher *et al.*, 1997a). The fragility curves are further segregated into components of the building (structural, non structural drift sensitive and non-structural acceleration sensitive). It is the fragility curves which convert peak displacement and acceleration (see 2.1.4) into damage.

The fragility curve for each damage state and building component combination is a cumulative log-normal distribution. Each fragility curve is described analytically using the damage state threshold and the variation parameter (closely related to the standard deviation). The peak spectral load (displacement or acceleration) is used together with the fragility curves to estimate the probability of exceeding each of the damage states (FEMA, 1999). Figure 4 illustrates how the variation parameter and hence aleatory uncertainty flattens the fragility curve causing probabilities of exceedence for a range of spectral loads. Without the aleatory uncertainty the fragility curve is a step function and the building will experience (or exceed) the given damage state with absolute certainty the moment the threshold spectral load is met. Similarly, when the variation parameter is zero the building will not experience (or

exceed) the damage state for spectral loads below the damage state threshold. Figure 5 illustrates the conversion of the cumulative probabilities of the fragility curves to incremental probabilities for each building component being in a given damage state. These incremental probabilities are used in the financial model to estimate the 'most probable' loss for the event. Note that the fragility curves are assumed to be correct and that no epistemic uncertainty has been considered in this study.

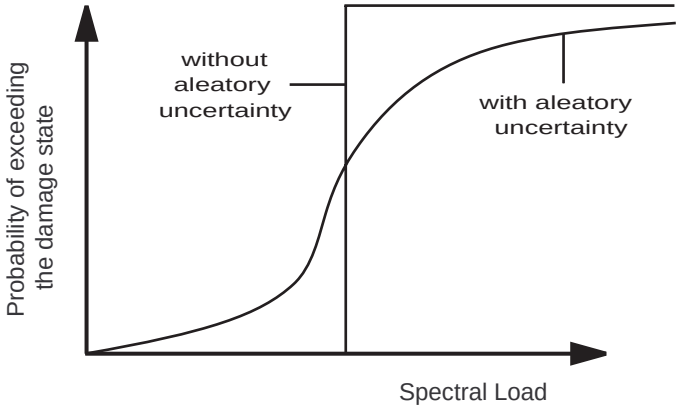

Figure 4 Fragility curve with and without aleatory uncertainty (step function).

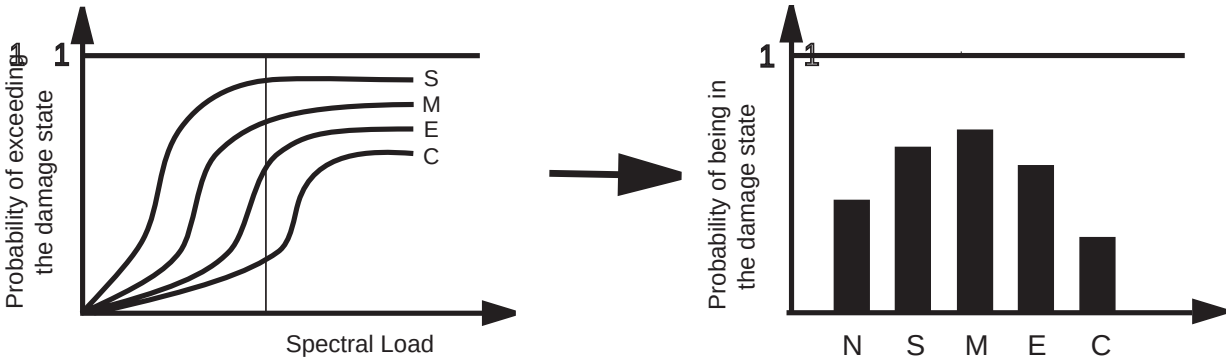

Figure 5 Converting the cumulative probabilities in the fragility curves to incremental probabilities for the building component being in a given damage state. The nomenclature N, S, M, E and C represents no, slight, moderate, extensive and complete damage respectively (Kircher et al., 1997b).

2.1.5 Financial Model

A financial model is used to estimate the loss in dollars associated with the damage for each of the three building components as well as for the contents. A total loss for each building is estimated by summing the individual component losses. For the purpose of this report the losses have been aggregated across the city to estimate a loss experienced by the region and then represented as a percentage of total building value for the region.

The financial model assumes the following for each building structural and usage type combination in the region:

1. a construction cost per meter square,
2. a pre-defined division of value across three building components, and
3. an estimate of contents value as a percentage of the total building value.

For the purpose of this report, points 1 to 3 above are assumed to be exact and no uncertainty has been considered.

2.2 SAMPLING THE PDF TO INCORPORATE ALEATORY UNCERTAINTY

The aleatory uncertainty associated with each model component is defined by a probability density function (PDF) with a mean (μ) and standard deviation (σ). Aleatory uncertainty is incorporated in risk estimates when the PDF is sampled to include variation from the mean. This can be done in a number of ways. Three techniques for sampling attenuation have been investigated; random sampling, spawning and sampling the mean of the PDF. These techniques are discussed below. Capacity curve uncertainty, amplification uncertainty and uncertainty associated with the earthquake catalogue, however, have all been modelled using only random sampling.

2.2.1 Spawning

Spawning incorporates an even sampling across the PDF and these are weighted against their respective probability of occurrence. The number of standard deviations sampled can be selected as required. This study used a default setting of 5 samples during spawning and a sample width of ±2.5 σ.

During spawning, the synthetic earthquake catalogue is generated the equivalent number of times the PDF is sampled, i.e. 5 samples corresponds to 5 earthquake catalogues generated (Figure 6). The actual motion is calculated at the bin centroid whereas the probability is determined by the width of the bin (Robinson and Fulford, 2005).

Risk is calculated by aggregating the loss across all sites of interest for each spawned event. Therefore, every point on the PML represents the loss for all buildings for a single event and a single spawned sample (refer to section 2.4.1). That is a high/low choice at one location corresponds with a high/low selection at all locations and therefore spawning introduces a high level of artificial spatial correlation. Whilst this study considers only one type of spawning, Robinson and Fulford (2005) introduce two different techniques of spawning which they refer to as

1. spawning without logic tree collapse, and
2. spawning with logic tree collapse.

It is not necessary to understand the details of these algorithms to understand the contents of this report (details can be found in Robinson and Fulford, 2005). However, it is important to realise only the first technique is used in this work. The second technique was designed to overcome some of the issues associated with spatial correlation introduced with the first technique. These issues are identified and described in detail later in this paper.

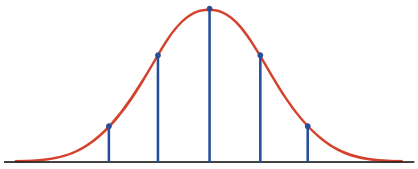

Figure 6 PDF showing 5 spawned values.

2.2.2 Random Sampling

Random sampling involves selecting a single random value from the PDF (Figure 7). Random sampling does not directly take into account the probability of selecting a particular value (Robinson and Fulford, 2005). In this method a randomly selected value is not weighted against its probability of occurrence. Extremely high or low values, however, have a naturally lower probability of selection and as such these values are less likely to be selected. Random sampling incorporates a very low level of spatial correlation. That is, a high/low choice at one location does not correspond with a high/low choice at other locations.

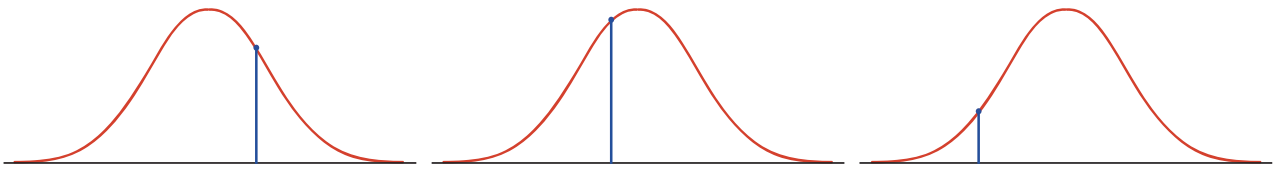

Figure 7 PDFs showing examples of randomly sampled values.

2.2.3 Mean and ± 1 standard deviation

This technique involves sampling only the mean or ± 1 standard deviation either side of the mean as specified (Figure 8).

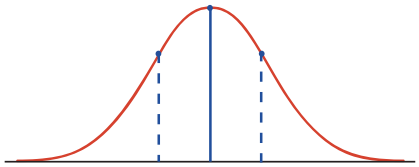

Figure 8 PDF showing the mean and ± 1 standard deviation.

2.2.4 Stratified Monte Carlo sampling

Traditionally the distribution of samples chosen from a PDF via Monte Carlo Sampling represents the original PDF. That is, there will be many samples in the vicinity of the expected value (or mean) and few samples corresponding to the tails of the PDF. Stratified Monte Carlo Sampling involves taking many samples (typically 1000 or more) from a PDF in a semi-controlled (or stratified) fashion. The algorithm encourages an even distribution of sampling across the dynamic range of the PDF. Therefore the number of samples generated in the vicinity of the expected value is roughly the same as the number generated in the tails.

The Stratified Monte Carlo sampling is usually applied to PDFs with a bounded range i.e. $X \in [x_{min},x_{max}]$ where X refers to the random variable, however it is possible to truncate PDFs with an un-bounded range i.e. $X \in (-\infty,\infty)$ (Figure 9a). The dynamic range of the PDF is divided into N_b bins (i.e. N_b discrete non-overlapping intervals, see Figure 9b). Typically the number of bins considered in this study is 15. The generation of N_s samples is then conducted in two stages. Firstly each of the N_s samples is constrained to one of the N_b bins by randomly sampling N_s values from a discrete uniform distribution containing 1,2,3,…,N_b. Here 1 refers to the first bin, 2 to the second bin and so on (Figure 9c). The N_b bins are similarly represented when a large number of samples are generated since any one of the N_b bins is equally likely to be chosen. A value for X is assigned to each of the N_s samples by randomly sampling a value from a continuous uniform distribution spanning the dynamic range of the bin (Figure 9d). Hence each of the samples can be any value in the range $X \in [x_{min},x_{max}]$ with equal likelihood and the N_s samples span the entire range of the original PDF. The samples are now ready for use in the simulation. However, conclusions drawn from such a simulation will not represent reality since the samples do not follow the original PDF. A final step is required to account for this. The probability of the random variable X equalling each of the sample values also needs to be calculated so that the final simulation results can be weighted against the likelihood of their occurrence. This is achieved by evaluating the probability of each of the samples occurring from the original PDF and normalising the probabilities to account for N_s and N_b. Robinson and Fulford (2005) discuss the calculation of this probability in detail as well as how it is used to weight the final results of the simulation.

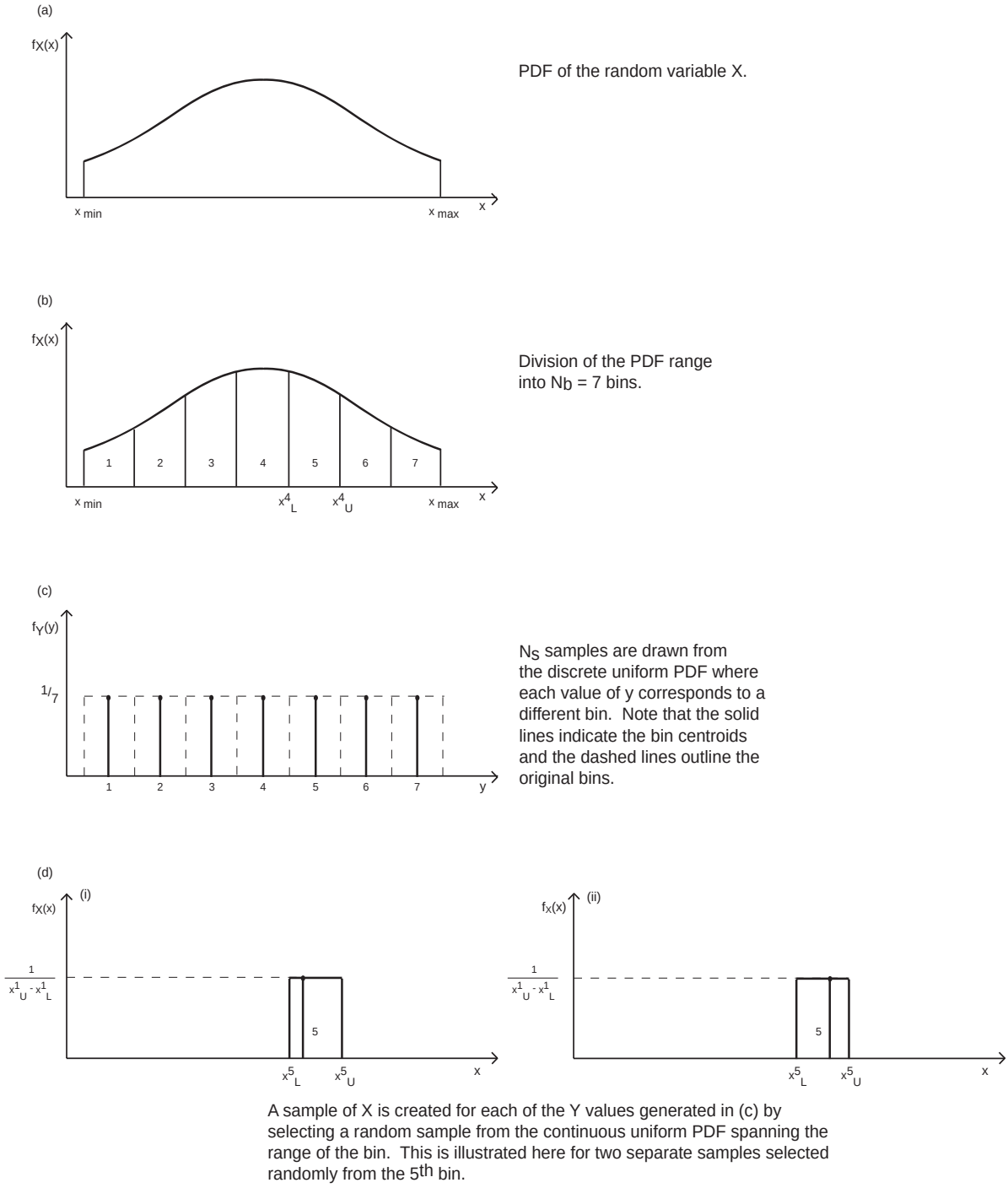

Figure 9 Four stages in stratified Monte Carlo sampling.

2.3 STUDY AREAS – NEWCASTLE AND PERTH

The Newcastle area is the principal focus of this study. The driving seismic source zone (or region of highest seismicity) is located directly below the metropolitan area and is described in detail by Dhu and Jones (2002). Newcastle has been classified into 6 source zones; the Newcastle Triangle Zone (NTZ), Newcastle Fault Zone (NFZ) and 4 segregations of the Tasman Sea Margin Zone (Dhu *et al.*, 2002). For this study approximately 1200 earthquakes were generated in each synthetic earthquake catalogue (500 in NTZ, 300 in NFZ, and 100 in each of TSMZ1 – TSMZ4).

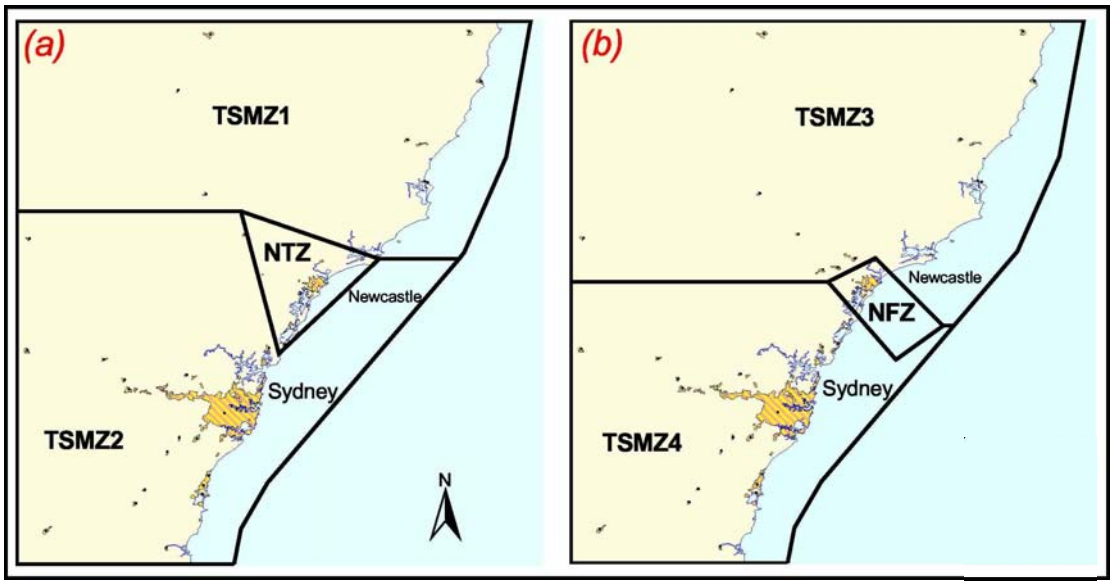

Figure 10 Two configurations of Earthquake Source Zones. Each configuration is believed to generate events with moment magnitude: (a) less than 5.4, and (b) between 5.41 and 6.5 (Dhu et al., 2002)

The Perth region has also been investigated in this study. The 5 primary source zones in the Perth area have been further divided into 7 separate zones for computational reasons. Unlike Newcastle, the highest seismic source zones are not directly underneath the metropolitan region, but rather are situated at some distance (approximately 150km). Hence, the drivers for risk are a combination of background seismicity and the high seismic zone some distance away.

Figure 11 illustrates the seismic source zones in Perth. The regions of highest seismicity are the SW seismic zone (SWSZ) and the SW seismic zone extension (Zone 2).

As the region of highest seismicity for Perth is located at a distance from the city itself, the Perth region is particularly useful in determining both the influence of distant seismicity on risk estimates, and how risk estimates are sensitive to background seismicity.

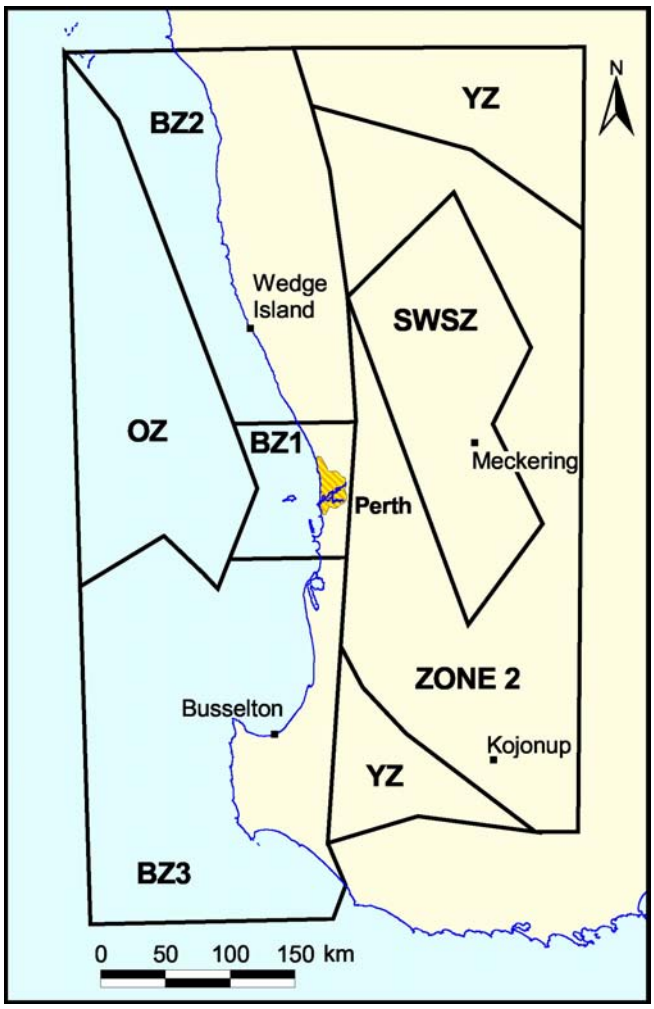

Figure 11 Perth Earthquake Source Zone configuration.

2.4 METHODOLOGY

The analyses herein involved running both the hazard and event versions of EQRM for a variety of test cases and comparing the results. Multiple simulations were performed for each test case and the results were aggregated to present risk in the Newcastle and Perth areas. Figures have been used to provide insight into the way PSRA is sensitive to changes in key parameters.

The PSRA has been conducted for residential structures only. Residential building databases for both Perth and Newcastle were sub-sampled to approximately 800 residential buildings. This was done in order to reduce the computational time and memory requirements. Sub-sampling involved the generation of 10 random spatial distributions of the buildings in each database followed by a visual inspection to select the most even distribution of buildings over the two study regions. It is important to note that the Perth building database was under development at the time this project was undertaken.

The sensitivity to several parameters was investigated. These parameters include:

- RSA periods – 10, 20, 30, 40, 50, 60, 70 and 80 fundamental periods;
- Return periods – 14, 56 and 123 return periods, where the number of return periods represents the number of points onto which the PML is interpolated. Typically these are logarithmically spaced across the range of the PML;
- Uncertainty associated with sampling the probability density function of the attenuation model – spawning, random sampling, mean, ± 1 standard deviation;
- Number of samples of the attenuation model PDF included during spawning – 3, 5, 7, and 9 samples;

- Attenuation models – three attenuation models have been considered. They are Toro *et al*. (1997), Atkinson and Boore (1997), Somerville *et al*., (2001). The Toro *et al.* (1997) model has been used as the default model unless otherwise stated;
- Capacity curve uncertainty (included and excluded);
- Amplification and amplification uncertainty (included and excluded); and
- Number of events in synthetic earthquake catalogue – 600, 1200 (default number) and 2400 earthquakes.

A number of assumptions have been made in this analysis. Specifically this study has incorporated a number of pre-existing models, the accuracy and appropriateness of which has been assumed. In particular, we assume accuracy of the engineer defined capacity/fragility curves as well as the suitability of the capacity spectrum method to modelling damage (Edwards *et* al., 2004; FEMA, 1999; Kircher *et al*., 1997a; Kircher *et al*., 1997b).

2.4.1 Data Presentation - PML Curve

Risk is represented by probable maximum loss (PML) curves which describe the probability of the study area exceeding a certain level of loss in a single year. The PML curve enables a graphical display of risk in terms of financial loss expressed as a percentage of the total value of the sub-sampled buildings and their contents in the study region. Figure 12 shows an example of PML curves for the hazard-based method using for the Newcastle region.

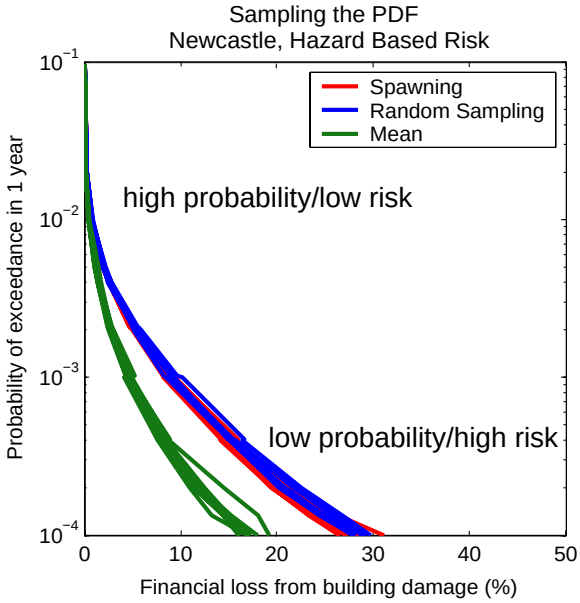

Figure 12 PML curve for the Newcastle Area. Financial loss is expressed as a percentage of the total value of the sub-sampled residential buildings and their contents in the Newcastle region.

The upper region of the curve represents events which have a relatively high probability of occurrence but low risk. The lower part of the curve represents those events with relatively low probability of occurrence and high associated risk. It is also important to note that each line represents the risk associated with a different synthetic catalogue of earthquakes.

In Chapter 3, two adjacent graphs have been presented for each series of simulations to show separate results for the hazard- (left) and event-based (right) approaches, unless otherwise specified. In such cases, results for both methods have been plotted together to facilitate direct comparison.

3 Results

3.1 SAMPLING THE PDF AND EVENT VS HAZARD

Figures 13 to 17 illustrate that hazard-based method produces smoother curves and estimates consistently higher loss than the event-based method across all three sampling techniques. Mean PML curves show consistently lower risk than those using either random sampling or spawning, regardless of whether other uncertainties are included or excluded. Furthermore, when the event-based approach is coupled with random sampling, estimates of loss are greatly reduced compared to those generated using either spawning or the hazard-based approach (Figure 13 and Figure 14). This is consistent in all results for Newcastle and Perth.

Both Newcastle and Perth display the same relative ranking of risk across the three sampling techniques and PML curves for each sampling technique display a comparable spread in results. Sampling only the mean of the RSA PDF consistently produces lower estimates of risk in both Newcastle and Perth (Figure 13 and Figure 14). Figure 13 indicates that random sampling produces marginally higher estimates of risk for high probability/low risk events, whereas spawning estimates higher risk than random sampling for low probability/high risk events in Newcastle, particularly when combined with the event-based approach. It should be noted that for ease of comparison with the corresponding results for Perth, these results have been calculated with amplification switched off. Amplification factors were not available for Perth at the time this work was undertaken.

The preliminary risk results contained herein for Perth are consistently higher than those for Newcastle. Figure 15 to Figure 17 show a comparison of results using spawning, random sampling and mean sampling techniques for both Perth and Newcastle and show that Perth (blue curves) produces consistently higher estimates of loss with a greater spread of results for both hazard-based and event-based methods than Newcastle (red curves).

NEWCASTLE

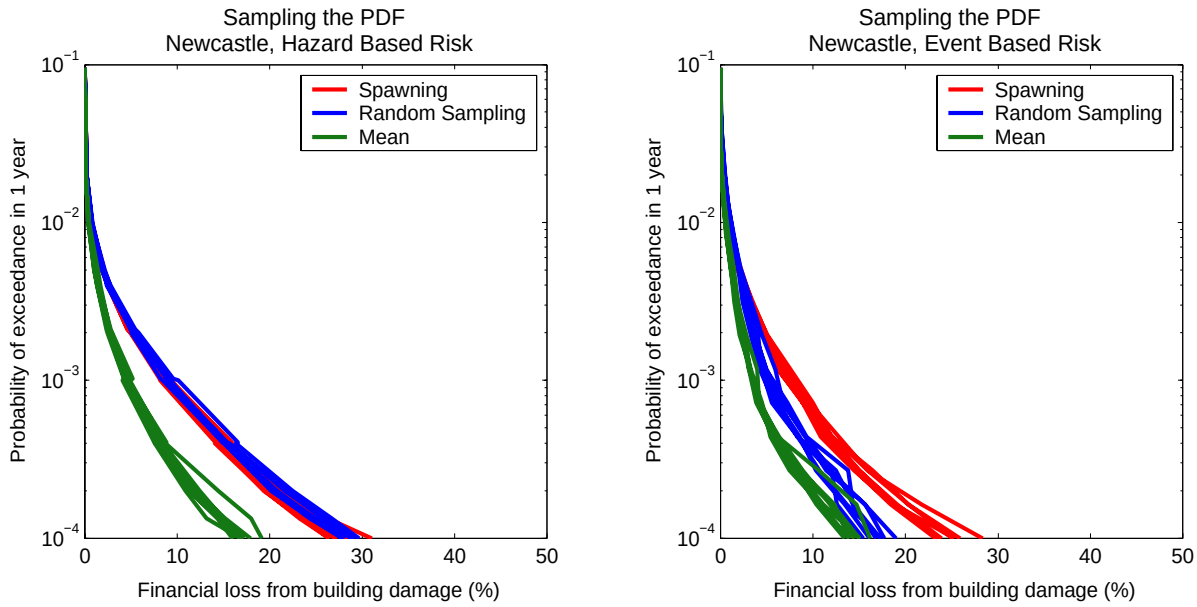

Figure 13 Effect of different sampling techniques on hazard- and event-based risk estimates in Newcastle.

PERTH

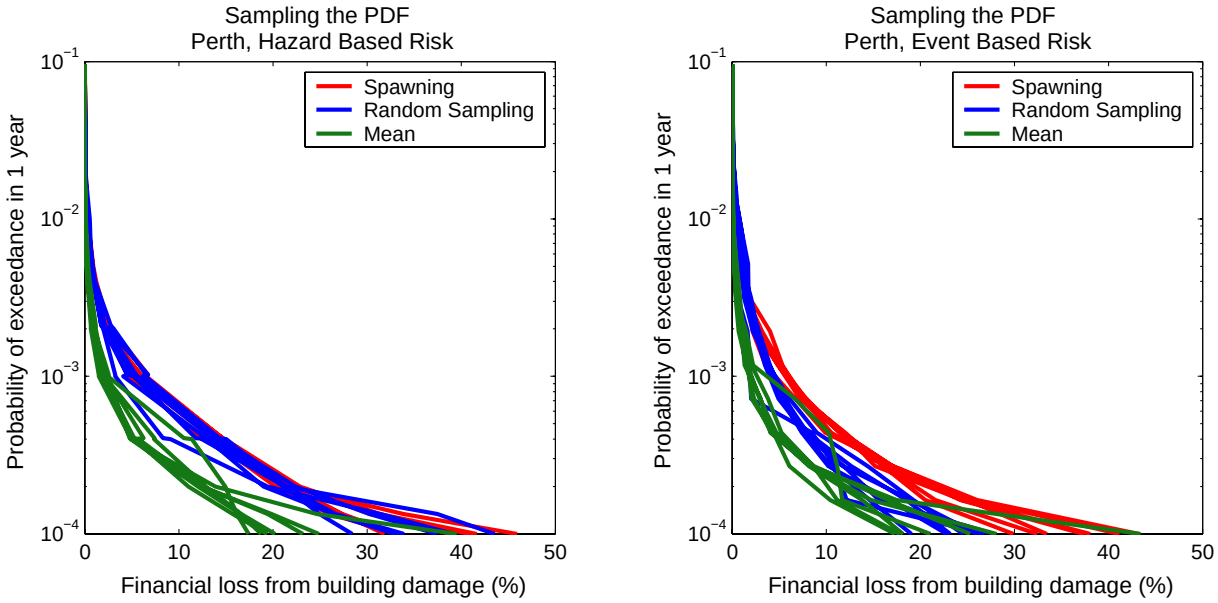

Figure 14 Effect of different sampling techniques on hazard- and event-based risk estimates in Perth.

PERTH VS NEWCASTLE - Spawning

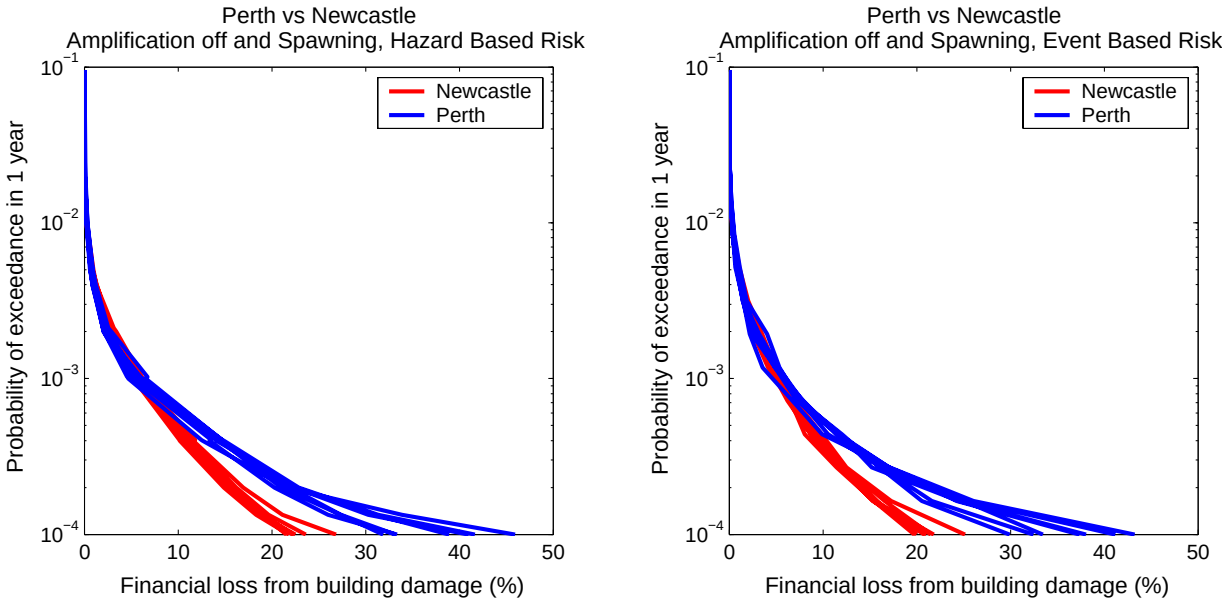

Figure 15 Comparison of results using spawning to estimate loss in Perth and Newcastle.

PERTH VS NEWCASTLE - Random Sampling

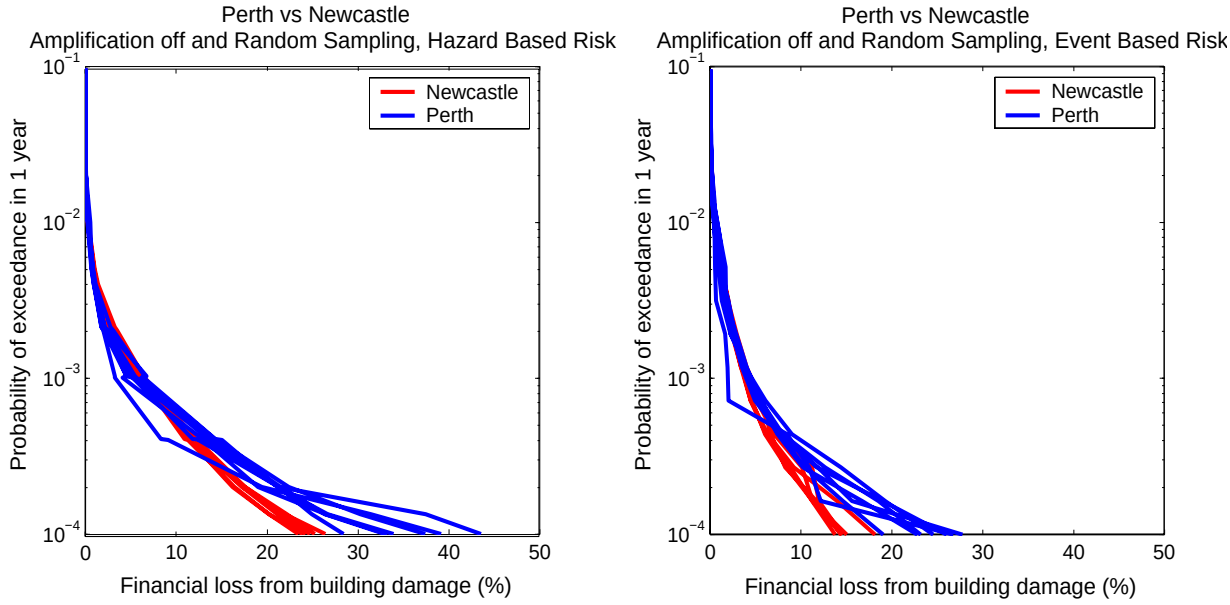

Figure 16 Comparison of results using random sampling to estimate loss in Perth and Newcastle.

PERTH VS NEWCASTLE - Mean

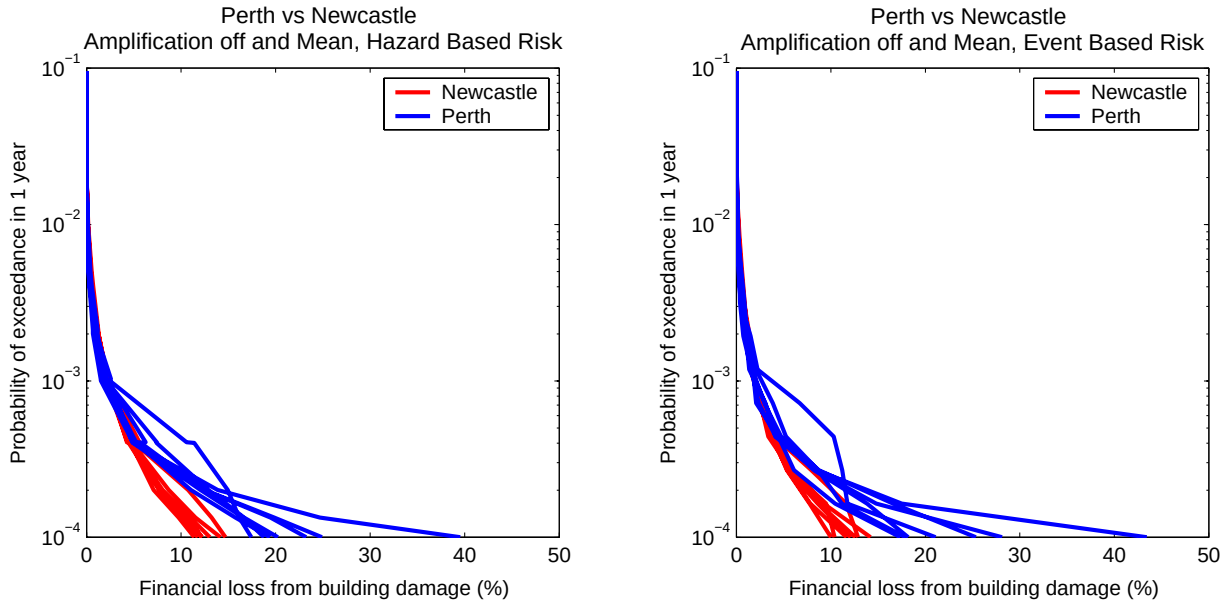

Figure 17 Comparison of results using mean to estimate loss in Perth and Newcastle.

3.2 NUMBER OF SAMPLES

Figure 18 demonstrates that simulations using 3, 5, 7, and 9 spawned samples with the RSA PDF show very little difference in loss and each display a reasonably consistent spread of results.

NEWCASTLE – Spawning

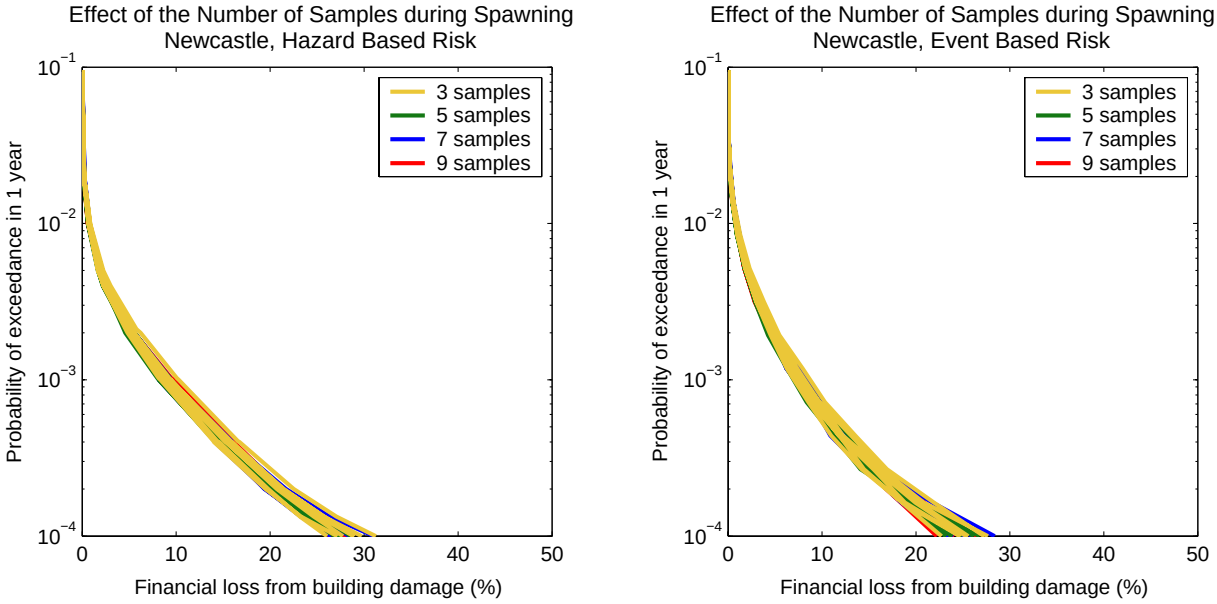

Figure 18 PML curves for different sample numbers with spawning.

3.3 VARYING THE NUMBER OF RSA PERIODS AND RETURN PERIODS

There does not appear to be any systematic trend in estimated losses when the number of RSA points is increased from 10 to 80 (Figure 19). Similarly, there is no apparent trend when the number of return periods is increased from 14 to 123 (Figure 20 and Figure 21).

NEWCASTLE - Random Sampling

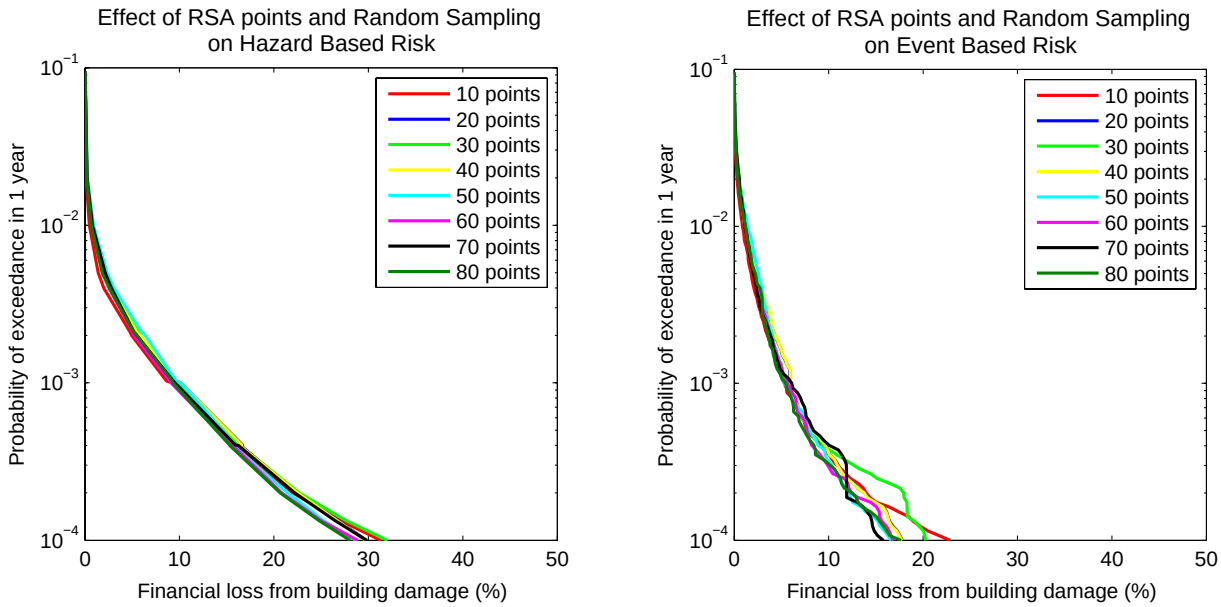

Figure 19 Comparison of different numbers of fundamental periods (T_o) when computing RSA.

NEWCASTLE - Spawning vs Random Sampling

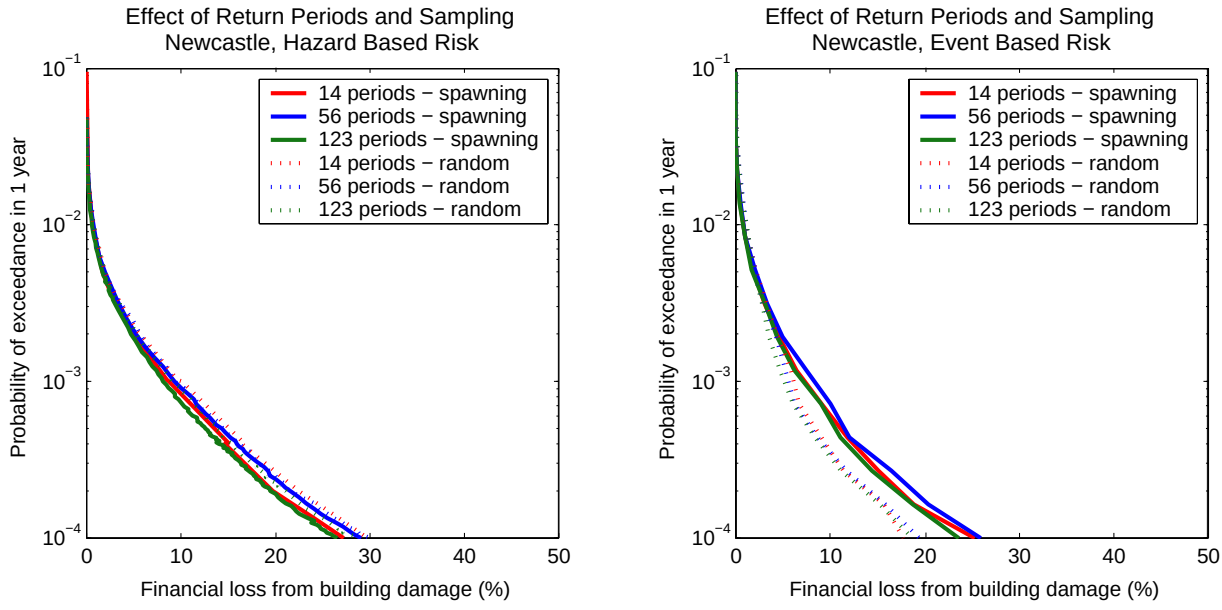

Figure 20 PML curves for 14, 56 and 123 return periods with random sampling and spawning.

NEWCASTLE - Event vs Hazard

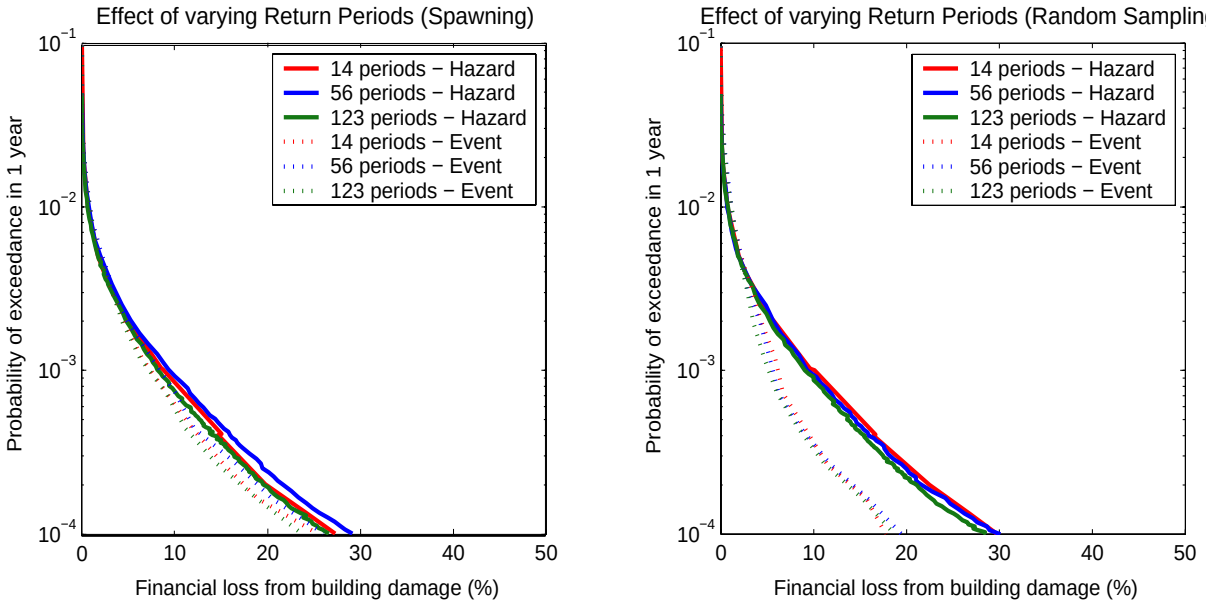

Figure 21 Comparison of different numbers of return periods for the event- and hazard-based methods.

3.4 UNDERSTANDING THE PML DISTRIBUTION - NEWCASTLE

Figures 22 to 24 were created with a greater number of synthetic catalogues to provide an indication of the distribution of resulting PML curves. In each case the amplification uncertainty and capacity curve uncertainty have been turned off. The dashed line in each of these figures represents lines of equal probability, across which the histograms of Figures 25 to 27 were created. Whilst it is far from conclusive, Figure 25 suggests that when random sampling is used with the attenuation model the distribution of loss may follow a normal distribution for low return periods (200 and 475 years) and a log-normal distribution for the higher return periods. Such a conclusion is only speculative at this stage and further investigation will be required to confirm the exact nature of the distribution. Figures 26 and 27 are less suggestive for the spawning and mean cases respectively. As with random sampling, further work is required to understand the distribution of the PML curves.

Random Sampling

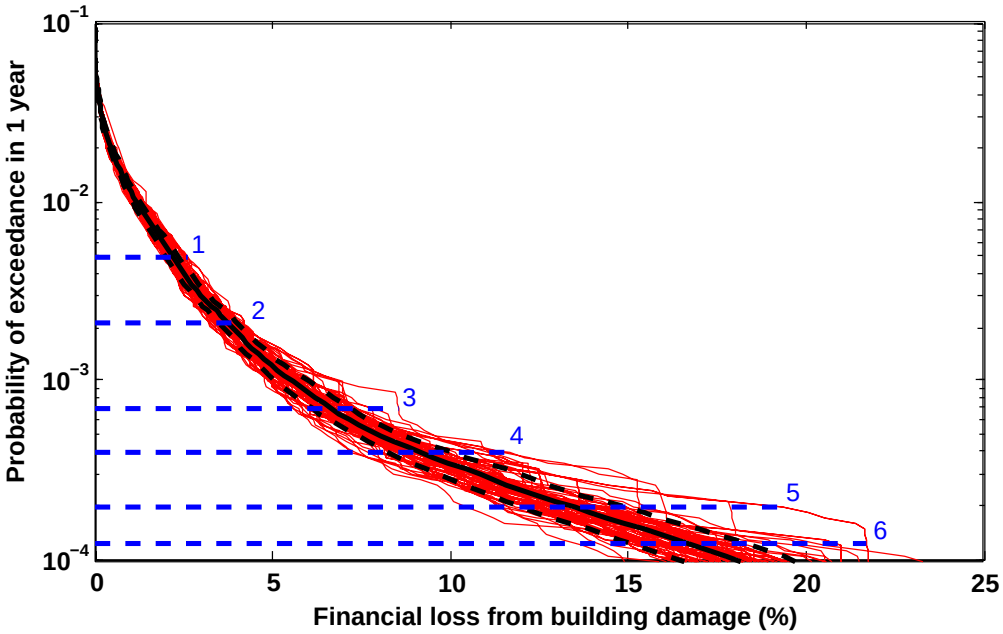

Figure 22 Eighty PML curves (red) created with amplification factor and building uncertainty ignored and attenuation uncertainty considered via random sampling. The mean, taken across lines of constant probability is shown with a black solid line, and +/- σ with black dashed lines. Blue dashed lines 1 to 6 indicate the probability of exceedence corresponding to return periods of (1) 200, (2) 475, (3) 1400, (4) 2475, (5) 5000, and (6) 8000 years, respectively.

Spawning

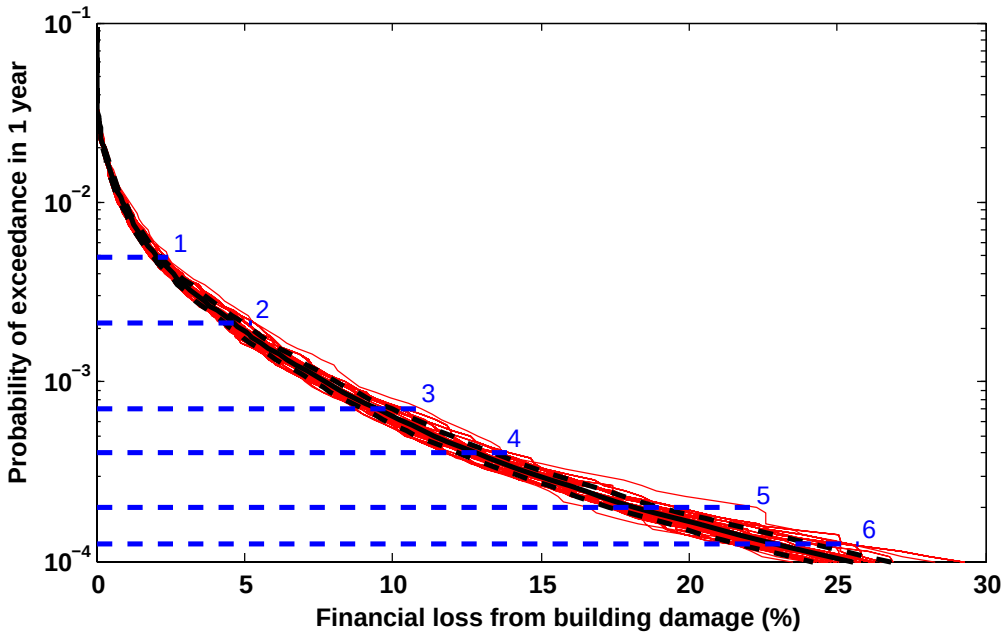

Figure 23 Eighty PML curves (red) created with amplification factor and building uncertainty ignored and spawned attenuation. The mean, taken across lines of constant probability is shown with a black solid line, and +/- σ with black dashed lines. Blue dashed lines 1 to 6 indicate the probability of exceedence corresponding to return periods of (1) 200, (2) 475, (3) 1400, (4) 2475, (5) 5000, and (6) 8000 years, respectively.

Mean

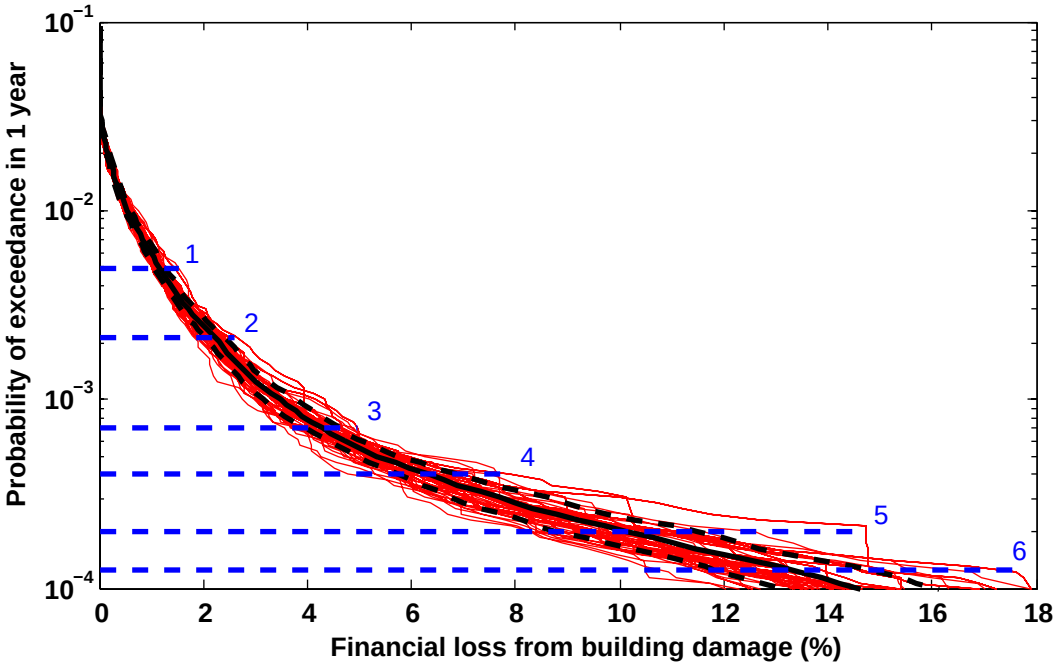

Figure 24 Eighty PML curves (red) created with amplification factor and building uncertainty ignored and only mean attenuation. The mean, taken across lines of constant probability is shown with a black solid line, and +/- σ with black dashed lines. Blue dashed lines 1 to 6 indicate the probability of exceedence corresponding to return periods of (1) 200, (2) 475, (3) 1400, (4) 2475, (5) 5000, and (6) 8000 years, respectively.

Random Sampling

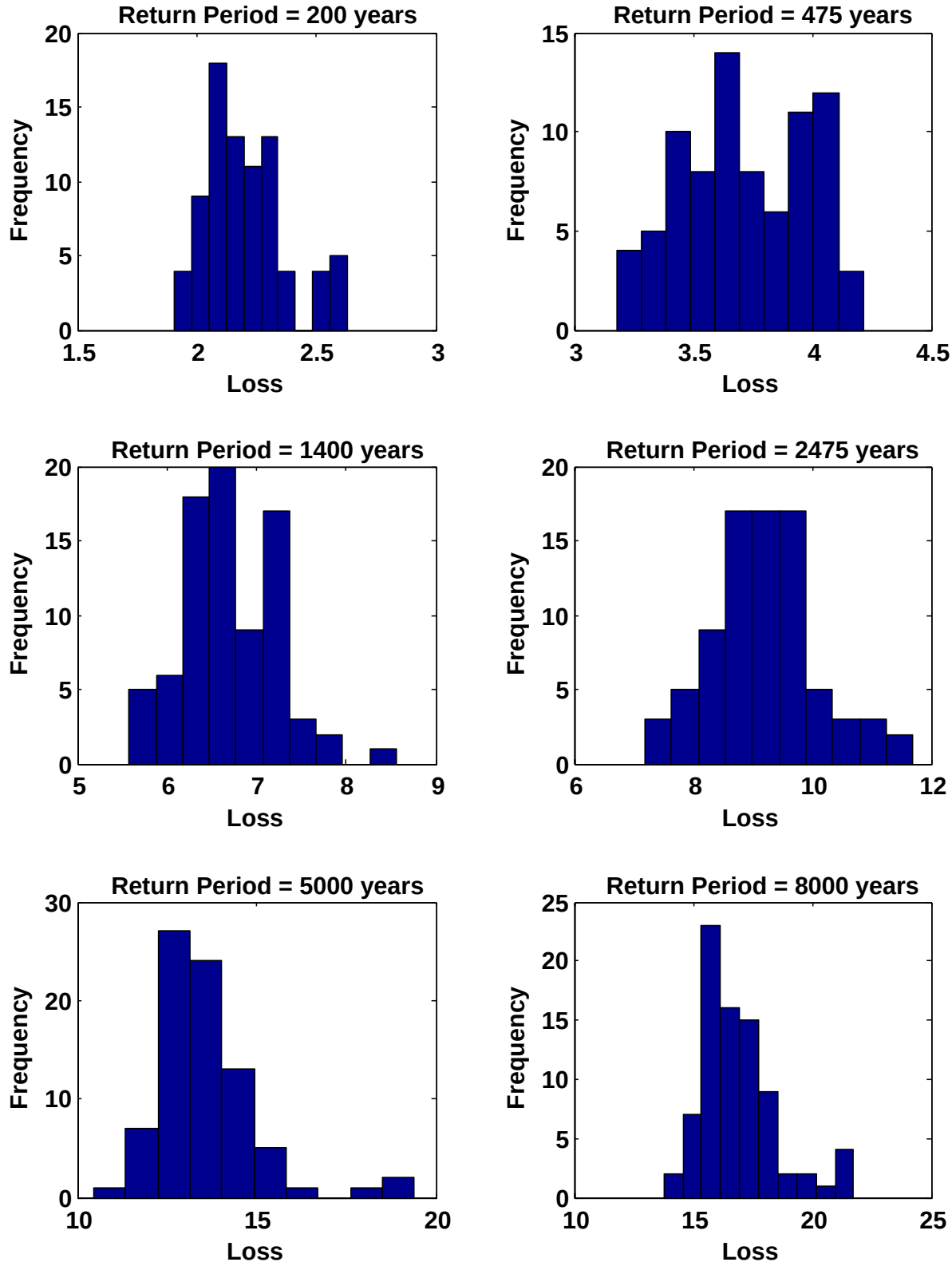

Figure 25 Histograms of total loss estimates for six return periods when amplification factor and building uncertainty are ignored and attenuation uncertainty considered via random sampling. Locations of the six return periods on the respective PML curves are illustrated in Figure 22.

Spawning

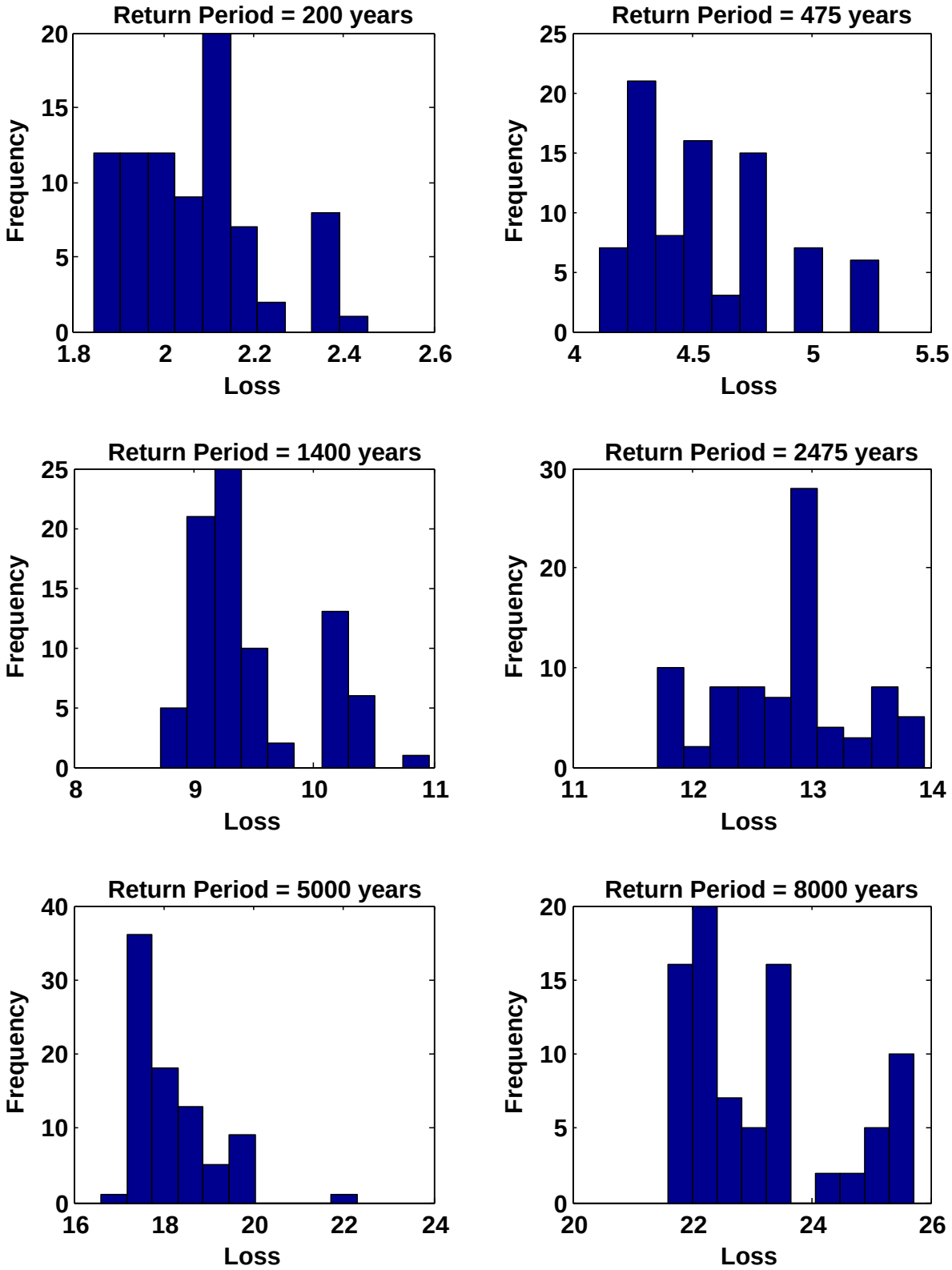

*Figure 26 Histograms of total loss estimates for six return periods when amplification factor and building uncertainty are ignored and attenuation uncertainty considered via spawning. Locations of the six return periods on the respective PML curves are illustrated in Figure **23**.*

Mean

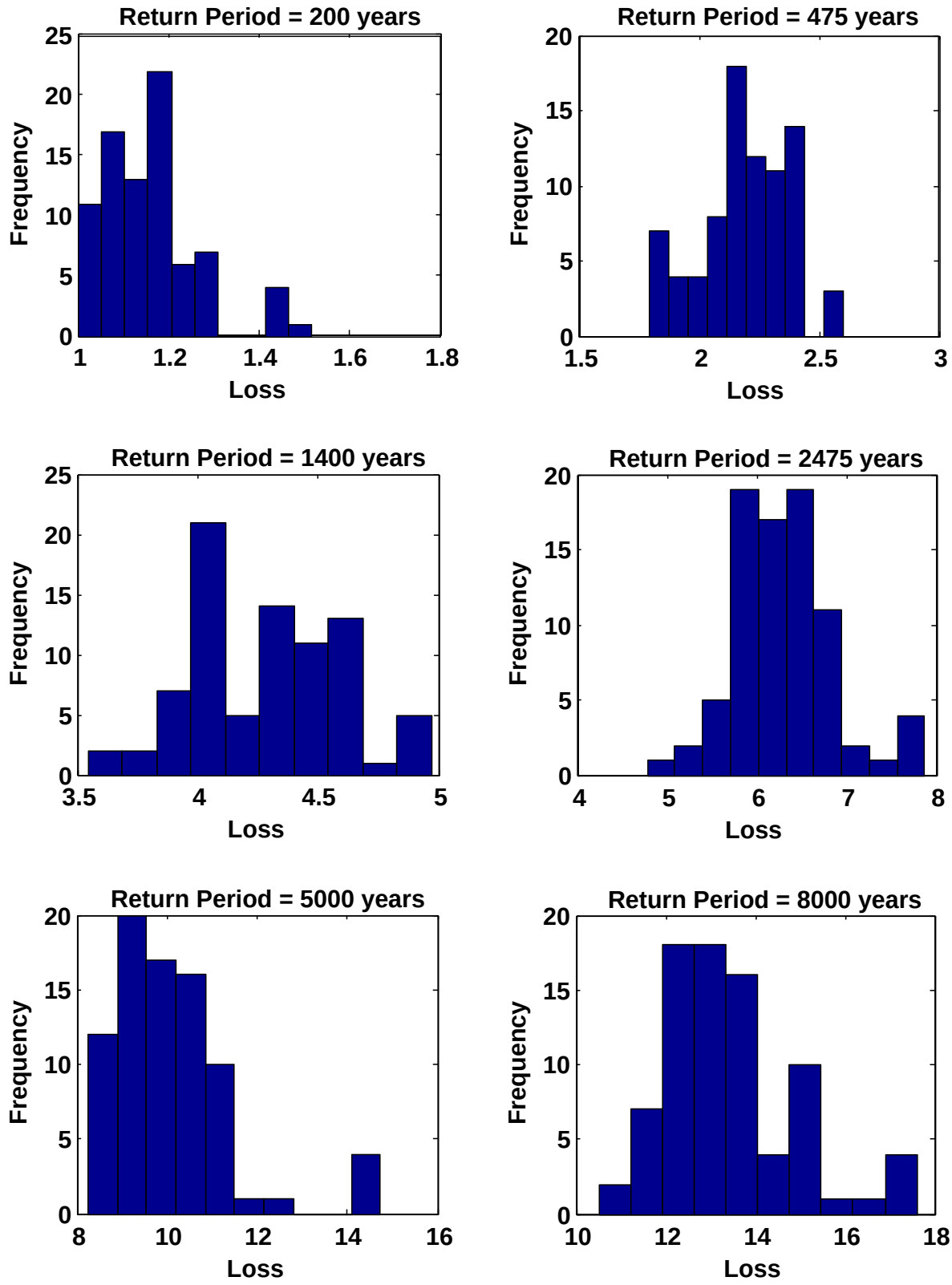

Figure 27 Histograms of total loss estimates for six return periods when amplification factor and building uncertainty are ignored and attenuation uncertainty considered via random sampling. Locations of the six return periods on the respective PML curves are illustrated in Figure 24.

3.5 COMPARISON OF ATTENUATION MODELS

Of all the uncertainties considered in this study, the attenuation model exerted the greatest influence on final estimates of risk. In general, the Atkinson and Boore (1997) and Somerville *et al.* (2001) attenuation models generate relatively comparable results regardless of the sampling technique employed. Furthermore, the hazard-based method shows marginally higher loss across all three attenuation models than the event-based method. This is consistent in both Newcastle (Figure 28 and Figure 29) and Perth (Figure 31 and Figure 32).

For low probability/high risk events, Perth shows greater estimated losses than Newcastle using all three attenuation models. For high probability/low risk events, however, Newcastle shows greater losses than Perth using the Somerville *et al.* (2001) and Toro et al. (1997), yet marginally lower losses using the Atkinson and Boore (1997) attenuation model.

Although the actual results for Perth and Newcastle differ, the two regions illustrate similar trends in the relative level of loss estimated by each attenuation model at high and low probabilities (Figure 37 and Figure 38). At high risk/low probability, the Toro *et al.* (1997) attenuation model estimates greater loss than the Somerville *et al.* (2001) model which, in turn generated greater loss than the Atkinson and Boore (1997) attenuation model for both the event- and hazard-based methods and for both study regions (Figure 28 and Figure 29). At low risk/high probability the Somerville *et al.* (2001) and Atkinson and Boore (1997) attenuation models estimated comparable levels of loss, while Toro *et al.* (1997) continues to generate much greater losses.

Figure 30 shows the percentage distribution towards annualised loss attributed to events of a particular moment magnitude and distance from buildings in Newcastle for each attenuation model. Two graphs for each attenuation model have been generated from different earthquake catalogues (e.g. Figure 30a shows Toro et al., 1997). Differences between pairs using the same attenuation model demonstrate uncertainty associated with the synthetic earthquake catalogue. Compared with Toro et al. (1997) and Atkinson and Boore (1997), Somerville et al. (2001) is shown to attribute a higher contribution towards annualised loss from high magnitude events at short distances.

Whilst the relative ranking of risk remains consistent across spawned and randomly sampled attenuation using the hazard-based method (i.e. Atkinson>Toro>Somerville for high probability low risk events and Toro>Somerville≥Atkinson for low probability high risk events), risk estimates are greatly reduced when the event-based method is combined with random sampling (Figure 31 and Figure 32).

NEWCASTLE - Spawning

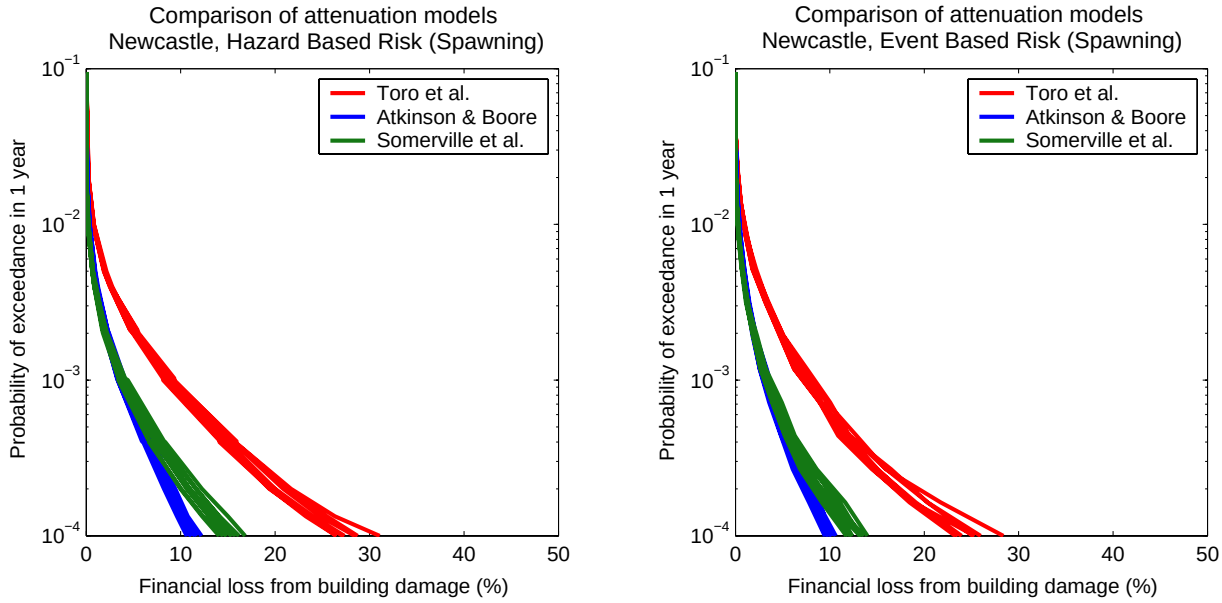

Figure 28 PML curves for Toro et al. (1997), Atkinson and Boore (1997) and Somerville et al. (2001) attenuation models using spawning.

NEWCASTLE - Random Sampling

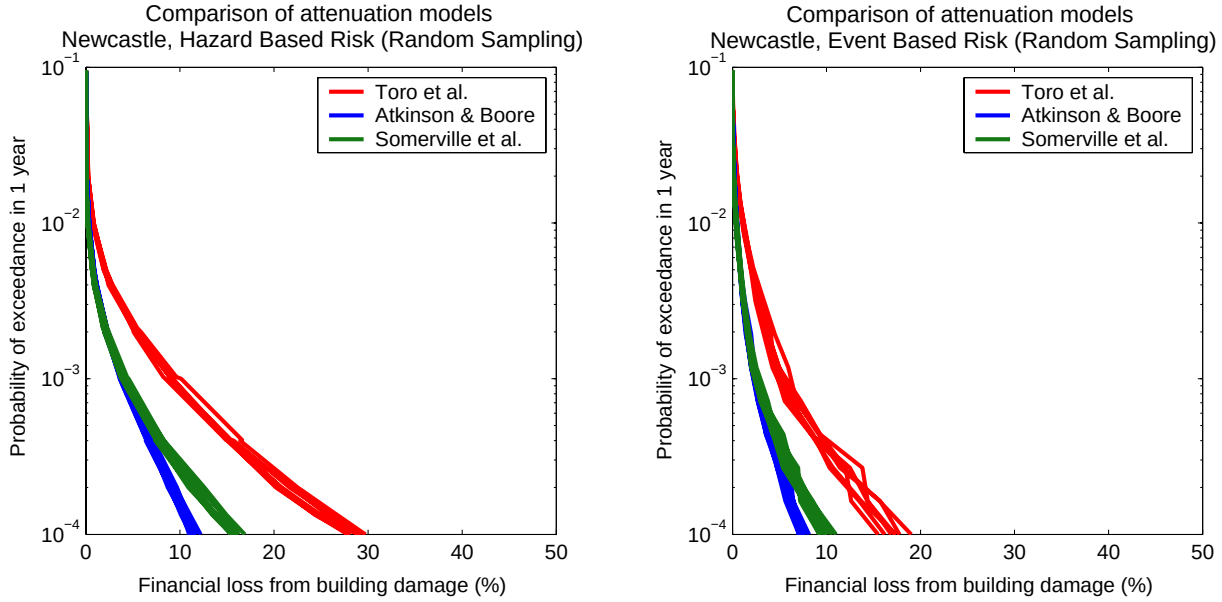

Figure 29 PML curves for Toro et al. (1997), Atkinson and Boore (1997) and Somerville et al. (2001) attenuation models using random sampling for Newcastle.

DISAGGREGATED RESULTS FOR NEWCASTLE - Spawning

(a) Toro et al. (1997)

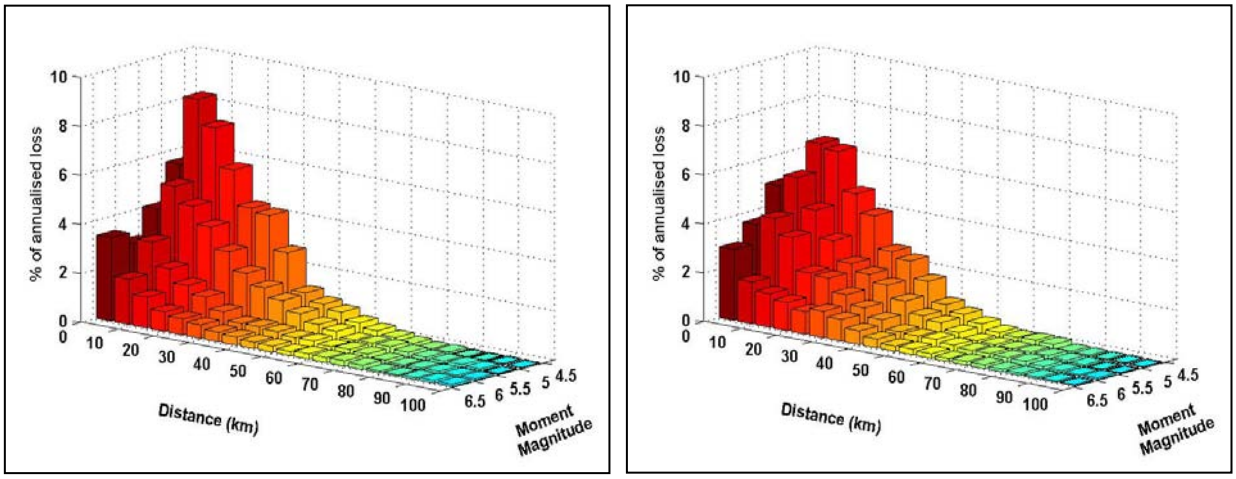

(b) Somerville et al. (2001)

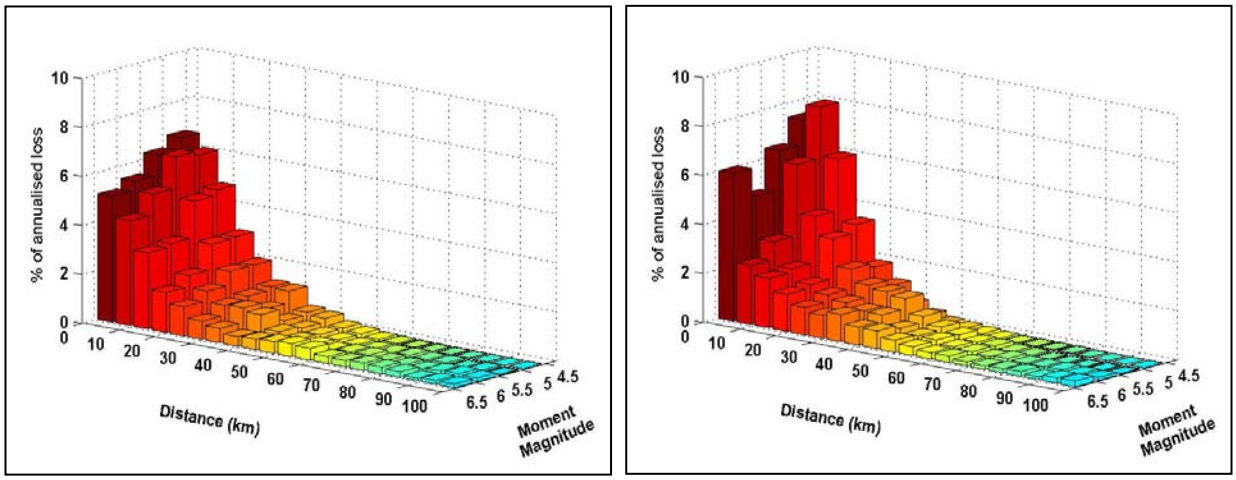

(c) Atkinson and Boore (1997)

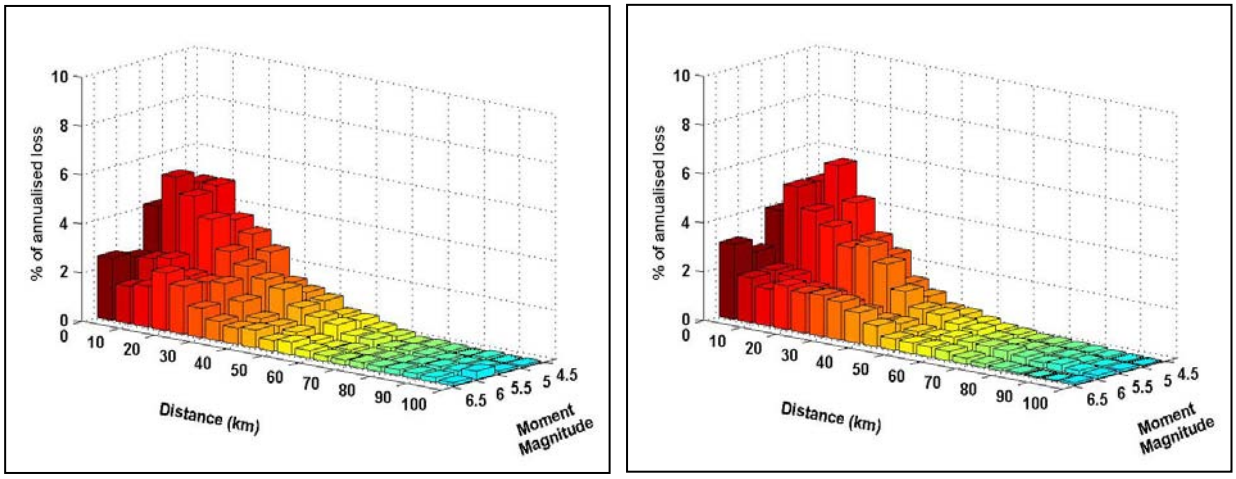

Figure 30 Disaggregated annualised loss estimates using spawning in Newcastle (a) Toro et al. (1997), (b) Somerville et al. (2001), and (c) Atkinson and Boore (1997). These plots partition the synthetic earthquake catalogue/building combination into magnitude and distance bins. Each partition illustrates the % of annualised loss attributed to the bin. Two graphs for each attenuation model have been generated from different earthquake catalogues. Differences between graphs using the same attenuation model demonstrate uncertainty associated solely with the synthetic earthquake catalogue.

PERTH - Spawning

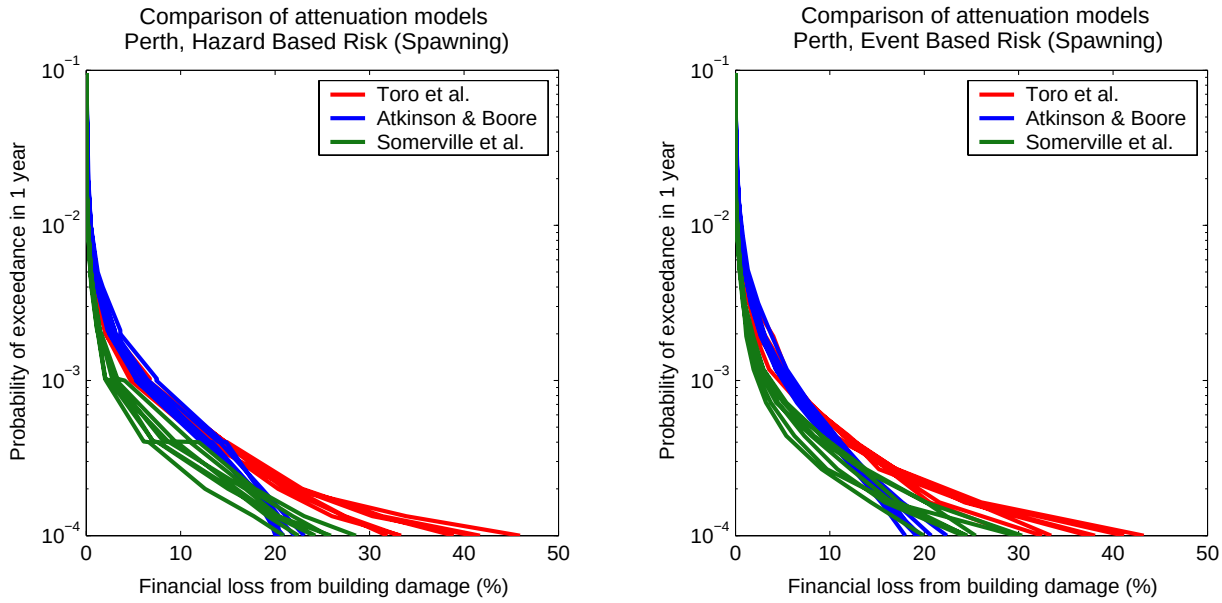

Figure 31 PML curves for Toro et al. (1997), Atkinson and Boore (1997), and Somerville et al. (2001) attenuation models with spawning

PERTH - Random Sampling

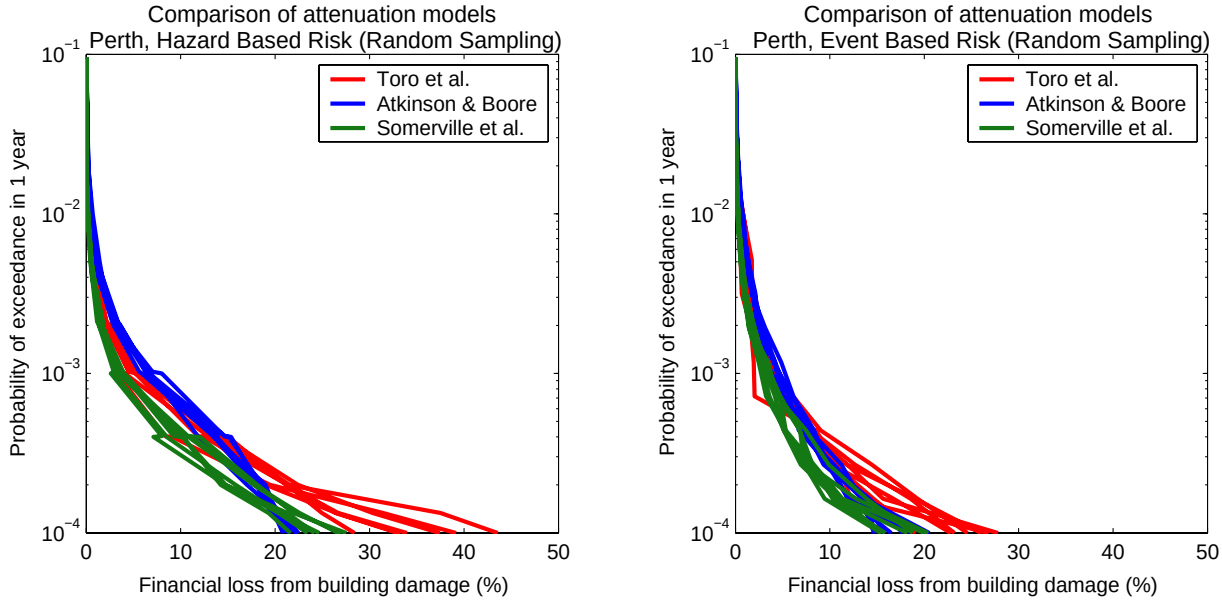

Figure 32 Comparison of the Toro et al. (1997), Atkinson and Boore (1997) and Somerville et al. (2001) attenuation models using random sampling for Perth.

Atkinson and Boore (1997) - spawning

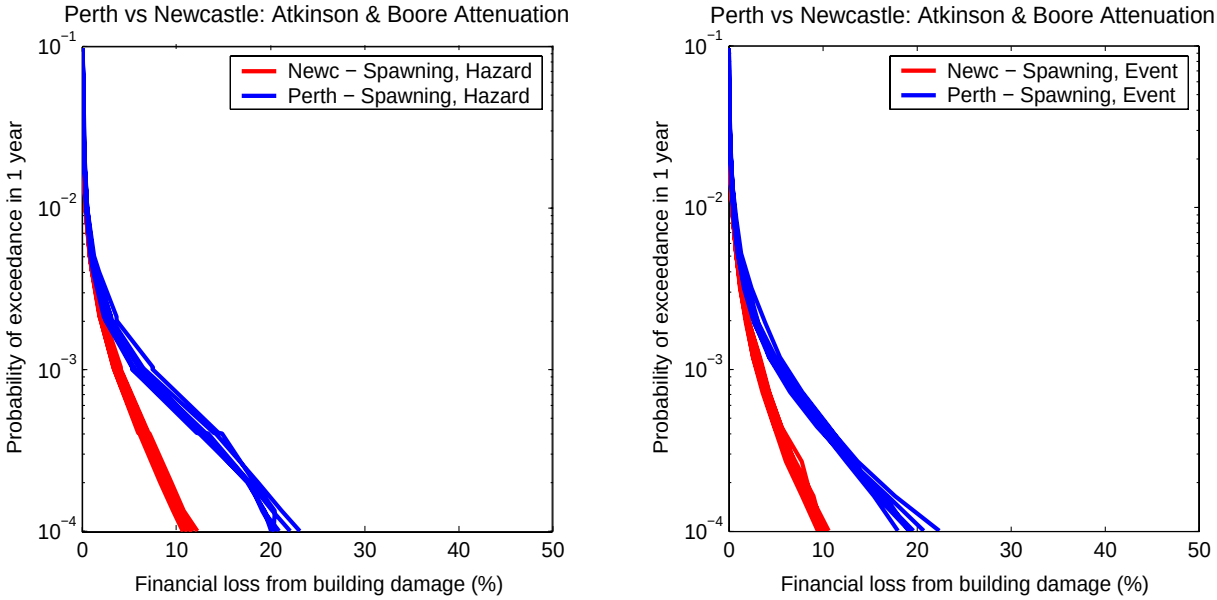

Figure 33 Effect of attenuation aleatory uncertainty by spawning for Perth and Newcastle using the Atkinson and Boore (1997) attenuation model.

Atkinson and Boore (1997) – random sampling

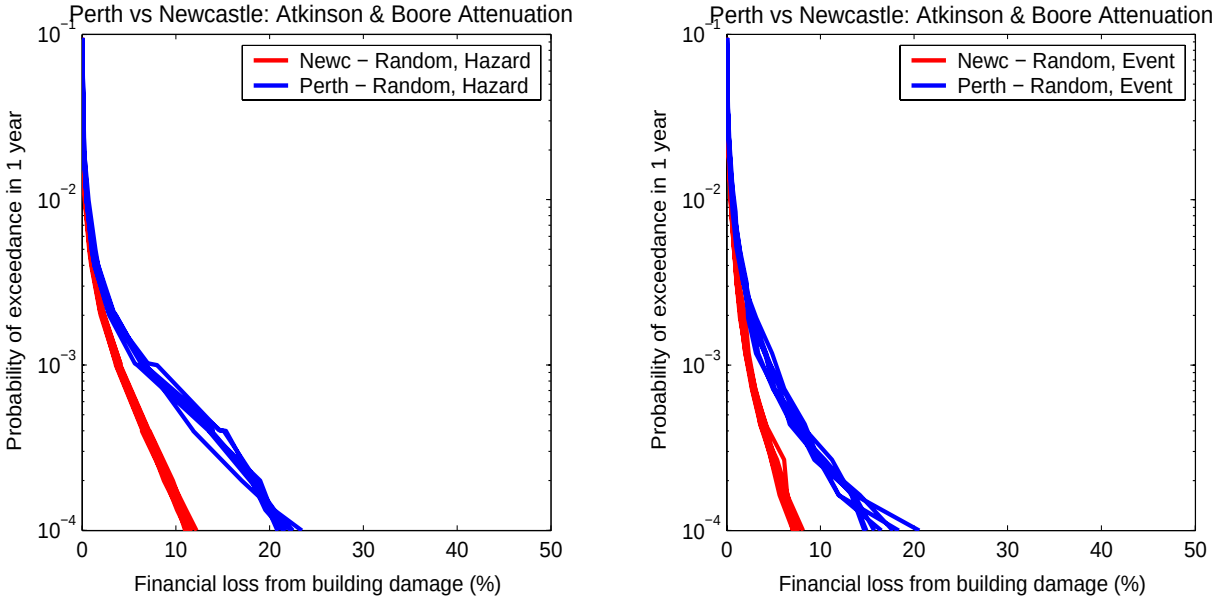

Figure 34 Effect of attenuation aleatory uncertainty by random sampling for Perth and Newcastle using the Atkinson and Boore (1997) attenuation model.

Somerville et al. (2001) - spawning

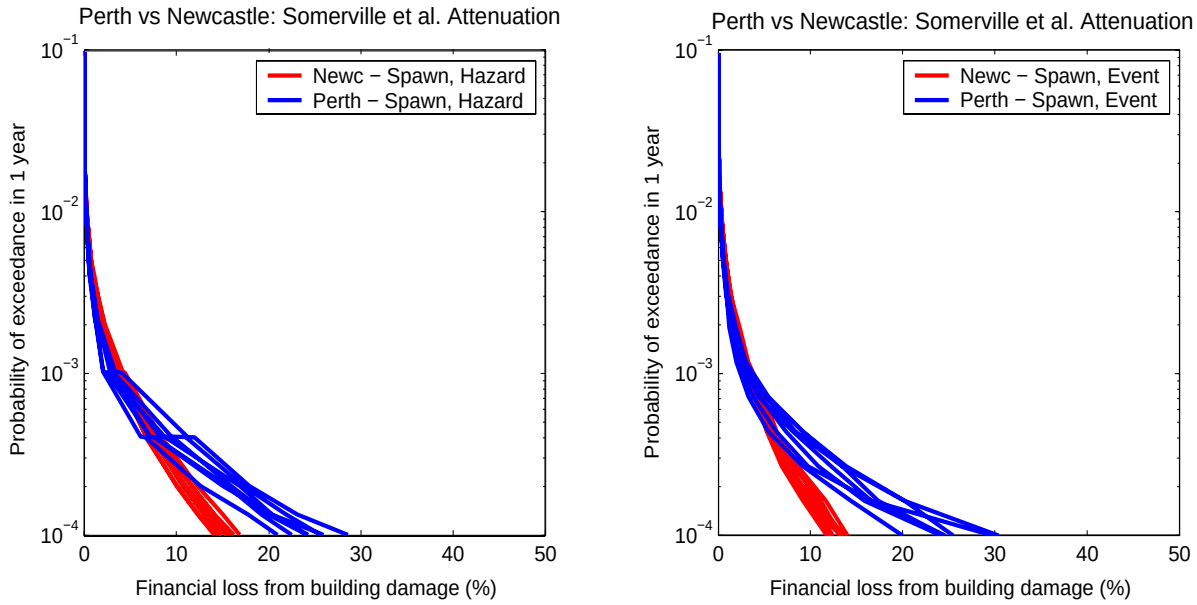

Figure 35 Effect of attenuation aleatory uncertainty by spawning for Perth and Newcastle using the Somerville et al. (2001) attenuation model.

Somerville et al. (2001) – random sampling

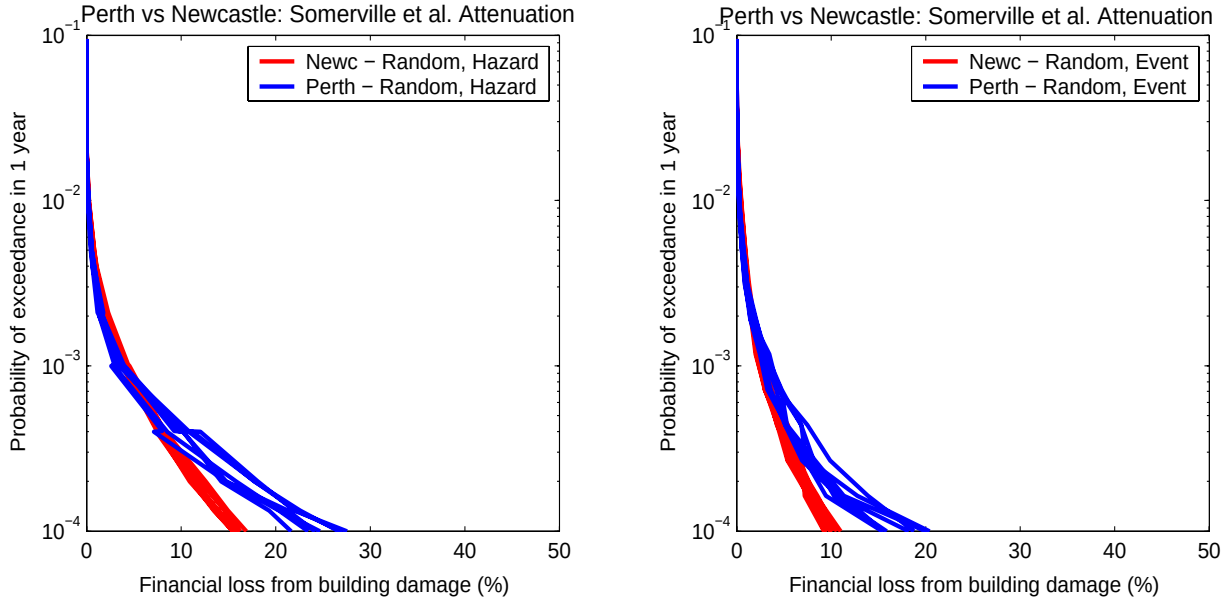

Figure 36 Effect of attenuation aleatory uncertainty by random sampling for Perth and Newcastle using the Somerville et al. (2001) attenuation model.

Toro et al. (1997) - spawning

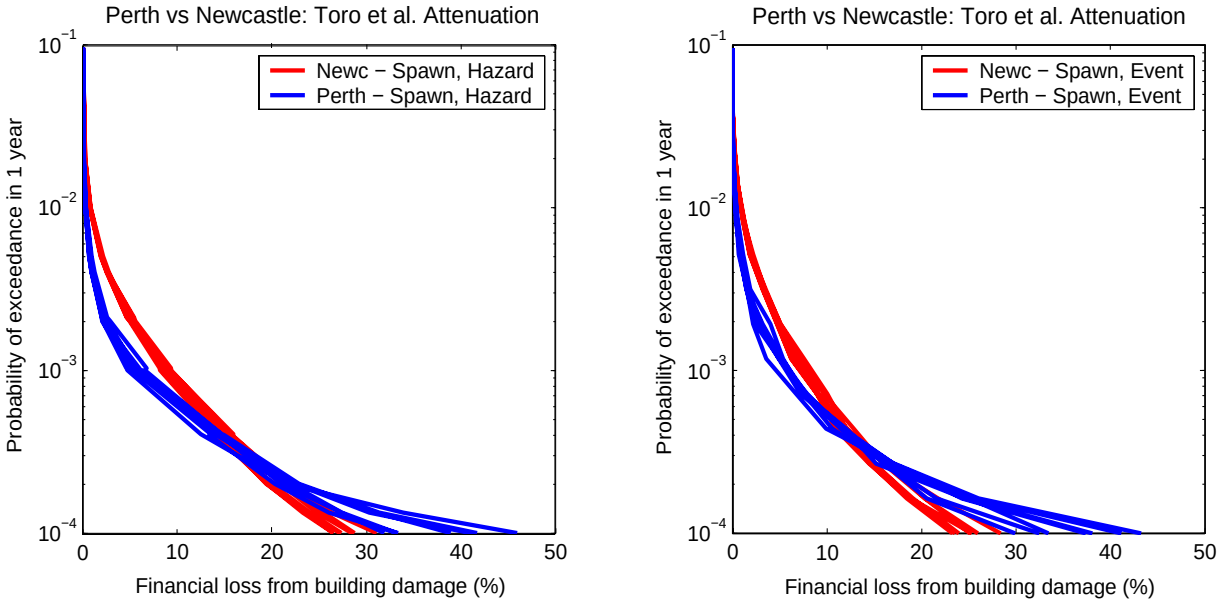

Figure 37 Effect of attenuation aleatory uncertainty by spawning for Perth and Newcastle using the Toro et al. (1997) attenuation model.

Toro et al. (1997) – random sampling

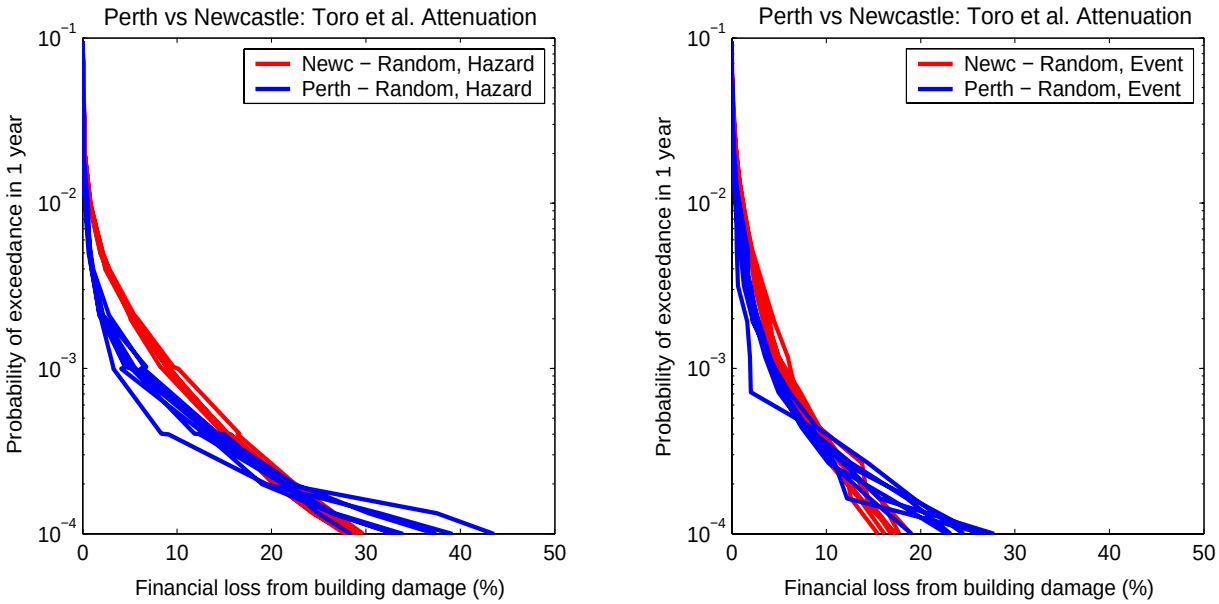

Figure 38 Effect of attenuation aleatory uncertainty by random sampling for Perth and Newcastle using the Toro et al, (1997) attenuation model.

3.6 REGOLITH AMPLIFICATION

The red PML curves of Figure 39 and Figure 40 illustrate the risk when regolith amplification is disregarded, and the blue curves show the risk when regolith amplification is included. These figures demonstrate that regolith amplification increases estimates of risk.

NEWCASTLE - Spawning

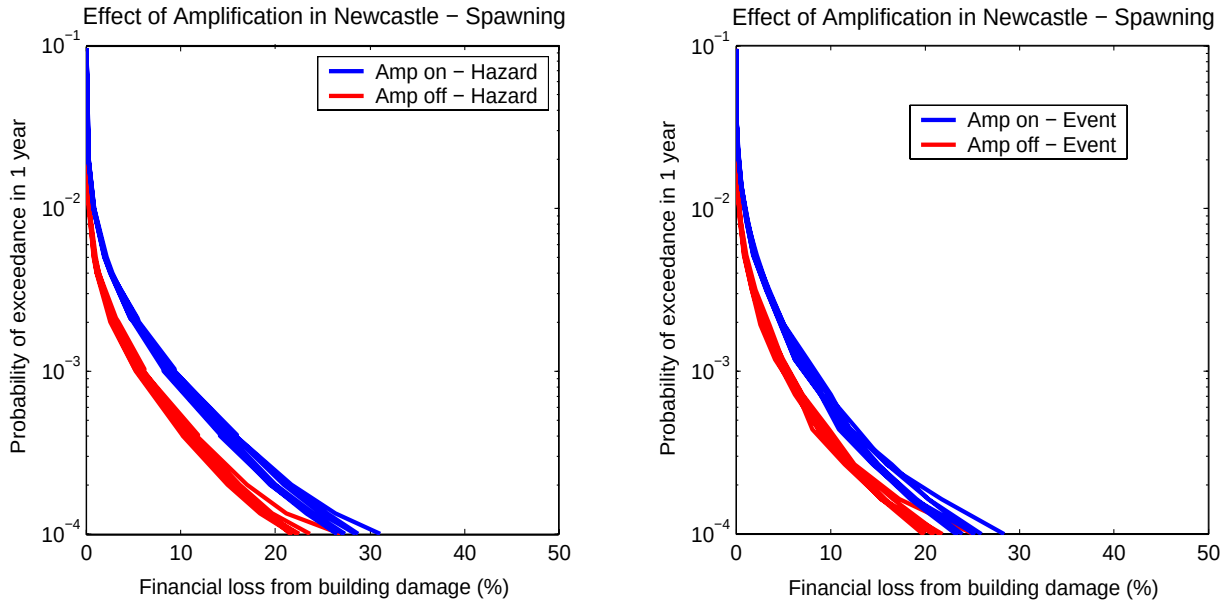

Figure 39 Effect of regolith amplification in Newcastle using spawning. The red curves show PML when the effects of amplification are excluded (i.e. bedrock), the blue curves show PML when regolith amplification is incorporated in risk analyses.

NEWCASTLE - Random Sampling

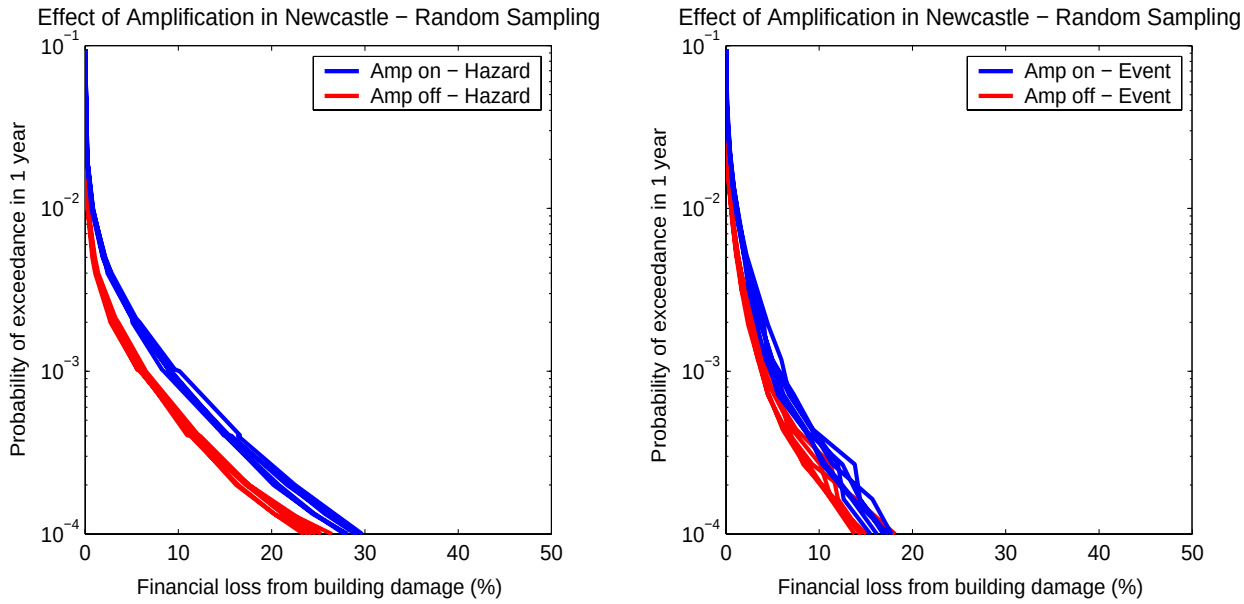

Figure 40 Effect of regolith amplification in Newcastle using random sampling.

3.7 AMPLIFICATION UNCERTAINTY

Although regolith amplification has a large impact on final risk estimates, aleatory uncertainty associated with amplification exerts only a minor effect on estimated risk which is slightly lower when amplification aleatory uncertainty is disregarded (Figure 41 and Figure 40). This is consistent for both high probability/low risk and low probability/high risk events using each of the three sampling techniques with either the event- or hazard-based approach (Figure 42 to Figure 44).

(a) NEWCASTLE - Amplification Uncertainty Included

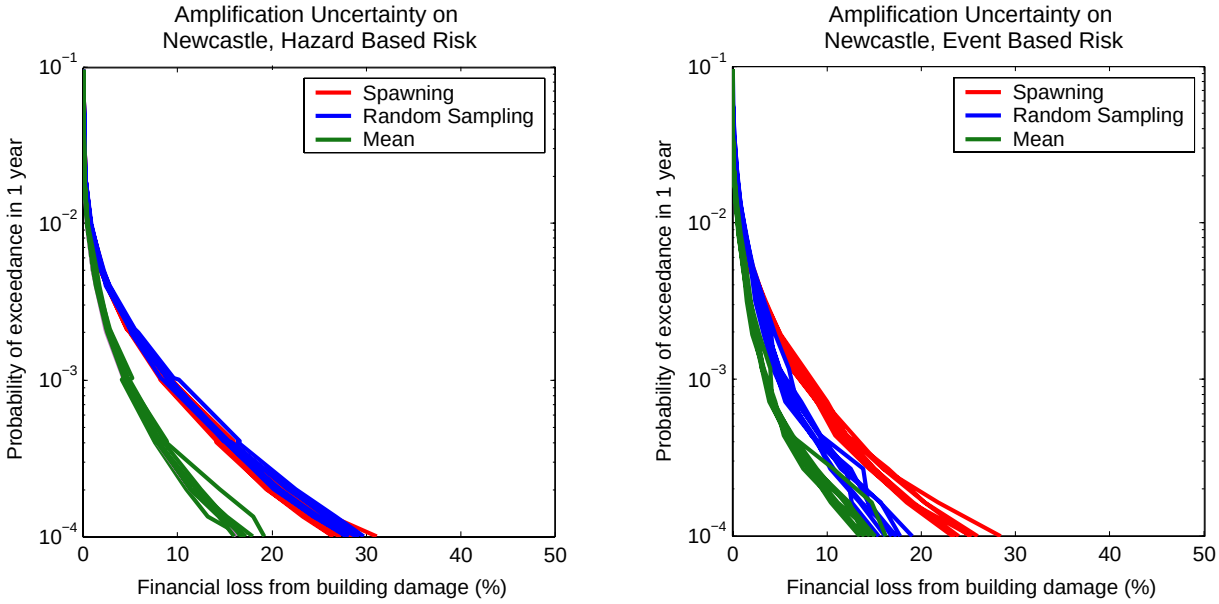

(b) NEWCASTLE - Amplification Uncertainty Excluded

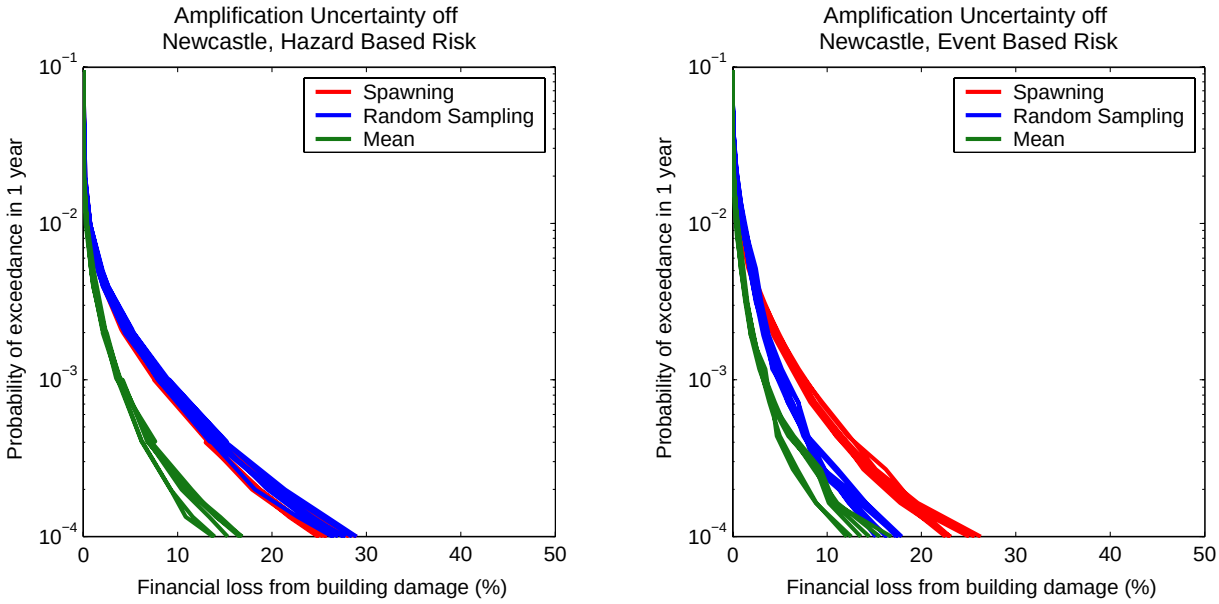

Figure 41 Effect of amplification uncertainty in Newcastle – a) amplification uncertainty is included by random sampling, and b) amplification uncertainty is excluded.

NEWCASTLE - Spawning

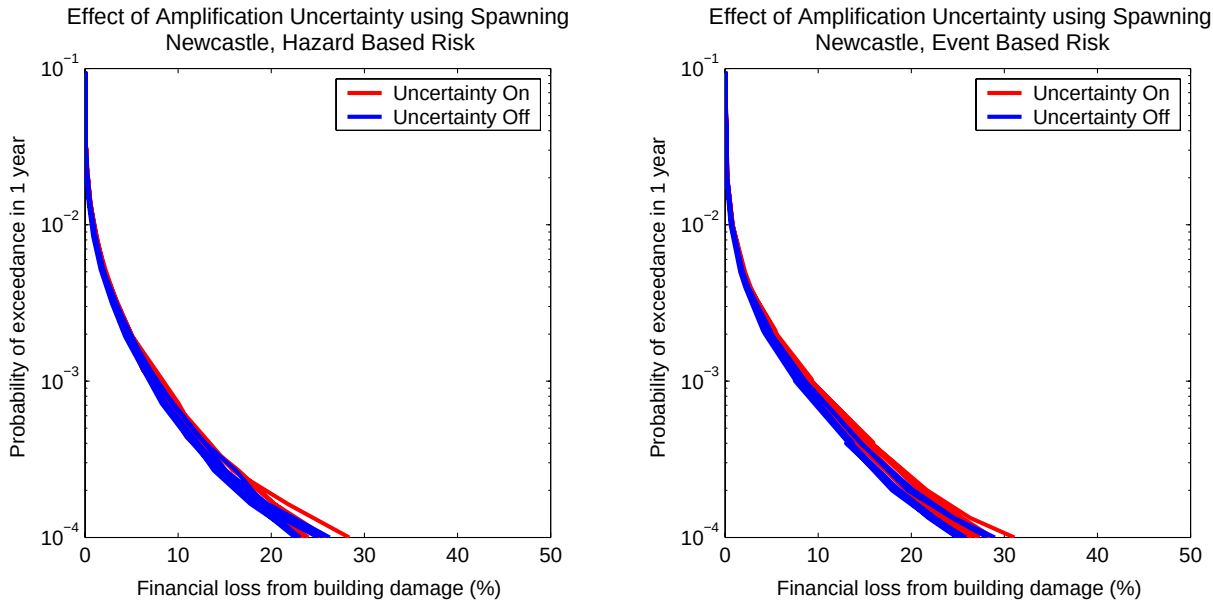

Figure 42 Comparison of the effect of amplification uncertainty using spawned attenuation for Newcastle.

NEWCASTLE - Random Sampling

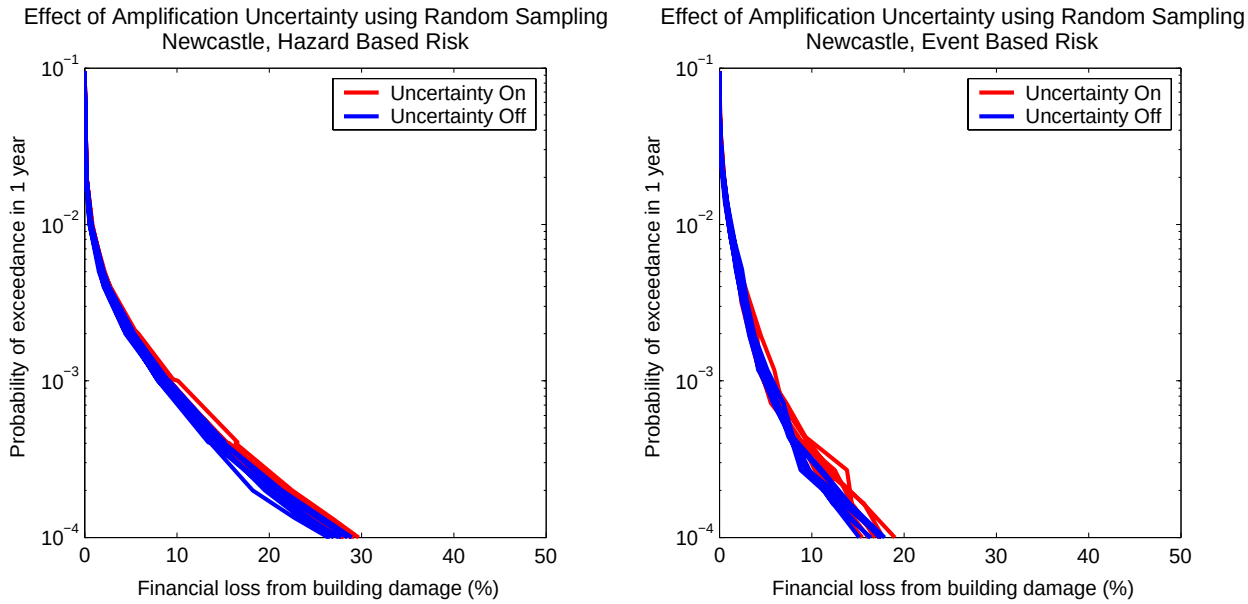

Figure 43 Comparison of the effect of amplification uncertainty using randomly sampled attenuation for Newcastle.

NEWCASTLE - Mean

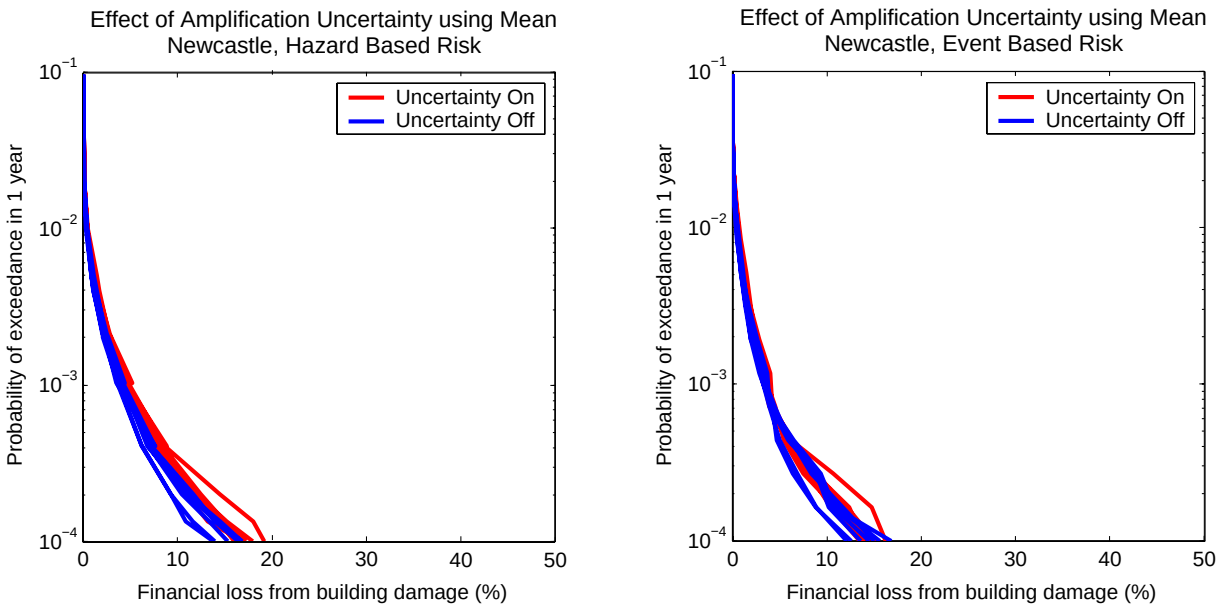

Figure 44 Comparison of the effect of amplification uncertainty using mean for Newcastle.

3.8 CAPACITY CURVE UNCERTAINTY

Figure 45 and Figure 47 illustrate the effect of a) excluding capacity curve aleatory uncertainty in simulations, and b) including capacity curve aleatory uncertainty in simulations, using all 3 sampling techniques in Newcastle and Perth respectively. Both regions display very little difference in estimated risk suggesting that capacity curve uncertainty exerts only a minor influence. The largest effect is seen when random sampling is combined with the event-based method (Figure 46 and Figure 50) although even this is small.

(a) NEWCASTLE - Capacity Curve Uncertainty Excluded

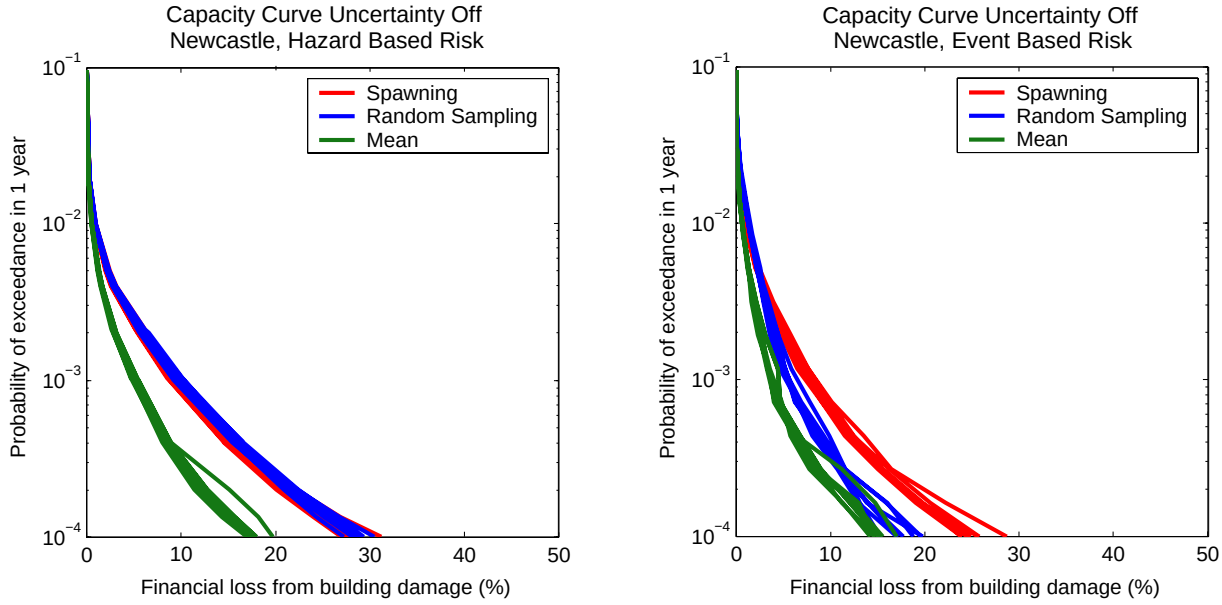

(b) NEWCASTLE - Capacity Curve Uncertainty Included

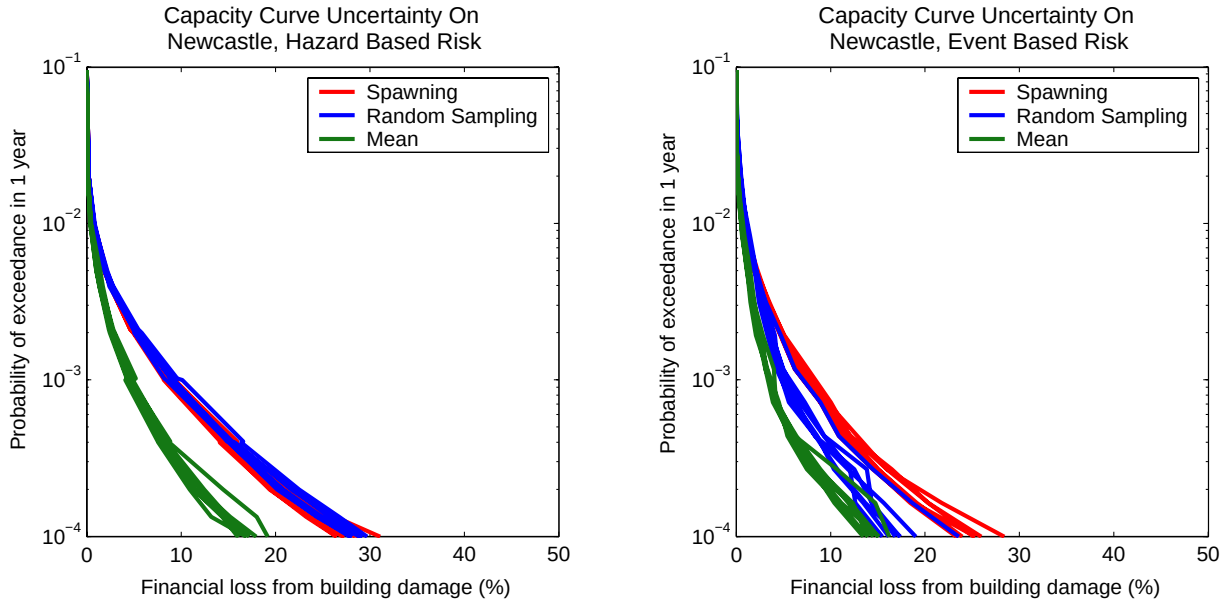

Figure 45 Comparison of the effect of capacity curve uncertainty using spawning for Newcastle for a) capacity curve uncertainty off, and b) capacity curve uncertainty on, in the Newcastle area. PML curves have been calculated without amplification uncertainty.

(a) Spawning

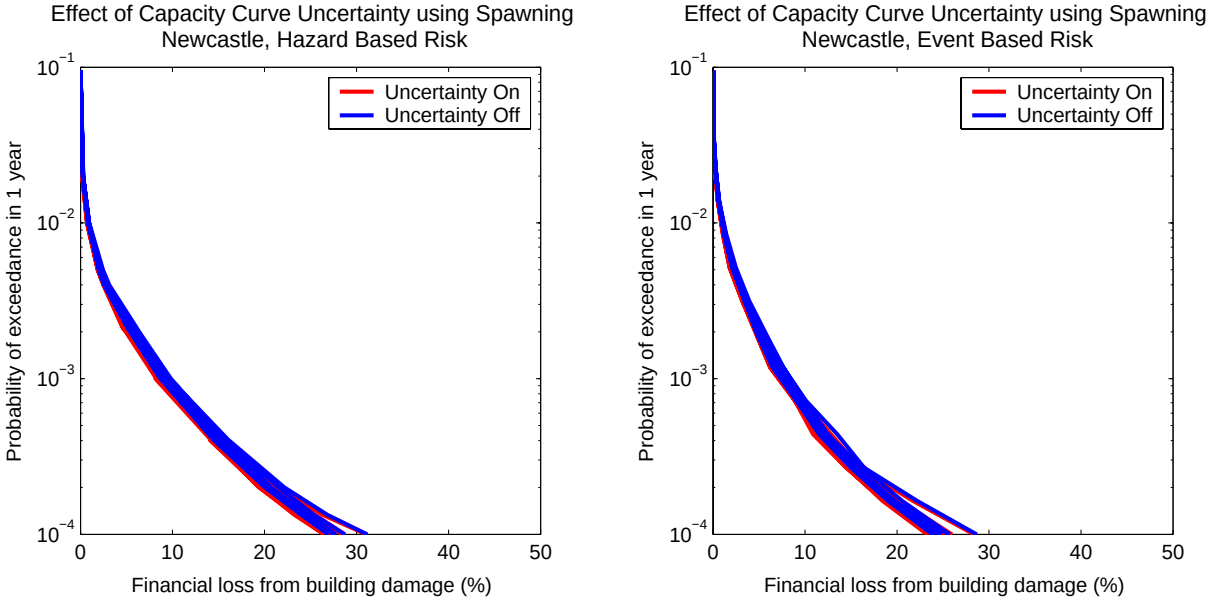

(b) Random Sampling

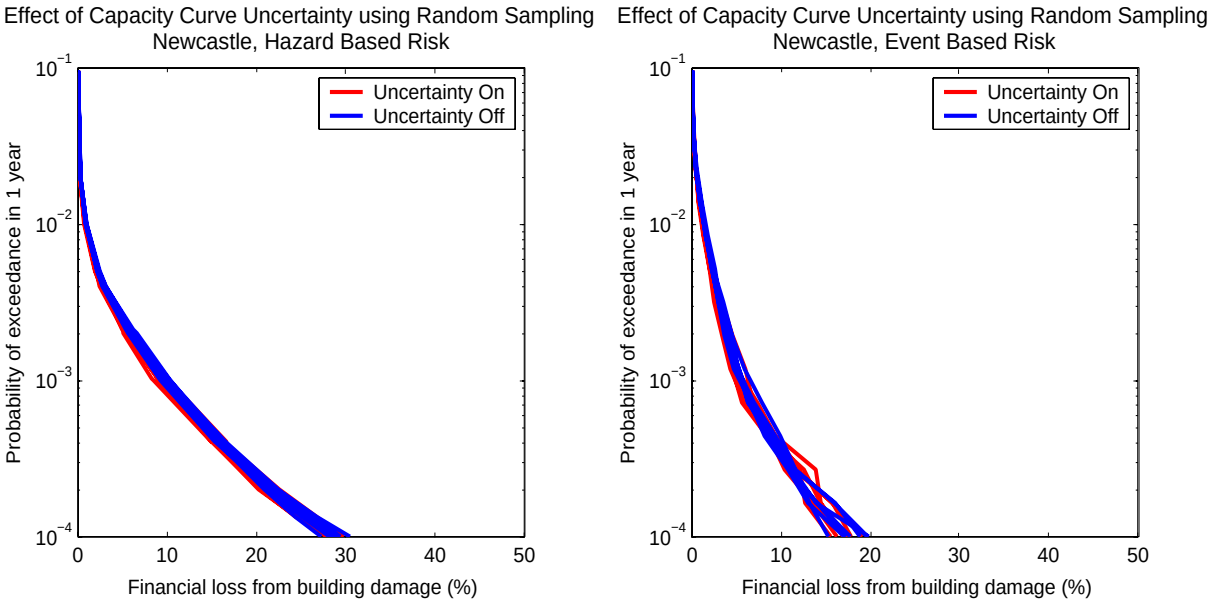

Figure 46 Effect of capacity curve uncertainty on Newcastle risk estimates when using a) spawning, and b) random sampling. The red curves show loss when the uncertainty is excluded and the blue curves show estimated loss when capacity curve aleatory uncertainty is included by random sampling.

(a) PERTH - Capacity Curve Uncertainty Excluded

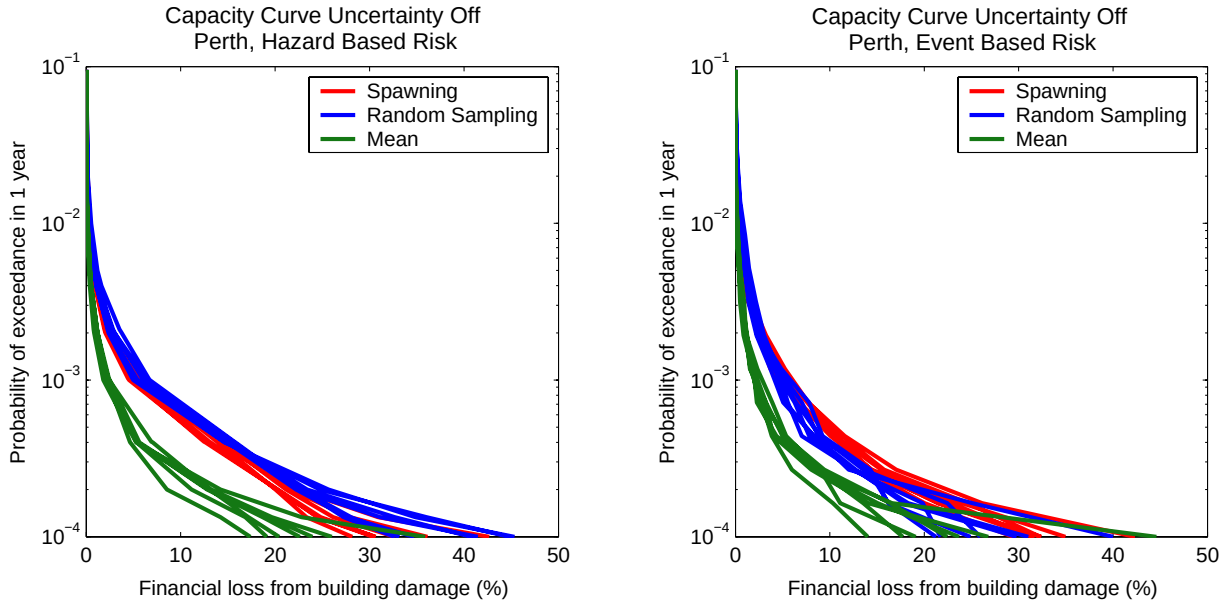

(b) PERTH - Capacity Curve Uncertainty Included

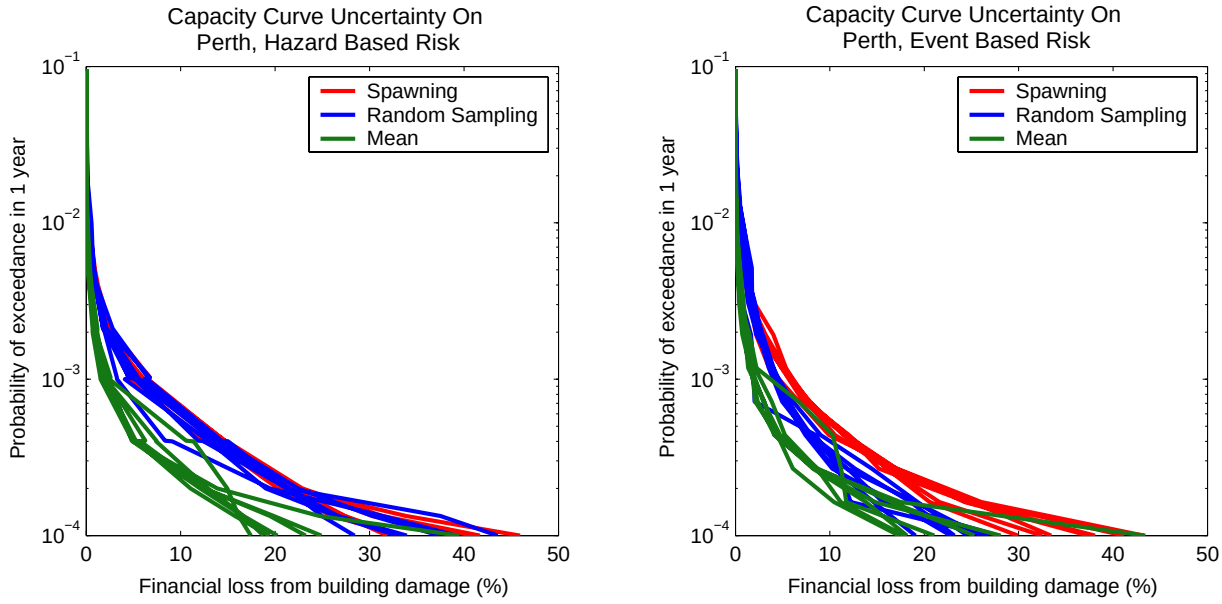

Figure 47 Effect of a) incorporating capacity curve uncertainty, and b) excluding capacity curve uncertainty, in the Perth area. PML curves have been calculated without amplification uncertainty.

Spawning

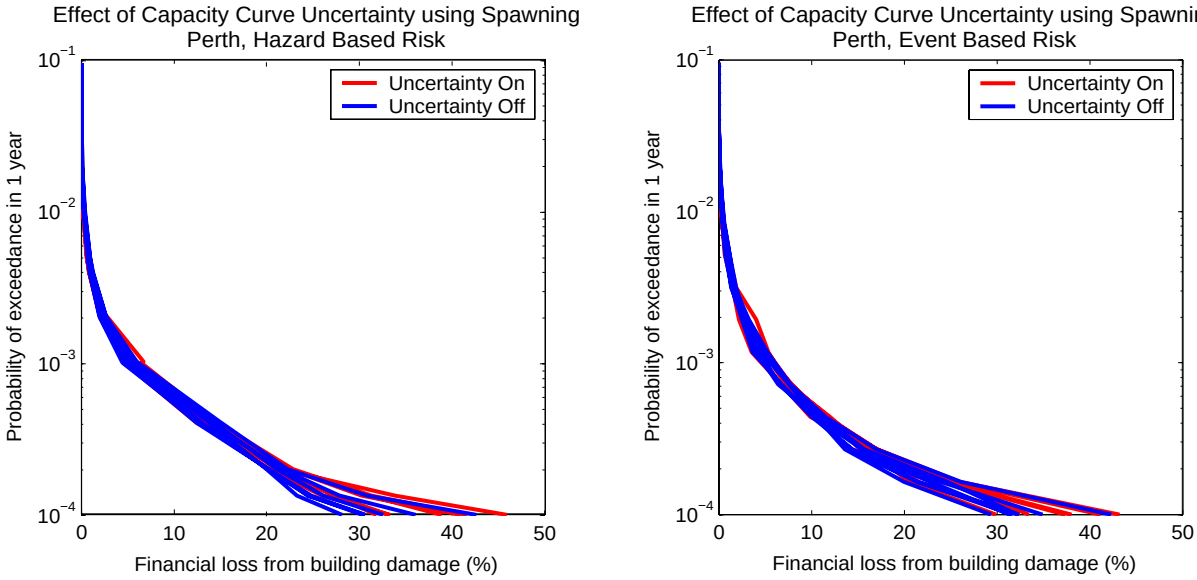

Figure 48 Effect of capacity curve uncertainty on Perth risk estimates when using spawning. The red curves show loss when the uncertainty is excluded and the blue curves show estimated loss when capacity curve aleatory uncertainty is included by random sampling.

Random Sampling

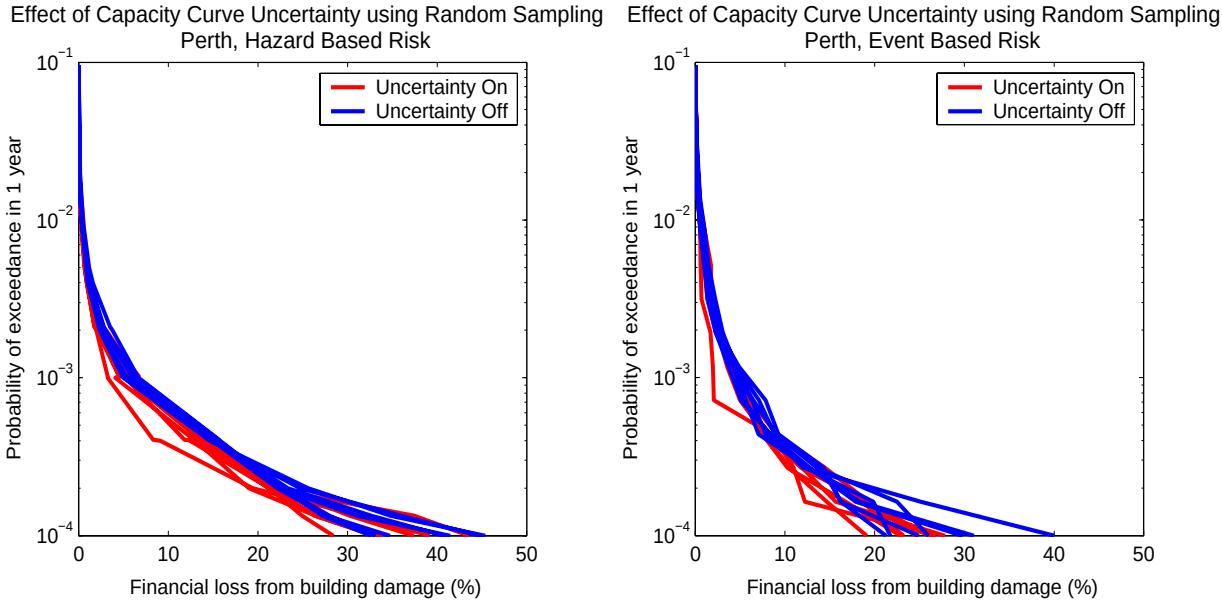

Figure 49 Effect of capacity curve uncertainty on Perth risk estimates when using random sampling. The red curves show loss when the uncertainty is excluded and the blue curves show estimated loss when capacity curve aleatory uncertainty is included by random sampling.

Mean

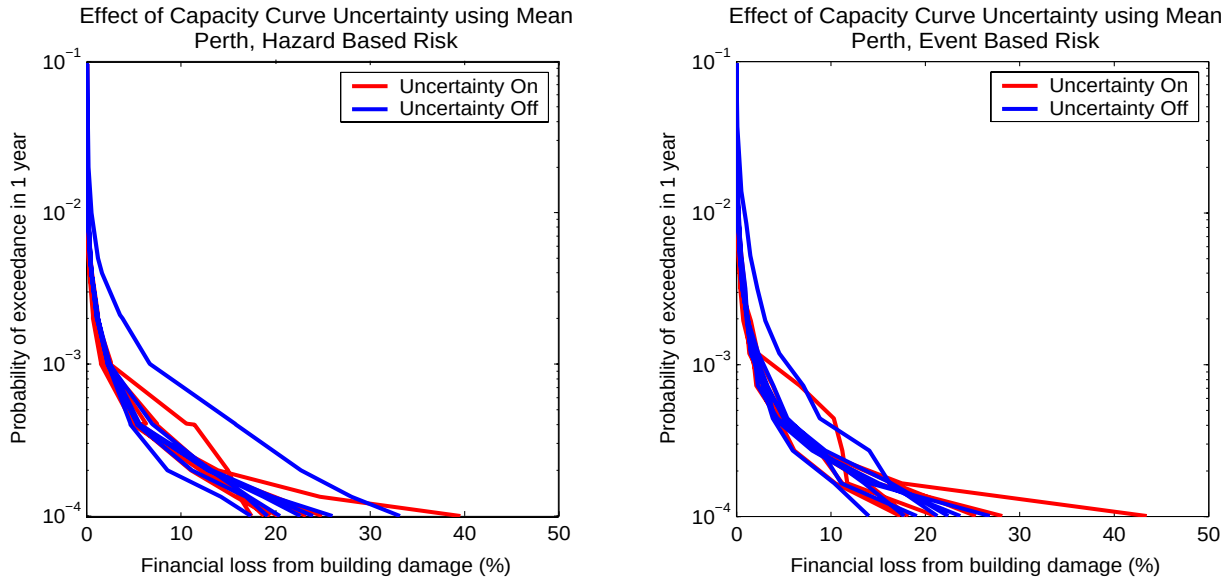

Figure 50 Effect of capacity curve uncertainty on Perth risk estimates when using mean attenuation. The red curves show loss when the uncertainty is excluded and the blue curves show estimated loss when capacity curve aleatory uncertainty is included by random sampling.

3.9 CHANGING THE NUMBER OF EARTHQUAKES IN EACH SOURCE REGION

Increasing the number of events within the synthetic earthquake catalogue leads to more tightly constrained risk estimates when multiple simulations are undertaken in both Newcastle (Figure 51 and Figure 52) and Perth (Figure 55 and Figure 56). The inverse occurs when the number of events is reduced, resulting in an increased spread of results, as shown for Newcastle in Figure 53 and Perth in Figure 57. Results also indicate that risk assessments in Perth require a greater number of synthetic earthquakes than Newcastle assessments to reach a similar distribution in estimated PML curves.

Although an increase in the number of earthquakes in the synthetic earthquake catalogue leads to a tighter spread of results, it does not cause any bulk shift in the PML curve (Figure 54 and Figure 58).

NEWCASTLE

Default Number of Earthquakes

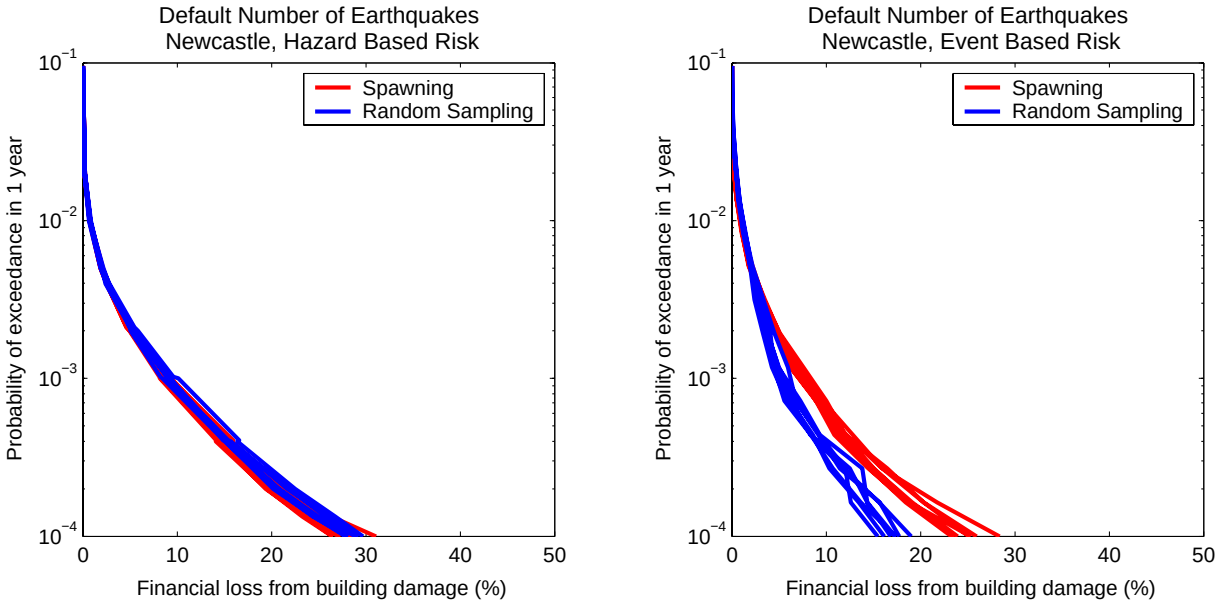

Figure 51 Risk estimates for Newcastle using the default number of earthquakes (approximately 1200 in total).

Doubled Number of Earthquakes

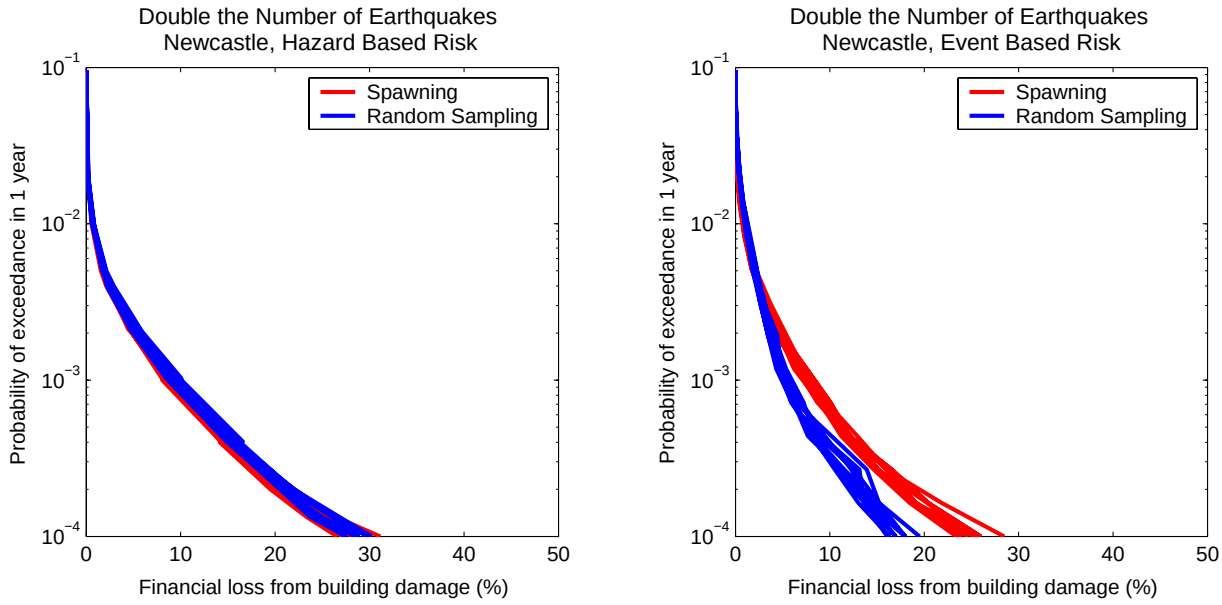

Figure 52 Risk estimates for Newcastle using double the default number of earthquakes (approximately 2400 in total).

Halved Number of Earthquakes

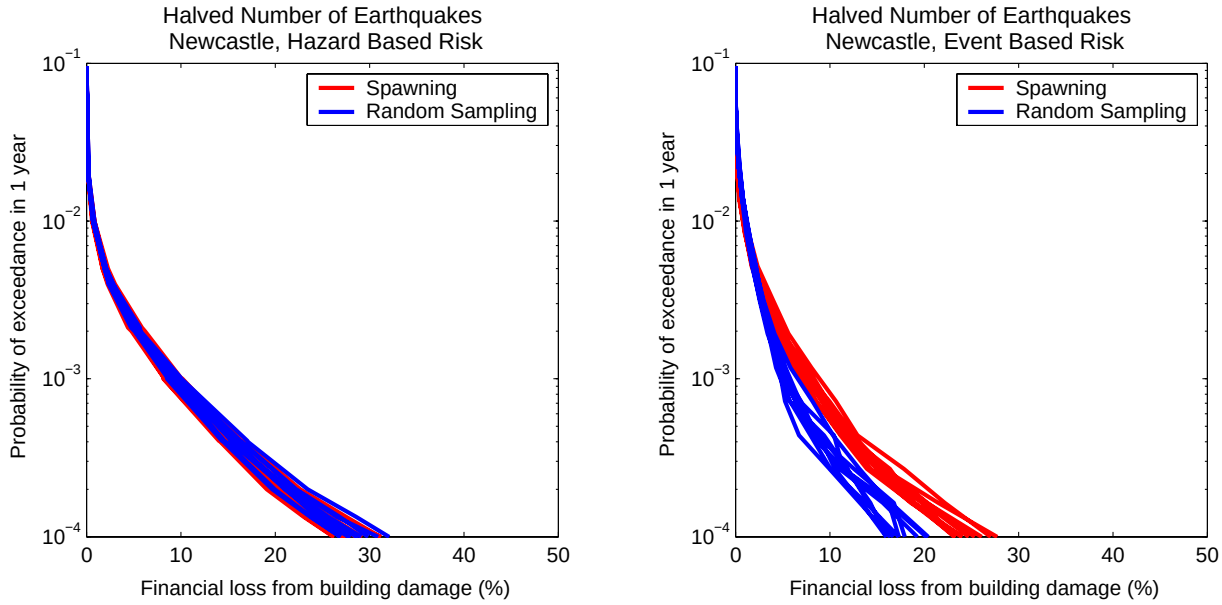

Figure 53 Risk estimates for Newcastle using half the default number of earthquakes in each source zone in Newcastle (approximately 600 in total).

(a) Spawning

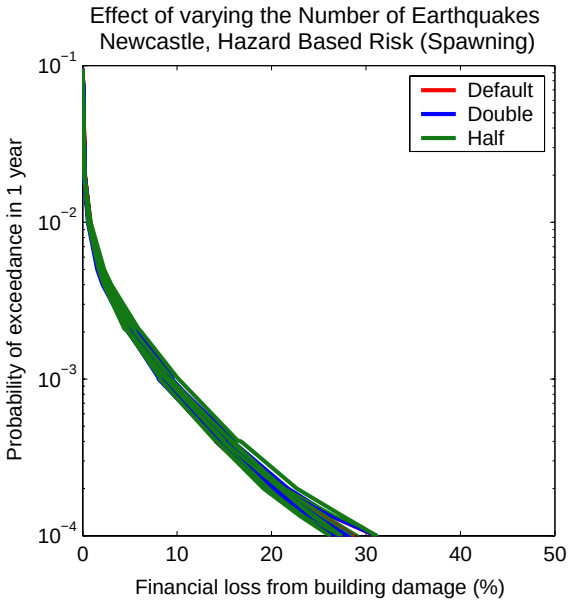

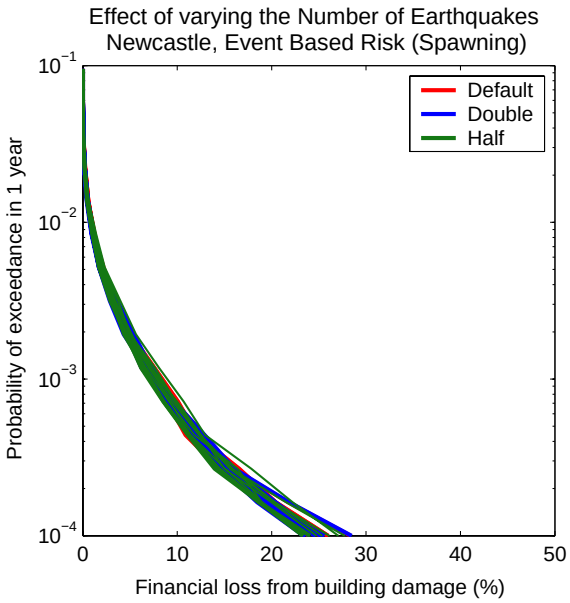

(b) Random Sampling

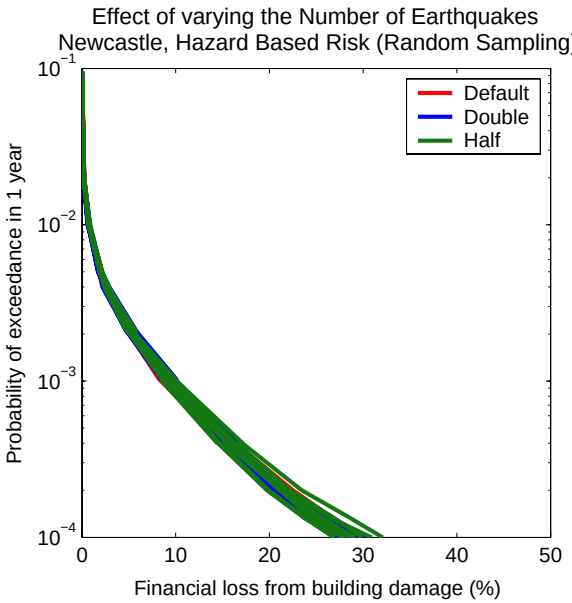

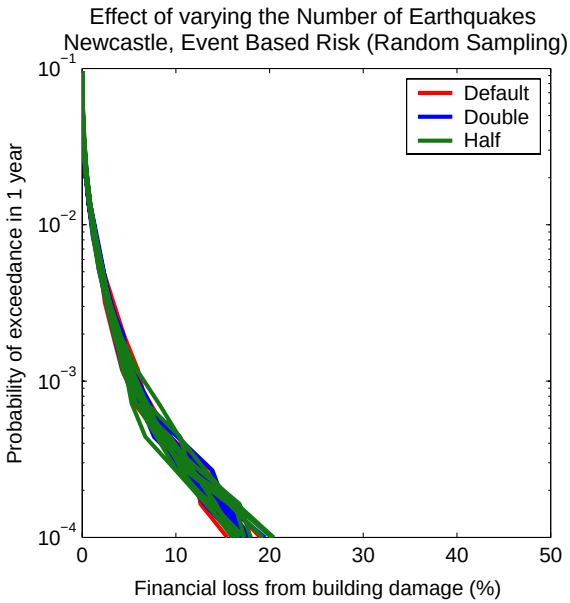

Figure 54 Effect of different sized earthquake catalogues in Newcastle (default, doubled and halved) with a) spawning, and b) random sampling.

PERTH

Default Number of Earthquakes

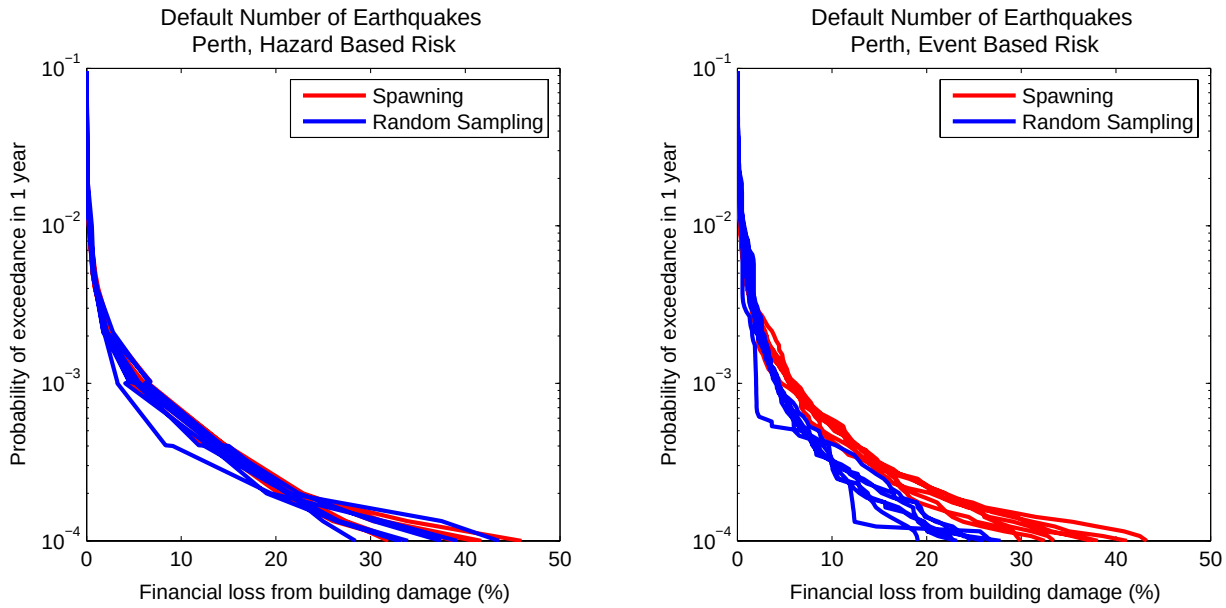

Figure 55 Risk estimates for Perth using the default number of earthquakes (approximately 1200 in total)

Doubled Number of Earthquakes

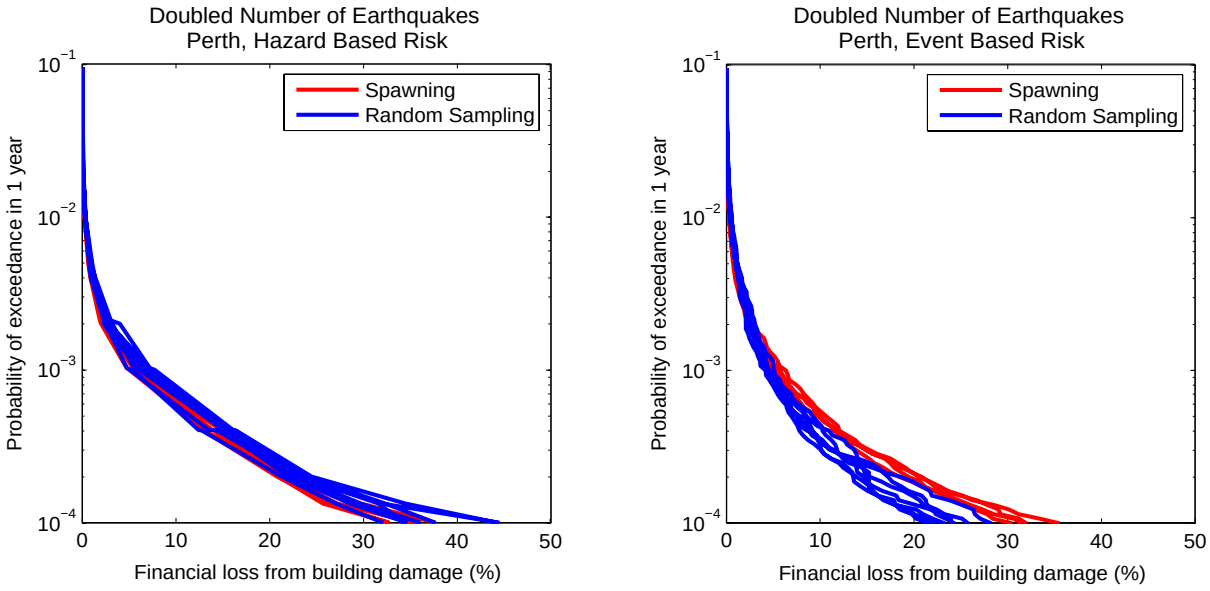

Figure 56 Risk estimates for Perth using double the number of earthquakes (approximately 2400 in total).

Halved Number of Earthquakes

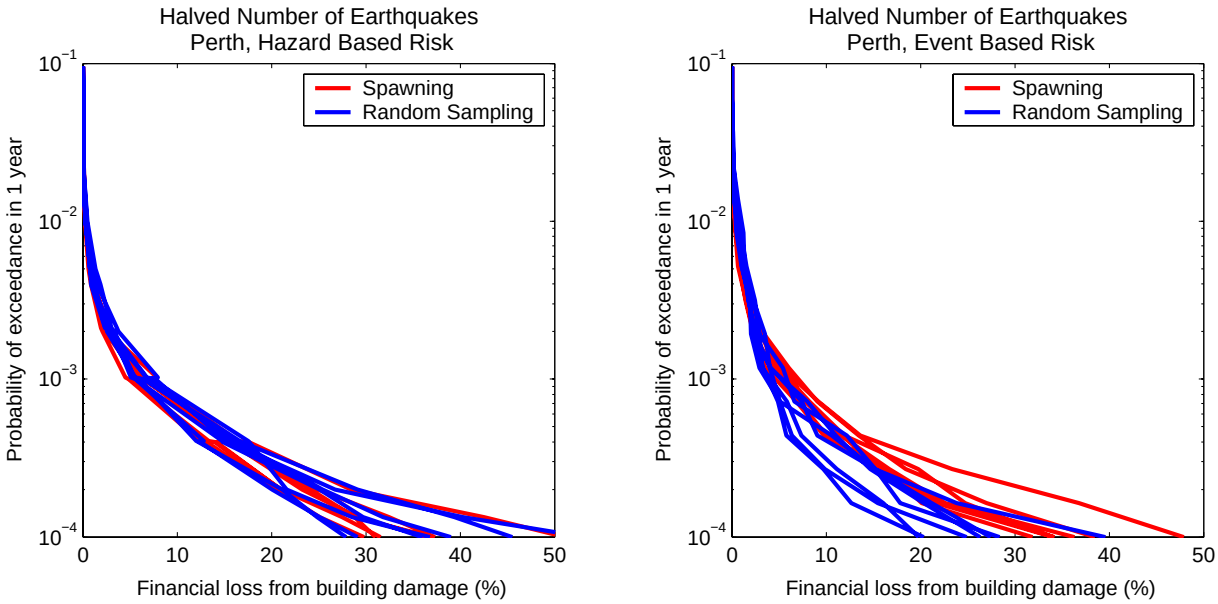

Figure 57 Risk estimates for Perth using half the number of earthquakes in each source zone (approximately 600 in total).

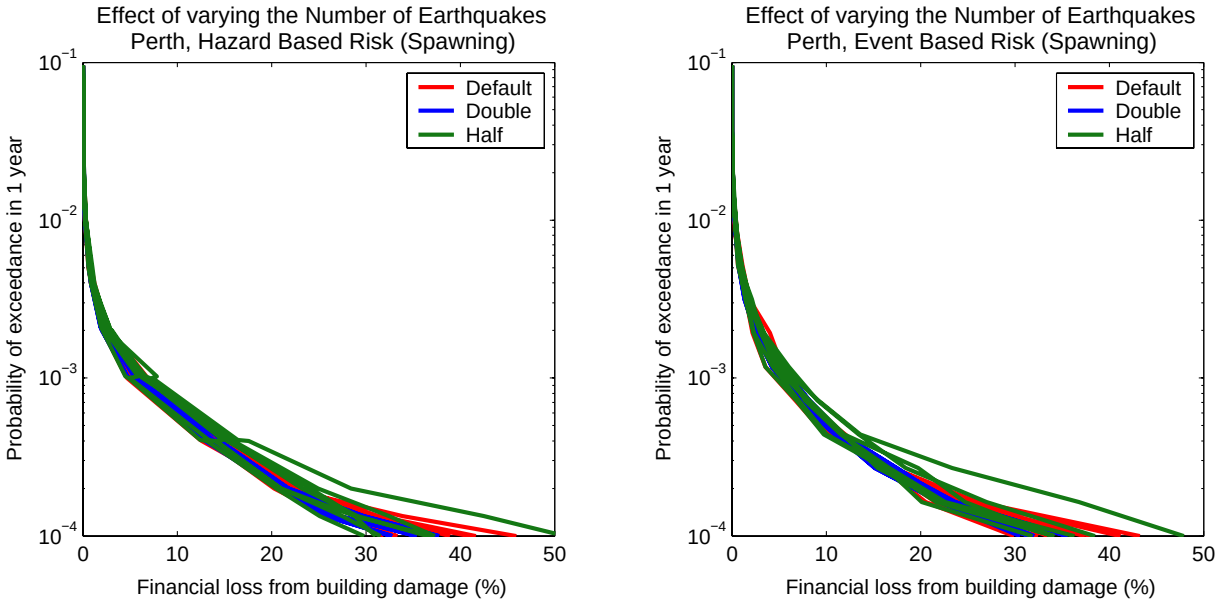

Figure 58 Effect of different sized earthquake catalogues in Perth (default, doubled and halved).

4 Discussion

4.1 CHOICE OF ATTENUATION MODEL

Attenuation models describe how the response spectral acceleration varies with increasing distance from the earthquake source and define both the mean and standard deviation of the response spectra (Toro *et al*., 1997). The three attenuation models considered in this study (Atkinson and Boore (1997), Toro *et al.* (1997) and Somerville *et al.* (2001)) each generate a different PDF by defining a unique mean and standard deviation (i.e. epistemic uncertainty). When different sampling techniques are applied to each attenuation model, the resultant risk also varies significantly (i.e. aleatory uncertainty).

The results presented herein suggest that attenuation *epistemic* uncertainty exerts a greater influence on observed loss than attenuation *aleatory* uncertainty. That is, uncertainty associated with using different attenuation models is significantly greater than the uncertainty observed using different sampling techniques in attenuation. Moreover, the results illustrate that epistemic uncertainty associated with the attenuation model exerts the greatest influence of all the uncertainties considered in this study.

The Somerville *et al.* (2001) attenuation model was originally designed to model risk for high magnitude earthquakes, and is known to underestimate ground motion for events of less than magnitude 6.5 (pers. comm. P. Somerville, 2004).

Figure 30 also suggests that Somerville *et al.*, (2001) estimates greater risk from closer events than the other attenuation models that were considered. The results suggest that multiple attenuation models should be considered in PSRA, particularly if it is not clear as to which attenuation model is the most appropriate to a particular area.

4.2 SAMPLING THE PDF FOR ATTENUATION

Different sampling techniques for incorporating aleatory uncertainty in attenuation are demonstrated to produce highly varying results. Sampling only the mean of the response spectra PDF does not provide a realistic representation of risk as, in nature, a consistent mean level of ground shaking is not likely to occur. Computationally, however, sampling the mean of the PDF is effective in isolating uncertainty caused by various parameters (e.g. randomness in the earthquake catalogue or capacity curve uncertainty) as it doesn't take into account any aleatory uncertainty associated with the ground motion (attenuation) itself. The mean RSA has been included in this study to assist the understanding of other uncertainties and therefore will not be discussed at length in this section. Random sampling and spawning can therefore be considered the two key sampling methods for incorporating natural variability, or aleatory uncertainty, in attenuation.

Spatial correlation is a critical difference between spawning and random sampling. In spawning, each sampled level of RSA is applied across all sites. Hence, when a high value is chosen at one site a high value will be correlated across all sites, and vice versa for low values. In this way spawning is highly correlated, and such a high level of spatial correlation is believed to be artificial. This high level of artificial spatial correlation introduced with spawning leads to higher estimates of risk than random sampling for the low probability high risk events, as a high selection of RSA at one location implies a high level everywhere.

Random sampling, by comparison, involves selecting a random RSA from the RSA PDF for each event-site combination. As such, two sites which are close together can produce dramatically different estimates of ground motion, and hence loss, for the same event. Random sampling therefore encompasses a much lower level of spatial correlation.

Spawning and random sampling also differ in the way that they account for the *probability* of selecting a particular RSA from the PDF. With spawning, each spawned level of RSA is weighted against its respective probability of occurrence. In random sampling, however, a randomly selected RSA is not weighted against its probability of occurrence (Robinson and Fulford, 2005). However, extremely high or low values have a naturally lower probability of selection and as such these values are less likely to be selected. Values closer to the mean are more likely to be selected during random sampling.

The impact of spawning, as demonstrated in this paper, suggests that it should be used with caution in PSRA. Ongoing work at Geoscience Australia suggests that a new formulation of spawning, spawning with logic tree collapse (Robinson and Fulford, 2005) shows promise as a viable sampling technique. In this report, spawning does not use logic tree collapse.

4.3 SYNTHETIC EARTHQUAKE CATALOGUE

Multiple simulations demonstrate uncertainty due to randomness (aleatory uncertainty) in generating the synthetic earthquake catalogue. Mean curves, in particular, isolate the uncertainty associated with the synthetic earthquake catalogue as they do not incorporate attenuation aleatory uncertainty (Figure 30a and Figure 32a for Newcastle and Perth respectively). This provides a useful way of considering variation in PML curves caused by the earthquake catalogue alone. The spread of results for each group of mean PML curves presented herein shows that the synthetic earthquake catalogue exerts a noticeable influence on estimated losses, although this does not appear to be as significant as either epistemic or aleatory uncertainty associated with the attenuation model.

An increase in the number of events within the earthquake catalogue results in a more even spatial distribution of earthquakes over each source region and therefore a tighter distribution of results (PML curves). When increasing the number of synthetic events, the *likelihood* of each synthetic event is also reduced as its likelihood is normalised by the total number of simulated events. Consequently each synthetic event becomes less dominant leading to spatially smoother estimates of hazard and hence more stable risk estimates. In other words, aleatory uncertainty is strongly influenced by limited numbers of earthquakes. Computational limitations bound the number of earthquakes that can be simulated in each source zone.

The geometry of the source areas in Perth and Newcastle is partly responsible for the range of results (and therefore uncertainty) in PML curves generated from both areas. Newcastle comprises three distinct seismic source zones, and the region of highest seismicity is located *directly under* the metropolitan area. In comparison, Perth encompasses five discrete seismic source zones, in which the region of highest seismicity (the South West Seismic Zone) is situated roughly 150 km away from the metropolitan area. A region of background seismicity occurs beneath the metropolitan area where, according to the Gutenberg-Richter magnitude-frequency relationship, earthquakes occur much less frequently than they do underneath Newcastle (Sinadinovski *et al*., 2005). The same number of earthquakes distributed in three zones in Newcastle is shared across five zones in Perth resulting in fewer earthquakes underneath the metropolitan area.

4.4 CAPACITY CURVE (BUILDING DAMAGE) AND AMPLIFICATION

Aleatory uncertainty can be associated with many stages of a PSRA and each uncertainty exerts a different level of influence over risk estimates. Aleatory uncertainty in capacity curve and amplification were also considered in this study.

It is commonly accepted that amplification can significantly increase risk. The results in Figure 39 through Figure 41 demonstrate that both the choice of attenuation model (attenuation epistemic uncertainty) and different sampling techniques used to incorporate attenuation aleatory uncertainty influence estimates of risk more than whether amplification is or is not included or not for the Newcastle study.

Aleatory uncertainty associated with both the capacity curve and amplification appears to be much less influential than whether amplification is applied and, therefore, less influential than attenuation uncertainty (aleatory and epistemic). Other studies have shown, however, that *epistemic* uncertainty associated with building damage and amplification may exert a large influence on risk estimates (Schneider *et al.*, 2003; Robinson *et al*., 2004). Epistemic uncertainty associated with the capacity curve and amplification, however, has not been investigated in this study. It should also be noted that the effect of uncertainties regarding building structure type has not been considered in this study.

4.5 RETURN PERIODS AND RSA PERIODS

The aleatory uncertainty associated with the number of return periods lies within the uncertainty associated with different synthetic earthquake catalogues.

Similarly, the aleatory uncertainty associated with varying the number of RSA periods is outweighed by uncertainty associated with different synthetic earthquake catalogues and is therefore

difficult to isolate without performing analyses using the same catalogue of events. Such an analysis was not undertaken in this study.

4.6 EVENT VS HAZARD

The hazard-based method estimates consistently higher risk than the event-based approach. This is because the hazard at any one site for a given return period represents the ***maximum*** probable level of ground motion at that site. The hazard-based method leads to a high level of spatial correlation as all building sites experience the maximum probable level of ground motion for a given return period. In the event-based method one demand curve is calculated for each synthetic earthquake at each individual building site. It is computed directly from the attenuation model and hence takes into account the magnitude and distance of each event at every building site. Therefore it is not as well correlated particularly when random sampling is used.

As the hazard model is spatially correlated at a much higher level than the event-based method it produces roughly comparable, though not identical, results to spawning. Due to this high level of spatial correlation, the hazard approach is not particularly realistic in theory as it relies on different combinations of events to estimate risk at each fundamental period on the demand curve. That is, the level of hazard experienced at different locations may be driven by different events. This means that the estimated losses across a portfolio of buildings can not be attributed to specific events and hence could not occur at any one time. In the event-based approach, however, each point on the PML curve represents a level of risk associated with a single event. This approach is somewhat more realistic as individual calculations of loss can be attributed to specific events and can therefore be considered as single impacts.

Neither the event-based approach nor random sampling introduces artificial spatial correlation and, therefore, computed losses are significantly reduced when the two methods are used in combination. Hazard-spawning, hazard-random sampling and event-spawning, however, all produce comparable results as each combination of techniques introduces an artificial spatial correlation.

5 Conclusions

The following conclusions were drawn from this study:

- The event-based approach is preferred over the hazard-based technique for computing risk because it does not introduce any artificial spatial correlation. The presence of artificial spatial correlation with the hazard-based approach suggests that care should be taken when using a hazard based approach to estimate risk.
- Spawning and random sampling lead to different risk estimates. Differences between spawning and random sampling occur due to an introduction of artificial spatial correlation, this time with spawning. This suggests that the application of spawning does not represent a good sampling technique.
- The choice of attenuation model has a direct and significant influence on risk estimates. An attenuation model designed specifically for Australia is critical.
- There are a number of uncertainties involved in PSRA and each uncertainty exerts a different level of influence over risk estimates. Uncertainties associated with attenuation are the dominant uncertainties explored in this study. In particular the attenuation uncertainty associated with using different attenuation models is significantly greater than the aleatory uncertainty observed by using different sampling techniques.
- Different sampling techniques for incorporating attenuation aleatory uncertainty lead to greater uncertainty in risk estimates than using or omitting amplification in the Newcastle study.
- Aleatory uncertainty associated with the synthetic earthquake catalogue also influences risk estimates.
- Epistemic uncertainty associated with the synthetic earthquake catalogue, amplification and capacity curve has not been considered in this study and hence represent areas for future investigation.

6 REFERENCES

Adams, J. and Halchuk, S., 2003. Fourth generation seismic hazard maps of Canada: Values for over 650 Canadian localities intended for the National Building Code of Canada. Geological Survey of Canada Report, Open File 4459, Ontario.

Atkinson, G. M. and Boore, D. M., 1997. Some comparisons between recent ground-motion relations. Seismological Research Letters, 68, 24-40.

Chopra, A. K., 2001. Dynamics of Structures; Theory and Applications to Earthquake Engineering: Second Edition, Prentice Hall, New Jersey.

Sinadinovski, C., Jones, T., Stewart, D. and Corby, N., 2002. Earthquake history, regional seismicity and the 1989 Newcastle earthquake. In: Dhu, T., and Jones, T., (eds) Earthquake risk in Newcastle and Lake Macquarie: ACT, Geoscience Australia, GA Record 2002/15, 31-42.

Council of Australian Governments, 2004. Natural Disasters in Australia: Reforming mitigation, relief and recovery arrangements, COAG, Canberra.

Dhu, T., Robinson, D., Sinadinovski, C., Jones, T., Corby, N., Jones, A. and Schneider, J., 2002. Earthquake Hazard, Chapter 4. In: Dhu, T., and Jones, T. (eds) Earthquake risk in Newcastle and Lake Macquarie: ACT, Geoscience Australia, GA Record 2002/15, 43-76.

Dhu, T. and Jones, T., 2002. Earthquake risk in Newcastle and Lake Macquarie: ACT, Geoscience Australia, GA Record 2002/15.

Dhu, T., Sinadinovski, C., Edwards, M., Robinson, D., Jones, T. and Jones, A., 2004. Earthquake risk assessment for Perth, Western Australia. 13th World Conference on Earthquake Engineering. Vancouver, Canada, August 2004.

Edwards, M. R., Robinson, D., McAneney, K. J. and Schneider, J., 2004. Vulnerability of residential structures in Australia. 13th World Conference on Earthquake Engineering, Vancouver, Canada, August 2004.

FEMA, 1999. HAZUS Technical Manual. National Institute of Building Science: Federal Emergency Management Agency, Washington DC, USA.

Frankel, A. D., Mueller, C. S., Barnhard, T. P., Leyendecker, E.V., Wesson, R.L., Harmsen, S.C., Klein, F.W., Perkins, D.M., Dickman, N.C., Hanson, S.L. and Hopper, M.G. (2000). USGS National Seismic Hazard Maps. Earthquake Spectra, 16(1), 1-19.

Jones, T., Middelmann, M. and Corby, N., 2005. Natural Hazard Risk in Perth, Western Australia, Geoscience Australia, Canberra, GeoCat # 62527.

Kircher, C. A., Nassar, A. A., Kustu, O. and Holmes, W. T., 1997a. Development of building damage function for earthquake loss estimation. Earthquake Spectra, 13, 663-683.

Kircher, C. A., Reitherman, R. K., Whitman, R. V. and Arnold, C., 1997b. Estimation of Earthquake Losses to Buildings. Earthquake Spectra, 13, 703-720.

Kramer, S. L., 1996. Geotechnical Earthquake Engineering. Prentice Hall, New Jersey.

Robinson, D. and Fulford, G., 2005. EQRM: Geoscience Australia's Earthquake Risk Model: Technical Manual: Version 3.0. Geoscience Australia Record 2005/01, Geoscience Australia, Canberra.

Robinson, D., Dhu, T. and Schneider, J., 2006. SUA: A computer program to compute regolith Site-response and estimate Uncertainty for probabilistic seismic hazard Analyses, Computers and Geosciences, 32(1), 109-123.

Robinson, D., Mendez, A., Fulford, G., Dhu, T., Jones, T. and Schneider, J., 2003. Recent advances in the modelling of earthquake hazard in Australia: part 2 – estimating the hazard. In: ASEG 16th Geophysical Conference and Exhibition, Adelaide, February 2003.

Robinson, D., Dhu, T. and Schneider, J., 2004. A sensitivity study on earthquake hazard in the Newcastle and Lake Macquarie Region, Australia. In: Proceedings of the Australian Society of Exploration Geophysics 2004 Conference, Sydney, August 2004.

Schneider, J., Robinson, D., Clark, D., Dhu, T. and Edwards, M., 2003. Earthquake risk in Australia: How well do we understand it? Catastrophic Risks and Insurability. In: Proceedings of the Aon Re Hazards and Capital Risk Management Series, 37-62, Gold Coast, Queensland, August 2003.

Somerville, P., Collins, N., Abrahamson, N., Graves, R. and Saika, C., 2001. Ground motion attenuation relations for the Central and Eastern United States: United States Geological Survey Report, 99HQGR0098, San Francisco.

Somerville, P. and Moriwaki, Y., 2003. Seismic hazards and risk assessments in engineering practice. In Lee, W. H. K., Kanamori, H., Jennings, P. C., and Kisslinger, C. (eds), International Handbook of Earthquake and Engineering Seismology. Academic Press, London, 1065 – 1080.

Toro, G. R., Abrahamson, N. A. and Schneider, J. F., 1997. Model of strong ground motions from earthquakes in Central and Eastern North America: best estimates and uncertainties. Seismological Research Letters, 68, 41-57.

7 Appendices

APPENDIX 1 DESCRIPTION OF RUNS LISTED BY FIGURE

Figure Number	*Comprisk runs used to generate figure*
13	*N: 002, 005,024-028, 032-037, 042-049*
14	*P: 001-021*
15	*N: 370-376* *P: 001-007*
16	*N: 377-383* *P: 008-014*
17	*N: 384-390* *P: 015-021*
18	*N: 023, 040, 041, 391-409*
19	*N: 004-006, 012, 013, 015, 016, 017*
20	*N: 002, 005, 008, 009, 010, 011*
21	*N: 002, 008, 010, 005, 009, 011*
22	*-*
23	*-*
24	*-*
25	*-*
26	*-*
27	*-*
28	*N: 002, 032-037, 310-329*
29	*N: 005, 014, 024-028, 330-339*
30	
31	*P: 001-007, 043-049, 057-063*
32	*P: 008-014, 050-056, 064-070*
33	*N: 310-319* *P:043-049*
34	*N: 330-339* *P: 050-056*
35	*N: 320-329* *P: 057-063*
36	*N: 340-349* *P: 064-070*
37	*N: 002, 032-037* *P: 001-007*
38	*N: 005, 014,024-028* *P: 008-014*
39	*N: 370-376, 002, 032-037*
40	*N: 005, 014, 024-028, 007*
41 a	*N: 050-070*

41 b	*N: 185-289*
42	*N: 057-063, 071-077*
43	*N: 064-070, 078-084*
44	*N: 050-056, 085-091*
45 a	*N: 071-091*
45 b	*N: 133-139, 154-174*
46 a	*N: 161-167, 071-077*
46 b	*N: 078-084, 168-174*
47 a	*N: 350-359, 360-369*
47 b	*P: 001-021*
48	*P: 001-014, 022-028* *N: 002, 032-037, 018, 290-299, 350-359; 005, 024-028, 300-309, 360-369*
49	*P: 008-014, 029-035*
50	*P: 015-021, 035-042*
51	*N: 002, 005, 014, 024-028, 032-037*
52	*N: 300-309, 290-299*
53	*N: 350-359, 360-369*
54 a	*N: 002, 032-037, 290-299, 350-359*
54 b	*N: 005, 014, 024-028, 300-309, 360-369*
55	*P: 001-014*
56	*P: 075-088*
57	*P: 089-102*
58 a	*P: 001-007, 075-081, 089-095,*
58 b	*P: 008-014, 082-088, 095-102*

APPENDIX 2: DESCRIPTION OF RUNS

NEWCASTLE

comprisk001

Default parameters

Variable	*Value*
Default setting	n/a

comprisk002

40 RSA Periods

Variable	*Value*
hzdrisk_param.Tlen	40
hzdrisk_param.Tlen_attn	40
hzdrisk_param.Tlen_vun	40
hzdrisk_param.periods	linspace(0,3.33,40)

comprisk003

60 RSA Periods

Variable	*Value*
hzdrisk_param.Tlen	60
hzdrisk_param.Tlen_attn	60
hzdrisk_param.Tlen_vun	60
hzdrisk_param.periods	linspace(0,3.33,60)

comprisk004

20 RSA Periods
Random Sampling

Variable	*Value*
hzdrisk_param.Tlen	20
hzdrisk_param.Tlen_attn	20
hzdrisk_param.Tlen_vun	20
hzdrisk_param.periods	linspace(0,3.33,20)
hzdrisk_param.var_attn_method	2

comprisk005

40 RSA Periods
Random Sampling

Variable	*Value*
hzdrisk_param.Tlen	40
hzdrisk_param.Tlen_attn	40
hzdrisk_param.Tlen_vun	40
hzdrisk_param.periods	linspace(0,3.33,40)
hzdrisk_param.var_attn_method	2

comprisk006

60 RSA Periods
Random Sampling

Variable	*Value*
hzdrisk_param.Tlen	60
hzdrisk_param.Tlen_attn	60
hzdrisk_param.Tlen_vun	60
hzdrisk_param.periods	linspace(0,3.33,60)
hzdrisk_param.var_attn_method	2

comprisk007

Regolith/amplification off
Random Sampling

Variable	*Value*
hzdrisk_param.amp_switch	0
hzdrisk_param.var_attn_method	2

comprisk008

Increased return periods (56)

Variable	*Value*
hzdrisk_param.rtrn_per	[20:20:200 300:100:3000 3250:250:5000 5500:500:10000]

comprisk009

Increased return periods (56)
Random Sampling

Variable	*Value*
hzdrisk_param.rtrn_per	[20:20:200 300:100:3000 3250:250:5000 5500:500:10000]
hzdrisk_param.var_attn_method	2

comprisk010

Increased return periods (123)

Variable	*Value*
hzdrisk_param.rtrn_per	[20:10:290 300:50:3000 3100:100:5000 5250:250:10000]

comprisk011

Increased return periods (123)
Random Sampling

Variable	*Value*
hzdrisk_param.rtrn_per	[20:10:290 300:50:3000 3100:100:5000 5250:250:10000]
hzdrisk_param.var_attn_method	2

comprisk012

Random Sampling
30 RSA Periods

Variable	*Value*
hzdrisk_param.Tlen	30
hzdrisk_param.Tlen_attn	30
hzdrisk_param.Tlen_vun	30
hzdrisk_param.periods	linspace(0,3.33,30)
hzdrisk_param.var_attn_method	2

comprisk013

Random Sampling
50 RSA Periods

Variable	*Value*
hzdrisk_param.Tlen	50
hzdrisk_param.Tlen_attn	50
hzdrisk_param.Tlen_vun	50
hzdrisk_param.periods	linspace(0,3.33,50)
hzdrisk_param.var_attn_method	2

comprisk014

as for comprisk005

comprisk015

Random Sampling
10 RSA Periods

Variable	*Value*
hzdrisk_param.Tlen	10
hzdrisk_param.Tlen_attn	10
hzdrisk_param.Tlen_vun	10
hzdrisk_param.periods	linspace(0,3.33,10)
hzdrisk_param.var_attn_method	2

comprisk016

Random Sampling
70 RSA Periods

Variable	*Value*
hzdrisk_param.Tlen	70
hzdrisk_param.Tlen_attn	70
hzdrisk_param.Tlen_vun	70
hzdrisk_param.periods	linspace(0,3.33,70)
hzdrisk_param.var_attn_method	2

comprisk017

Random Sampling
80 RSA Periods

Variable	*Value*
hzdrisk_param.Tlen	80
hzdrisk_param.Tlen_attn	80
hzdrisk_param.Tlen_vun	80
hzdrisk_param.periods	linspace(0,3.33,80)
hzdrisk_param.var_attn_method	2

comprisk018

Doubled the number of earthquakes in each source zone

Variable	*Value*
hzdrisk_param.ntgrvector	[1000 200 200 600 200 200]

comprisk019

10 bins

Variable	*Value*
hzdrisk_param.nbins	10

comprisk020

20 bins

Variable	*Value*
hzdrisk_param.nbins	20

comprisk021

10 bins
Random Sampling

Variable	*Value*
hzdrisk_param.nbins	10
hzdrisk_param.var_attn_method	2

comprisk022

20 bins
Random Sampling

Variable	*Value*
hzdrisk_param.nbins	20

comprisk023

nsamples = 3

Variable	*Value*
hzdrisk_param.nsamples	3

comprisk024 – comprisk028

as for comprisk005

comprisk029

25 Magnitude Bins

Variable	*Value*
hzdrisk_param.nbins	25

comprisk030

30 Magnitude Bins

Variable	*Value*
hzdrisk_param.nbins	30

comprisk031

5 Magnitude Bins

Variable	*Value*
hzdrisk_param.nbins	5

comprisk032 – comprisk 037

as for comprisk002

comprisk038

Halve the number of earthquakes in each source zone

Variable	*Value*
hzdrisk_param.ntgrvector	[250 50 50 150 50 50]

comprisk039

Quarter of the number of earthquakes in each source zone

Variable	*Value*
hzdrisk_param.ntgrvector	[125 25 25 75 25 25]

comprisk040

nsamples = 7

Variable	*Value*
hzdrisk_param.nsamples	7

comprisk041

nsamples = 9

Variable	*Value*
hzdrisk_param.nsamples	9

comprisk042 – comprisk049

40 RSA Periods
Mean variability

Variable	*Value*
hzdrisk_param.Tlen	40
hzdrisk_param.Tlen_attn	40
hzdrisk_param.Tlen_vun	40
hzdrisk_param.periods	linspace(0,3.33,40)
hzdrisk_param.var_attn_flag	0

comprisk050 – comprisk056

40 RSA Periods
Mean variability
Building Damage Variability off

Variable	*Value*
hzdrisk_param.Tlen	40
hzdrisk_param.Tlen_attn	40
hzdrisk_param.Tlen_vun	40
hzdrisk_param.periods	linspace(0,3.33,40)
hzdrisk_param.var_attn_flag	0
hzdrisk_param.var_bcap_flag	0

comprisk057 – comprisk 063

40 RSA Periods
Spawning
Building Damage Variability off

Variable	*Value*
hzdrisk_param.Tlen	40
hzdrisk_param.Tlen_attn	40
hzdrisk_param.Tlen_vun	40
hzdrisk_param.periods	linspace(0,3.33,40)
hzdrisk_param.var_bcap_flag	0
hzdrisk_param.var_attn_flag	0

comprisk064 – comprisk070

40 RSA Periods
Random Sampling
Building Damage Variability off

Variable	*Value*
hzdrisk_param.Tlen	40
hzdrisk_param.Tlen_attn	40
hzdrisk_param.Tlen_vun	40
hzdrisk_param.periods	linspace(0,3.33,40)
hzdrisk_param.var_bcap_flag	0
hzdrisk_param.var_attn_method	2

comprisk071 – comprisk077

40 RSA Periods
Spawning
Building Damage Variability off
Amplification Variability off

Variable	*Value*
hzdrisk_param.Tlen	40
hzdrisk_param.Tlen_attn	40
hzdrisk_param.Tlen_vun	40
hzdrisk_param.periods	linspace(0,3.33,40)
hzdrisk_param.var_amp_flag	0
hzdrisk_param.var_bcap_flag	0

comprisk078 – comprisk084

40 RSA Periods
Random Sampling
Building Damage Variability off
Amplification Variability off

Variable	*Value*
hzdrisk_param.Tlen	40
hzdrisk_param.Tlen_attn	40
hzdrisk_param.Tlen_vun	40
hzdrisk_param.periods	linspace(0,3.33,40)
hzdrisk_param.var_amp_flag	0
hzdrisk_param.var_bcap_flag	0
hzdrisk_param.var_attn_method	2

comprisk085 – comprisk091

40 RSA Periods
Mean variability
Building Damage Variability off
Amplification Variability off

Variable	*Value*
hzdrisk_param.Tlen	40
hzdrisk_param.Tlen_attn	40
hzdrisk_param.Tlen_vun	40
hzdrisk_param.periods	linspace(0,3.33,40)
hzdrisk_param.var_attn_flag	0
hzdrisk_param.var_amp_flag	0
hzdrisk_param.var_bcap_flag	0

comprisk092 – comprisk098

40 RSA Periods
1 standard deviation up
Building Damage Variability off
Amplification Variability off

Variable	*Value*
hzdrisk_param.Tlen	40
hzdrisk_param.Tlen_attn	40
hzdrisk_param.Tlen_vun	40
hzdrisk_param.periods	linspace(0,3.33,40)
hzdrisk_param.var_attn_method	4
hzdrisk_param.src_eps_switch	0
hzdrisk_param.var_amp_flag	0
hzdrisk_param.var_bcap_flag	0

comprisk099 – comprisk106

40 RSA Periods
1 standard deviation up
Building Damage Variability off
Amplification Variability On

Variable	*Value*
hzdrisk_param.Tlen	40
hzdrisk_param.Tlen_attn	40
hzdrisk_param.Tlen_vun	40
hzdrisk_param.periods	linspace(0,3.33,40)
hzdrisk_param.var_attn_method	4
hzdrisk_param.src_eps_switch	0
hzdrisk_param.var_amp_flag	1
hzdrisk_param.var_bcap_flag	0

comprisk113 – comprisk119

-1 σ
40 RSA Periods
Building Damage Variability off
Amplification Variability off

Variable	*Value*
hzdrisk_param.Tlen	40
hzdrisk_param.Tlen_attn	40
hzdrisk_param.Tlen_vun	40
hzdrisk_param.periods	linspace(0,3.33,40)
hzdrisk_param.var_amp_flag	0
hzdrisk_param.var_bcap_flag	0
hzdrisk_param.var_attn_method	5

comprisk120 – comprisk125

-1 σ
40 RSA Periods
Building Damage Variability off
Amplification Variability on

Variable	*Value*
hzdrisk_param.Tlen	40
hzdrisk_param.Tlen_attn	40
hzdrisk_param.Tlen_vun	40
hzdrisk_param.periods	linspace(0,3.33,40)
hzdrisk_param.var_amp_flag	1
hzdrisk_param.var_bcap_flag	0
hzdrisk_param.var_attn_method	5

comprisk126 – comprisk132

-1 σ
40 RSA Periods
Building Damage Variability on
Amplification Variability off

Variable	*Value*
hzdrisk_param.Tlen	40
hzdrisk_param.Tlen_attn	40
hzdrisk_param.Tlen_vun	40
hzdrisk_param.periods	linspace(0,3.33,40)
hzdrisk_param.var_amp_flag	0
hzdrisk_param.var_bcap_flag	1
hzdrisk_param.var_attn_method	5

comprisk133 – copmrisk139

Random Sampling
40 RSA Periods
Building Damage Variability on
Amplification Variability off

Variable	*Value*
hzdrisk_param.Tlen	40
hzdrisk_param.Tlen_attn	40
hzdrisk_param.Tlen_vun	40
hzdrisk_param.periods	linspace(0,3.33,40)
hzdrisk_param.var_amp_flag	0
hzdrisk_param.var_bcap_flag	1
hzdrisk_param.var_attn_method	2

comprisk140 – comprisk146

-1 σ
40 RSA Periods
Building Damage Variability on
Amplification Variability on

Variable	*Value*
hzdrisk_param.Tlen	40
hzdrisk_param.Tlen_attn	40
hzdrisk_param.Tlen_vun	40
hzdrisk_param.periods	linspace(0,3.33,40)
hzdrisk_param.var_amp_flag	1
hzdrisk_param.var_bcap_flag	1
hzdrisk_param.var_attn_method	5

comprisk147 – comprisk153

+1 σ
40 RSA Periods
Building Damage Variability on
Amplification Variability off

Variable	*Value*
hzdrisk_param.Tlen	40
hzdrisk_param.Tlen_attn	40
hzdrisk_param.Tlen_vun	40
hzdrisk_param.periods	linspace(0,3.33,40)
hzdrisk_param.var_amp_flag	0
hzdrisk_param.var_bcap_flag	1
hzdrisk_param.var_attn_method	4

comprisk154 – comprisk160

Mean
40 RSA Periods
Building Damage Variability on
Amplification Variability off

Variable	*Value*
hzdrisk_param.Tlen	40
hzdrisk_param.Tlen_attn	40
hzdrisk_param.Tlen_vun	40
hzdrisk_param.periods	linspace(0,3.33,40)
hzdrisk_param.var_amp_flag	0
hzdrisk_param.var_bcap_flag	1
hzdrisk_param.var_attn_flag	0

comprisk161 – comprisk167

Spawning
40 RSA Periods
Building Damage Variability on
Amplification Variability off

Variable	*Value*
hzdrisk_param.Tlen	40
hzdrisk_param.Tlen_attn	40
hzdrisk_param.Tlen_vun	40
hzdrisk_param.periods	linspace(0,3.33,40)
hzdrisk_param.var_amp_flag	0
hzdrisk_param.var_bcap_flag	1

comprisk168 – comprisk174

Random Sampling
40 RSA Periods
Building Damage Variability on
Amplification Variability off

Variable	*Value*
hzdrisk_param.Tlen	40
hzdrisk_param.Tlen_attn	40
hzdrisk_param.Tlen_vun	40
hzdrisk_param.periods	linspace(0,3.33,40)
hzdrisk_param.var_amp_flag	0
hzdrisk_param.var_bcap_flag	1
hzdrisk_param.var_attn_method	2

comprisk175 – comprisk181

Random Sampling
40 RSA Periods
Building Damage Variability on
Amplification Variability on

Variable	*Value*
hzdrisk_param.Tlen	40
hzdrisk_param.Tlen_attn	40
hzdrisk_param.Tlen_vun	40
hzdrisk_param.periods	linspace(0,3.33,40)
hzdrisk_param.var_amp_flag	1
hzdrisk_param.var_bcap_flag	1
hzdrisk_param.var_attn_method	2

comprisk182

Mean

Variable	*Value*
hzdrisk_param.var_attn_flag	0

comprisk183

mean variability
56 return periods

Variable	*Value*
hzdrisk_param.var_attn_flag	0
hzdrisk_param.rtrn_per	[20:20:200 300:100:3000 3250:250:5000 5500:500:10000]

comprisk184

mean variability
123 return periods

Variable	*Value*
hzdrisk_param.var_attn_flag	0
hzdrisk_param.rtrn_per	[20:10:290 300:50:3000 3100:100:5000 5250:250:10000]

comprisk185 – comprisk219

Spawning
40 RSA Periods
Building Damage Variability off
Amplification Variability off

Variable	*Value*
hzdrisk_param.Tlen	40
hzdrisk_param.Tlen_attn	40
hzdrisk_param.Tlen_vun	40
hzdrisk_param.periods	linspace(0,3.33,40)
hzdrisk_param.var_amp_flag	0
hzdrisk_param.var_bcap_flag	0

comprisk220 – comprisk254

Random Sampling
40 RSA Periods
Building Damage Variability off
Amplification Variability off

Variable	*Value*
hzdrisk_param.Tlen	40
hzdrisk_param.Tlen_attn	40
hzdrisk_param.Tlen_vun	40
hzdrisk_param.periods	linspace(0,3.33,40)
hzdrisk_param.var_amp_flag	0
hzdrisk_param.var_bcap_flag	0
hzdrisk_param.var_attn_method	2

comprisk255 – comprisk289

Mean variability
40 RSA Periods
Building Damage Variability off
Amplification Variability off

Variable	*Value*
hzdrisk_param.Tlen	40
hzdrisk_param.Tlen_attn	40
hzdrisk_param.Tlen_vun	40
hzdrisk_param.periods	linspace(0,3.33,40)
hzdrisk_param.var_amp_flag	0
hzdrisk_param.var_bcap_flag	0
hzdrisk_param.var_attn_flag	0

comprisk290 – comprisk299

Doubled the number of earthquakes in each source zone
40 RSA Periods

Variable	*Value*
hzdrisk_param.ntgrvector	[1000 200 200 600 200 200]
hzdrisk_param.Tlen	40
hzdrisk_param.Tlen_attn	40
hzdrisk_param.Tlen_vun	40
hzdrisk_param.periods	linspace(0,3.33,40)

comprisk300 – comprisk309

Doubled the number of earthquakes in each source zone
Random Sampling
40 RSA Periods

Variable	*Value*
hzdrisk_param.ntgrvector	[1000 200 200 600 200 200]
hzdrisk_param.Tlen	40
hzdrisk_param.Tlen_attn	40
hzdrisk_param.Tlen_vun	40
hzdrisk_param.periods	linspace(0,3.33,40)
hzdrisk_param.var_attn_method	2

comprisk310 – comprisk319

Spawning
40 RSA Periods
Atkinson and Boore (1997) attenuation model

Variable	*Value*
hzdrisk_param. attenuation_flag	2
hzdrisk_param.Tlen	40
hzdrisk_param.Tlen_attn	40
hzdrisk_param.Tlen_vun	40
hzdrisk_param.periods	linspace(0,3.33,40)

comprisk320 – comprisk329

Somerville attenuation model
40 RSA Periods

Variable	*Value*
hzdrisk_param. attenuation_flag	4
hzdrisk_param.Tlen	40
hzdrisk_param.Tlen_attn	40
hzdrisk_param.Tlen_vun	40
hzdrisk_param.periods	linspace(0,3.33,40)

comprisk330 – comprisk339

Random Sampling
40 RSA Periods
Atkinson and Boore (1997) attenuation model

Variable	*Value*
hzdrisk_param. attenuation_flag	2
hzdrisk_param.Tlen	40
hzdrisk_param.Tlen_attn	40
hzdrisk_param.Tlen_vun	40
hzdrisk_param.periods	linspace(0,3.33,40)
hzdrisk_param.var_attn_method	2

comprisk340 – comprisk349

Random Sampling
Somerville attenuation model
40 RSA Periods

Variable	*Value*
hzdrisk_param. attenuation_flag	4
hzdrisk_param.Tlen	40
hzdrisk_param.Tlen_attn	40
hzdrisk_param.Tlen_vun	40
hzdrisk_param.periods	linspace(0,3.33,40)
hzdrisk_param.var_attn_method	2

comprisk350 – comprisk359

Halve the number of earthquakes in each source zone

Variable	*Value*
hzdrisk_param.ntgrvector	[250 50 50 150 50 50]

comprisk360 – comprisk369

Random Sampling
Halve the number of earthquakes in each source zone

Variable	*Value*
hzdrisk_param.ntgrvector	[250 50 50 150 50 50]
hzdrisk_param.var_attn_method	2

comprisk370 – comprisk376

40 RSA Periods
Amplification off

Variable	*Value*
hzdrisk_param.Tlen	40
hzdrisk_param.Tlen_attn	40
hzdrisk_param.Tlen_vun	40
hzdrisk_param.periods	linspace(0,3.33,40)
hzdrisk_param.amp_switch	0

comprisk377 – comprisk383

Random Sampling
40 RSA Periods
Amplification off

Variable	*Value*
hzdrisk_param.Tlen	40
hzdrisk_param.Tlen_attn	40
hzdrisk_param.Tlen_vun	40
hzdrisk_param.periods	linspace(0,3.33,40)
hzdrisk_param.amp_switch	0
hzdrisk_param.var_attn_method	2

comprisk384 – comprisk390

Mean variability
Amplification off
40 RSA Periods

Variable	*Value*
hzdrisk_param.Tlen	40
hzdrisk_param.Tlen_attn	40
hzdrisk_param.Tlen_vun	40
hzdrisk_param.periods	linspace(0,3.33,40)
hzdrisk_param.amp_switch	0
hzdrisk_param.var_attn_flag	0

comprisk391 - comprisk396
as for comprisk023

comprisk397 – comprisk402
as for comprisk040

comprisk403 – comprisk409
as for comprisk041

comprisk410 – comprisk450
as for comprisk185

comprisk451 – comprisk490
as for comprisk220

comprisk491 – comprisk531
as for comprisk255

PERTH

comprisk001 – comprisk 007

40 RSA Periods
spawning

Variable	*Value*
hzdrisk_param.Tlen	40
hzdrisk_param.Tlen_attn	40
hzdrisk_param.Tlen_vun	40
hzdrisk_param.periods	linspace(0,3.33,40)

comprisk008 – comprisk014

40 RSA Periods
Random Sampling

Variable	*Value*
hzdrisk_param.Tlen	40
hzdrisk_param.Tlen_attn	40
hzdrisk_param.Tlen_vun	40
hzdrisk_param.periods	linspace(0,3.33,40)
hzdrisk_param.var_attn_method	2

comprisk015 – comprisk021

40 RSA Periods
Mean variability

Variable	*Value*
hzdrisk_param.Tlen	40
hzdrisk_param.Tlen_attn	40
hzdrisk_param.Tlen_vun	40
hzdrisk_param.periods	linspace(0,3.33,40)
hzdrisk_param.var_attn_flag	0

comprisk022 – comprisk 028

40 RSA Periods
Spawning
Building Damage Variability off

Variable	*Value*
hzdrisk_param.Tlen	40
hzdrisk_param.Tlen_attn	40
hzdrisk_param.Tlen_vun	40
hzdrisk_param.periods	linspace(0,3.33,40)
hzdrisk_param.var_bcap_flag	0
hzdrisk_param.var_attn_flag	0

comprisk029 – comprisk035

40 RSA Periods
Random Sampling
Building Damage Variability off

Variable	*Value*
hzdrisk_param.Tlen	40
hzdrisk_param.Tlen_attn	40
hzdrisk_param.Tlen_vun	40
hzdrisk_param.periods	linspace(0,3.33,40)
hzdrisk_param.var_bcap_flag	0
hzdrisk_param.var_attn_method	2

comprisk035 – comprisk042

40 RSA Periods
Mean variability
Building Damage Variability off

Variable	*Value*
hzdrisk_param.Tlen	40
hzdrisk_param.Tlen_attn	40
hzdrisk_param.Tlen_vun	40
hzdrisk_param.periods	linspace(0,3.33,40)
hzdrisk_param.var_attn_flag	0
hzdrisk_param.var_bcap_flag	0

comprisk043 - 049

Spawning
40 RSA Periods
Atkinson and Boore (1997) attenuation model

Variable	*Value*
hzdrisk_param. attenuation_flag	2
hzdrisk_param.Tlen	40
hzdrisk_param.Tlen_attn	40
hzdrisk_param.Tlen_vun	40
hzdrisk_param.periods	linspace(0,3.33,40)

comprisk050 - 056

Random Sampling
40 RSA Periods
Atkinson and Boore (1997) attenuation model

Variable	*Value*
hzdrisk_param. attenuation_flag	2
hzdrisk_param.Tlen	40
hzdrisk_param.Tlen_attn	40
hzdrisk_param.Tlen_vun	40
hzdrisk_param.periods	linspace(0,3.33,40)
hzdrisk_param.var_attn_method	2

comprisk057 - 063

Spawning
Somerville attenuation model
40 RSA Periods

Variable	*Value*
hzdrisk_param. attenuation_flag	4
hzdrisk_param.Tlen	40
hzdrisk_param.Tlen_attn	40
hzdrisk_param.Tlen_vun	40
hzdrisk_param.periods	linspace(0,3.33,40)

comprisk064 - 070

Random Sampling
Somerville attenuation model
40 RSA Periods

Variable	*Value*
hzdrisk_param. attenuation_flag	4
hzdrisk_param.Tlen	40
hzdrisk_param.Tlen_attn	40
hzdrisk_param.Tlen_vun	40
hzdrisk_param.periods	linspace(0,3.33,40)
hzdrisk_param.var_attn_method	2

comprisk071

Spawning
nsamples = 3

Variable	*Value*
hzdrisk_param.nsamples	3

comprisk072

Spawning
nsamples = 7

Variable	*Value*
hzdrisk_param.nsamples	7

comprisk073

Spawning
nsamples = 9

Variable	*Value*
hzdrisk_param.nsamples	9

comprisk074

Spawning
nsamples = 11

Variable	*Value*
hzdrisk_param.nsamples	11

comprisk075 - comprisk081

Spawning
40 RSA Periods
Doubled the number of earthquakes in each source zone

Variable	*Value*
hzdrisk_param.ntgrvector	[1000 200 200 600 200 200]
hzdrisk_param.Tlen	40
hzdrisk_param.Tlen_attn	40
hzdrisk_param.Tlen_vun	40
hzdrisk_param.periods	linspace(0,3.33,40)

comprisk082 – comprisk088

Random Sampling
40 RSA Periods
Doubled the number of earthquakes in each source zone

Variable	*Value*
hzdrisk_param.ntgrvector	[1000 200 200 600 200 200]
hzdrisk_param.Tlen	40
hzdrisk_param.Tlen_attn	40
hzdrisk_param.Tlen_vun	40
hzdrisk_param.periods	linspace(0,3.33,40)
hzdrisk_param.var_attn_method	2

comprisk089 - comprisk095

Spawning
40 RSA Periods
Halved the number of earthquakes in each source zone

Variable	*Value*
hzdrisk_param.ntgrvector	[250 50 50 150 50 50]
hzdrisk_param.Tlen	40
hzdrisk_param.Tlen_attn	40
hzdrisk_param.Tlen_vun	40
hzdrisk_param.periods	linspace(0,3.33,40)

comprisk095 – comprisk102

Random Sampling
40 RSA Periods
Halved the number of earthquakes in each source zone

Variable	*Value*
hzdrisk_param.ntgrvector	[250 50 50 150 50 50]]
hzdrisk_param.Tlen	40
hzdrisk_param.Tlen_attn	40
hzdrisk_param.Tlen_vun	40
hzdrisk_param.periods	linspace(0,3.33,40)
hzdrisk_param.var_attn_method	2